UNIVERSITE DE STRASBOURG

Ecole doctorale de la Vie et de la Santé

Laboratoire de Biophotonique et Pharmacologie
UMR CNRS 7213 – Faculté de Pharmacie

THESE

pour obtenir le grade de

DOCTEUR DE L'UNIVERSITE DE STRASBOURG

Discipline: Sciences du Vivant

Specialité: Aspects moléculaires et cellulaires de la Biologie

par

PIKHARTOVA-MARTINKOVA Eva

COMBINATION OF ELLIPTICINE CHEMOTHERAPY AND α5β1 INTEGRIN TARGETED THERAPY IN HUMAN GLIOBLASTOMA

Présentée et soutenue publiquement le 27.4.2010

Docteur Monique DONTENWILL	Directrice de Thèse
Professeur Marie STIBOROVA	Co-directrice de Thèse, Prague
Professeur José LUIS	Rapporteur Externe, Marseille
Docteur Muriel BARBERI-HEYOB	Rapporteur Externe, Nancy
Docteur Dominique GUENOT	Rapporteur Interne, Strasbourg
Professeur Tomáš ECKSCHLAGER	Examinateur, Prague
Docteur Pavel SOUČEK	Examinateur, Prague
Docteur Petr HODEK	Examinateur, Prague

Charles University Prague

Faculty of Science

Department of Biochemistry

THESIS

COMBINATION OF ELLIPTICINE CHEMOTHERAPY AND α5β1 INTEGRIN-TARGETED THERAPY IN HUMAN GLIOBLASTOMA.

by

MARTÍNKOVÁ Eva

Supervisors: Prof. RNDr. Marie STIBOROVÁ, DrSc.
Dr. Monique DONTENWILL

« Ms Eva Martinkova was a member of the European Doctoral College of Strasbourg during the preparation of her PhD, from 2007 to 2010, class name Marco Polo. She has benefited from specific financial supports offered by the College and, along with her mainstream research, has followed a special course on topics of general European interests presented by international experts. This PhD research project has been led with the collaboration of two universities: the Charles University Prague, Czech Republic and the University of Strasbourg, France. »

Acknowledgements

The following thesis benefited from the insights and direction of several people and therefore it is my pleasure to thank those who made this thesis possible:

I am heartily thankful to my supervisors, Dr. Monique Dontenwill and Prof. Marie Stiborova (in alphabetical order), whose encouragement, guidance and support from the initial to the final level enabled me to develop an understanding of the subject. In addition, they provided timely and instructive comments and evaluation at every stage of the thesis process, allowing me to complete this project on schedule.

Prof. José Luis, Dr. Muriel Barberi-Heyob, Dr. Dominique Guenot, Prof. Tomáš Eckschlager, Dr. Petr Hodek, Dr. Pavel Souček deserve special thanks as my thesis committee members and advisors.

I owe my deepest gratitude to Anne without whose knowledge and assistance this study would not have been successful. She always expressed never-ending patience and readiness to listen, help and coach. She introduced me new methods, provided me myriads of invaluable pieces of advice, and I thank her for willingness to always stand by me when needed, not only at work. She is the closest person in Strasbourg and France for me.

I greatly appreciate Sophie`s help and never-ending patience while introducing me to new experimental techniques and the basics of molecular biology. As well, I will never forget Jérôme who was always there and offered his never-ending smile and encouragement when I became sad or homesick. My special thanks also belong to Claudine for her great help with understanding the basics of flow cytometry.

My sincere thanks also go to all the UMR7213 technical and administrative staff for creating me great conditions to work.

I am deeply grateful to Petr for supporting and encouraging me to pursue this degree. Without Petr’s encouragements, I would not have finished the project. He also provided insights that guided and challenged my thinking, substantially improving the finished product.

It is an honor for me to show my deepest appreciation to my parents for their unflagging love

and support throughout my life. They spare no effort to provide the best possible environment for me to grow up. I have no suitable word that can fully describe my parents` everlasting love to me.

I am indebted to many of my colleagues particularly to Jitka, Martina, Jana, Barbora, Jan and David who have the attitude and the substance of a genius: they continually and convincingly conveyed a spirit of adventure in regard to research and an excitement in regard to helping others. Without their guidance and persistent help this dissertation would not have been possible. I thank to Petr Bartík who helped a lot in the beginning with overcoming those thousands of papers and forms needed to be filled in.

My sincere thanks belong to the institutions that supported me financially during my whole studies: The French Embassy in Prague, with whom I benefited from the scholarship "BGF"; The European Doctoral College, where all the people were always very kind and helpful, and where the studios provided me an unbelievable comfort; Barrande program co-organized by AIP ČR and EGIDE, helping me with the traveling costs and short-term stays for finishing important experiments in Strasbourg.

Lastly, I offer my regards and blessings to all of those others who supported me in any respect during the completion of the project.

Table of Contents

APPENDIX 1: Martinkova E, Maglott A, Leger, DY, Bonnet D, Stiborova M, Takeda K, Martin S, Dontenwill M: *α5β1 integrin antagonists reduce chemotherapy-induced premature senescence and facilitate apoptosis in human glioblastoma cells.* Int J Cancer. Accepted. (2010 Jan 22)

APPENDIX 2: Martinkova E, Dontenwill M, Frei E, Stiborová M: *Cytotoxicity of and DNA adduct formation by ellipticine in human U87MG glioblastoma cancer cells.* Neuro Endocrinol Lett 30(Suppl), 60-66 (2009)

APPENDIX 3: Martinkova E, Hodek P, Hudecek J, Frei E, Dontenwill M, Stiborova M: *Oxidation of ellipticine by human and rat cytochromes P450 correlates with its binding to DNA.* Chem. Listy 101, s73−s310 (2007)

Summary of Figures and Tables

Figures

Tables

Abbreviations

AA	anaplastic astrocytoma
ADMIDAS	Additional Metal Ion Dependent Adhesion Site
ADP	adenosine diphophosphate
Akt	serine/threonine-specific protein kinase family
APC	adenomatosis polyposis coli
ATP	adenosine triphosphate
Bad	Bcl-2-associated death promoter
Bcl-2	human proto-oncogene located on chromosome 18
BCNU	bis-chloronitrosourea, carmustine
bFGF	basic fibroblast growth factor
CBTRUS	Central Brain Tumor Registry of the United States
CDK2/4/6	cyclin-dependent kinase 2/4/6
CHK2	CHK2 checkpoint homolog
CNS	central nervous system
COP1	Caspase recruitment domain-containing protein 16
CYP	cytochrome P450
cyt b5	cytochrome b5
DMSO	dimethylsuphoxide
ECM	extracellular matrix
EGF	Epidermal growth factor
EGFR	epidermal growth factor receptor
ERK	extracellular signal-regulated kinases
FA	focal adhesion
FACS	fluorescence assisted cell sorting / flow cytometry
FAK	focal adhesion kinase
FBS	fetal bovine serum
Fn	fibronectin
Fyn	tyrosine protein kinase 5
GBM	glioblastoma multiforme
GIT	gastrointestinal tract
Graf	GTPase Regulator Associated with Focal Adhesion Kinase
Grb2	rowth factor receptor-bound protein 2
GSK3β	glycogen synthase kinase 3 beta

GTP	guanosine triphosphate
HGF/SF	Hepatocyte growth factor/scatter factor
HIF	Hypoxia-inducible factors
hMLH1 (2)	human MutL homolog 1 (2)
IL-8	interleukin 8
ILK	integrin-linked kinase
JNK	c-Jun N-terminal kinases
MAPK	Mitogen-activated protein (MAP) kinases
MDM2	murine double minute oncogene
MFO	mixed function oxidases
MGMT	O6-Methylguanine-DNA Methyl Transferase
MIDAS	Metal Ion Dependent Adhesion Site
MMP	Matrix metalloproteinase
MTIC	3-methyl-(triazen-1-yl)imidazole-4-carboxamide
mTOR	mammalian target of rapamycin
NAD+	Nicotinamide adenine dinucleotide
NADP+	Nicotinamide adenine dinucleotide phosphate
NCI	National Cancer Institute (USA)
NF1 (2)	neurofibromin 1 (2)
NFκB	nuclear factor kappa-light-chain-enhancer of activated B cells
p130Cas	Crk-associated substrate
p16INK4a	Cyclin-dependent kinase inhibitor 2A
PAH	polycyclic aromatic hydrocarbons
PAPS	3'-Phosphoadenosine-5'-phosphosulfate
PDGF	platelet-derived growth factor
PDGFR	platelet-derived growth factor receptor
PI	propidium iodide
PI3K	phosphoinositide 3-kinases
PIP2	phosphatidylinositol 4,5-bisphosphate
PIP3	Phosphatidylinositol (3,4,5)-trisphosphate
PIRH2	p53-induced ubiquitin-protein ligase
PMS2	Mismatch repair endonuclease
POLR2A	polymerase (RNA) II (DNA directed) polypeptide A
PTB	phosphotyrosine-binding
PTCH	protein patched homolog
PTEN	phosphatase and tensin homolog

Raf	Serine/threonine-specific protein kinase
Ras	small GTPase
RB1	retinoblastoma protein
SA-β-gal	senescence-associated β-galactosidase
SDS-PAGE	sodium dodecyl sulphate polyacrylamide gel electrophoresis
Src	proto-oncogenic tyrosine kinases
TGF-α	Transforming growth factor α
TMZ	temozolomide
TSC1 (2)	tuberous sclerosis protein 1 (2)
VEGF	Vascular endothelial growth factor receptor
WHO	World Health Organization

Part I. Introduction

This work is dealing with treating glioblastoma multiforme (or glioblastoma or GBM), type of central nervous system (CNS) tumor originating from astrocytic cells. Glioblastoma represent the most abundant and most aggressive type of CNS tumors in adults with a survival median of less than one year. Moreover, these tumors often embody chemo- and/or radioresistance and easily recur. Therefore, novel therapeutic strategies are highly needed to be found.

CNS tumors

Primary malignant CNS tumors represent about 2% of all cancers (http://www.cancer.org/docroot/PRO/content/PRO_1_1_Cancer_Statistics_2009_Presentation.asp, cached 19.2.2010). By estimation, 1,479,350 new cases of benign and malignant brain tumors have been diagnosed in 2009 in the United States. Mortality reaches 38%.

The incidence of brain tumors in the United States is 14.8 cases per 100,000 population annually, with approximately half being histologically benign. But even benign tumors, if not amenable to excision or radiation therapy, can be fatal as a result of progressive growth in the closed space of the skull (Buckner et al., 2007). Meningiomas are the most abundant ones, but exhibit usually benign histology and slow growth. The most important group is glioma representing 40% and 78% of all and malignant CNS tumors, respectively [**Table 1**].

Table 1: Distribution of all primary brain and CNS tumors by histology, CBTRUS 1998-2002 (N=63,698)*

Histology	Percentage
Lymphoma	3.1
Nerve sheath	8.0
Craniopharyngioma	0.7
Pituitary	6.3
Glioblastoma†	20.3
Astrocytomas	9.8
Ependymomas	2.3
Oligodendrogliomas	3.7
Embryonal, including medulloblastoma	1.7
Meningioma	30.1
All other	13.9

*CBTRUS = Central Brain Tumor Registry of the United States; CNS = central nervous system.
†Gliomas account for 40% of all tumors and 78% of malignant tumors.

CNS tumors can be classified regarding the specific cell type they are originating from (ependymomas, gliomas, oligodendrogliomas etc.) or their grade according to the World Health Organization (WHO) classification established in 1993 [**Table 2**].

Table 2: General CNS tumor classification according to WHO including malignancy grades (Louis et al., 2007).

	I	II	III	IV
Astrocytic tumours				
Subependymal giant cell astrocytoma	•			
Pilocytic astrocytoma	•			
Pilomyxoid astrocytoma		•		
Diffuse astrocytoma		•		
Pleomorphic xanthoastrocytoma		•		
Anaplastic astrocytoma			•	
Glioblastoma				•
Giant cell glioblastoma				•
Gliosarcoma				•
Oligodendroglial tumours				
Oligodendroglioma		•		
Anaplastic oligodendroglioma			•	
Oligoastrocytic tumours				
Oligoastrocytoma		•		
Anaplastic oligoastrocytoma			•	
Ependymal tumours				
Subependymoma	•			
Myxopapillary ependymoma	•			
Ependymoma		•		
Anaplastic ependymoma			•	
Choroid plexus tumours				
Choroid plexus papilloma	•			
Atypical choroid plexus papilloma		•		
Choroid plexus carcinoma			•	
Other neuroepithelial tumours				
Angiocentric glioma	•			
Chordoid glioma of the third ventricle		•		
Neuronal and mixed neuronal-glial tumours				
Gangliocytoma	•			
Ganglioglioma	•			
Anaplastic ganglioglioma			•	
Desmoplastic infantile astrocytoma and ganglioglioma	•			
Dysembryoplastic neuroepithelial tumour	•			
Central neurocytoma		•		
Extraventricular neurocytoma		•		
Cerebellar liponeurocytoma		•		
Paraganglioma of the spinal cord	•			
Papillary glioneuronal tumour	•			
Rosette-forming glioneuronal tumour of the fourth ventricle	•			
Pineal tumours				
Pineocytoma	•			
Pineal parenchymal tumour of intermediate differentiation		•	•	
Pineoblastoma				•
Papillary tumour of the pineal region		•	•	
Embryonal tumours				
Medulloblastoma				•
CNS primitive neuroectodermal tumour (PNET)				•
Atypical teratoid / rhabdoid tumour				•
Tumours of the cranial and paraspinal nerves				
Schwannoma	•			
Neurofibroma	•			
Perineurioma	•	•	•	
Malignant peripheral nerve sheath tumour (MPNST)		•	•	•
Meningeal tumours				
Meningioma	•			
Atypical meningioma		•		
Anaplastic / malignant meningioma			•	
Haemangiopericytoma		•		
Anaplastic haemangiopericytoma			•	
Haemangioblastoma	•			
Tumours of the sellar region				
Craniopharyngioma	•			
Granular cell tumour of the neurohypophysis	•			
Pituicytoma	•			
Spindle cell oncocytoma of the adenohypophysis	•			

Histological grading is a mean of predicting the biological behavior of a neoplasm. In the clinical setting, tumor grade is a key factor influencing the choice of therapies, especially determining the use of adjuvant radiation and specific chemotherapy protocols. The WHO classification of tumors of the nervous system includes a grading scheme that is a 'malignancy scale' ranging across a wide variety of neoplasms rather than a strict histological grading system (Kleihues et al., 1993, Louis et al. , 2007).

Glioblastoma

Gliomas are CNS tumors originating from glial cells usually occurring in brain, more rarely also in spinal cord. The annual incidence of glioma in the United States is 5.4 cases per 100,000 population which is comparable to the rest of the world (http://emedicine.medscape.com/article/283453-overview, cached 30.11.2009).

Table 3: Astrocytic tumors classification by grade according to WHO (http://rad.usuhs.mil/rad/who/who2b.html; cached 30.11.2009; (Louis et al. , 2007).

WHO tumor name	**WHO grade**	**Characteristics**
Pilocytic Astrocytoma	I	lesions with low proliferative potential and the possibility of cure following surgical resection alone; children at age 5-15 survival median: > 20 years
Low-grade Astrocytoma	II	generally infiltrative; despite low-level proliferative activity often recur; tend to progress to higher grades of malignancy survival median: cca 10 years
Anaplastic Astrocytoma	III	lesions with histological evidence of malignancy, including nuclear atypia and brisk mitotic activity; adults at age superior 40 years survival median: 2 – 3 years
Glioblastoma	IV	cytologically malignant, mitotically active, necrosis-prone neoplasms; typically associated with rapid pre- and postoperative disease evolution and a fatal outcome; most common type in adults survival median: 8 months

Glioblastomas as well as all astrocytomas originate from non-neuron star-shaped glial cells - astrocytes, providing biochemical support to neurons as well as to epithelial cells forming the blood-brain barrier. They are essential for sustaining homeostasis and providing nutrients

supply for neural cells. Glioblastoma represent the most common and also the most aggressive solid CNS tumors [**Table 3**]. It is present in two histological variants: giant cell glioblastoma containing a portion of multinucleated giant cels, and gliosarcoma representing only 2.1% of all glioblastomas.

Median survival of patients diagnosed with GBM without any treatment is approximately 90 days, and is extended to from about six to twelve months using conventional therapies, while long term survival (at least five years) falls under 3% (Buckner et al. , 2007).

Causes of Glioblastoma

Predominant and exact causes and mechanisms of astrocytic tumor formation remain unknown. Genetic predisposition to these tumors appears to be relatively rare, although they can be inherited as a part of several familial diseases, such as type 1 neurofibromatosis (mutation of NF1), Turcot syndrome (mutation of APC), basal cell nevus (or Gorlin) syndrome mutation of PTCH), and Li-Fraumeni syndrome (mutation of TP53 or CHEK2) [**Table 4**].

Table 4: Inherited mutations in members of families at increased risk of glioma (Schwartzbaum et al., 2006)

Syndrome	Gene name	Chromosomal location
Neurofibromatosis 1	*NF1*	17q11
Neurofibromatosis 2	*NF2*	22q12
Tuberous sclerosis	*TSC1*	9q34
	TSC2	16p13
Retinoblastoma	*RB1*	13q14
Li–Fraumeni syndrome	*TP53*	17p13
Turcot's syndrome and multiple hamartoma	*APC*	5q21
	hMLH1	3p21.3
	hMSH2	2p22–21
	PMS2	7p22
	PTEN	10q23.3

In addition, environmental risk factors associated with primary brain tumors have been difficult to identify. Except therapeutic irradiation and exposure to some chemical stress stimuli such as formaldehyde, vinylchloride or acrylonitrile, the identification of specific environmental causal factors has been unsuccessful (http://emedicine.medscape.com/article/283453-overview, cached 30.11.2009).

Molecular physiopathology of glioblastoma

Despite a great effort and more than 20 years of ongoing clinical studies, current clinical medicine is still lacking an efficient glioblastoma therapy. The lack of glioma-targeted agents predicts a very limited chance of finding a successful therapy using this approach. An important clue to pathways involved in glioma genesis may lie in the two GBM subtypes that have been identified clinically: primary and secondary GBM [**Figure 1**].

Primary GBM typically presents in older patients (mean age 62 years) as an aggressive, highly invasive tumor, usually without any evidence of prior clinical disease. It usually loses heterozygosity on chromosome 10q (in almost 70% cases). Among other genetic alterations, *EGFR* amplification, *TP53* and *PTEN* mutations, and $p16^{INK4a}$ are often present in primary GBM (Ohgaki and Kleihues, 2005, Ohgaki and Kleihues, 2007).

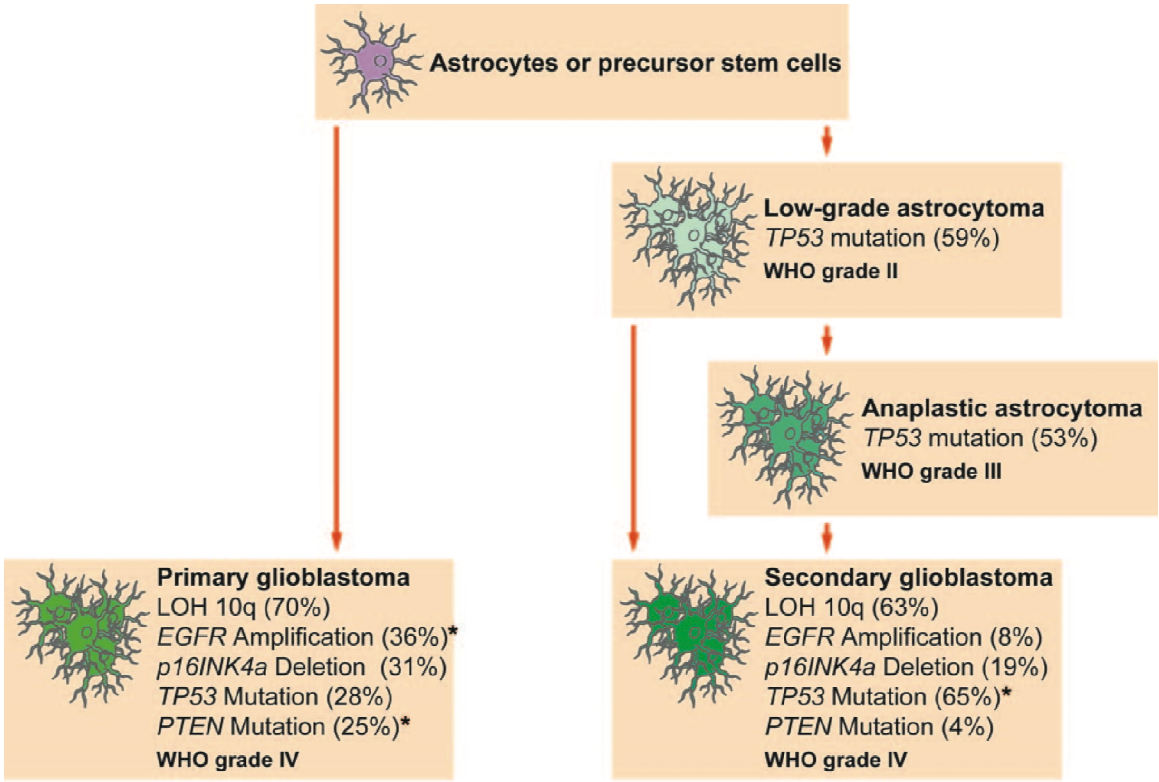

Figure 1: Two GBM entities with their most frequent genetic alterations. GBM can develop over 5–10 years from a low-grade astrocytoma (secondary GBM), or it can be the initial pathology at diagnosis (primary GBM). The clinical features of GBM are the same regardless of clinical route, whereas their genetic background differ. *Genetic alterations significantly different in frequency between primary and secondary glioblastomas. (Ohgaki and Kleihues, 2007).

Secondary GBM has a very different clinical history. It is usually observed in younger patients (mean age 45 years) who initially present with a low-grade astrocytoma that transforms into GBM within 5 – 10 years of the initial diagnosis, regardless of prior therapy. They also embody loss of heterozygosity on chromosome 10q (63%) and *TP53* mutations, which are in 57% cases located in hotspot codons 248 and 273, whereas in primary GBM *TP53* mutations are more widely spread (Maher et al., 2001, Ohgaki and Kleihues, 2005).

EGFR/PTEN/Akt/mTOR signaling pathway is crucial for primary GBM development. *EGFR* amplification occur in about 40% of primary GBM, whereas is very rare in the secondary glioblastomas. *EGFR* amplicons often become (deletion of exons 2 and 7 are the most common) and such constitutively active EGFRvIII with concurrent overexpressed EGFR result in p27 inhibition via PI3K/Akt pathway activation and subsequently in enhanced cell proliferation. Growth factors such as TGF-α and EGF are responsible for EGFR activation resulting in PI3K recruitment to the cell membrane, phosphorylation of phosphatidylinositol to PIP3, that subsequently phosphorylates the effectors: Akt and mTOR leading to apoptosis inhibition and thus cell proliferation [**Figure 2**]. *PTEN* (phosphatase and tensin homology) gene counteracts PI3K signals resulting in cell proliferation inhibition. PTEN has been found to be mutated in 15 - 40% primary GBM, but not in secondary ones.

TP53/MDM2/p14^{ARF} pathway is the key signaling system, primarily for secondary glioblastoma development. TP53 is mutated in two-thirds and about 30% of secondary and primary GBM, respectively. In secondary glioblastomas, 57% of mutations have been reported to be located in the two hotspot codons 248 and 273. However, in primary glioblastomas, mutations were more equally distributed through all exons, with only 17% occurring in codons 248 and 273 (Ohgaki and Kleihues, 2005, Ohgaki and Kleihues, 2007). The less specific pattern of TP53 mutations in primary glioblastomas may constitute, at least in part, secondary events due to increasing genomic instability during tumor development (Ohgaki and Kleihues, 2007).

Amplification of *MDM2* is present in 10% of glioblastomas (exclusively in primary ones) that lack a *TP53* mutation. 36,37 Loss of p14^{ARF} expression has frequently been observed in glioblastomas (76%), and this typically correlates with homozygous deletion or promoter methylation of the p14^{ARF} gene (Bogler et al., 1995). Promoter methylation of p14^{ARF} was more frequent in secondary than primary glioblastomas, but there was no significant

difference in the overall frequency of p14ARF alterations (homozygous deletion and promoter methylation) between glioblastoma subtypes (Nakamura et al., 2001).

The *TP53* gene at 17p13.1 encodes a protein that plays a key role in regulation of cell proliferation, cell death, cell differentiation, and neovascularization (Bogler et al. , 1995). In normal unstressed cells, the level of p53 protein is downregulated via the binding of proteins such as MDM2, COP1, PIRH2 or JNK that promote p53 degradation via the ubiquitin/proteasome pathway. As most of these genes are up regulated by p53, this lead to a regulation loop that will keep p53 level very low in a normal cells (http://p53.free.fr/index.html, cached 1.12.2009).

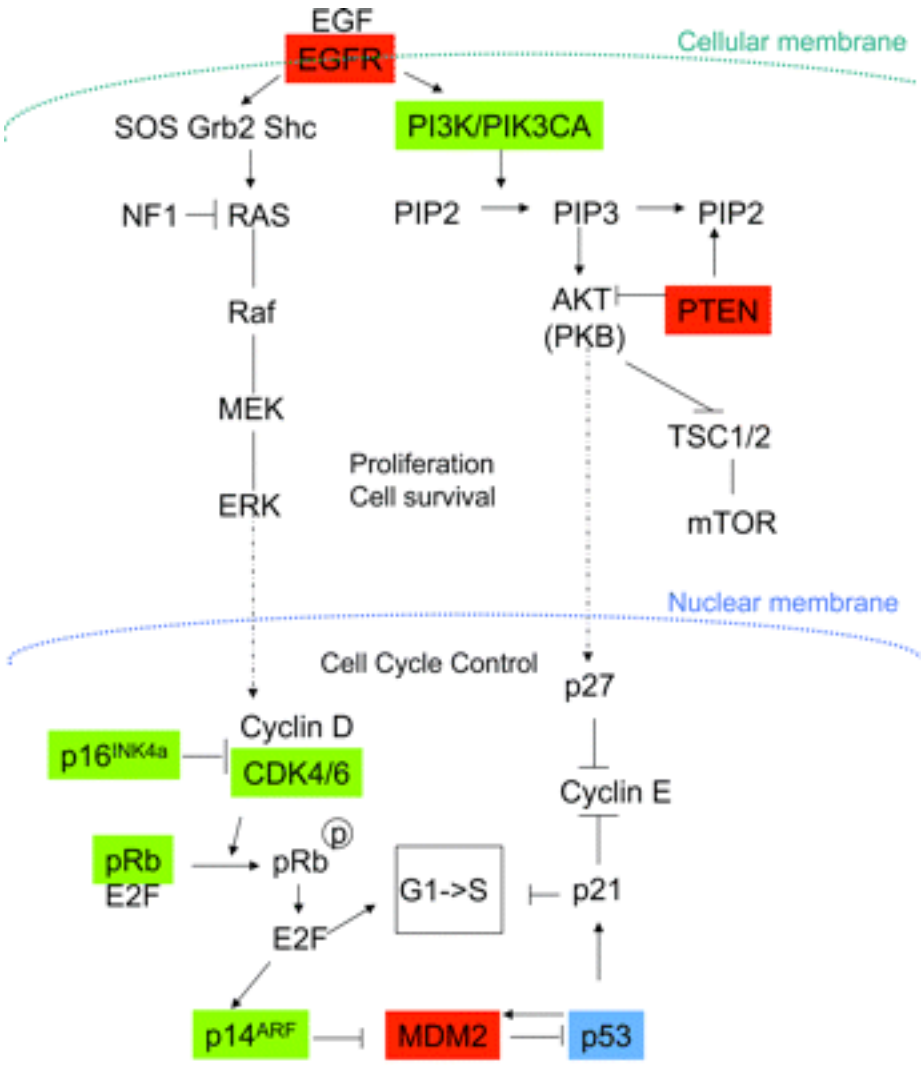

Figure 2: Principal signaling pathways involved in the pathogenesis of glioblastoma (in red: primary GBM, in blue: secondary GBM, in green: both GBM subtypes) (Ohgaki and Kleihues, 2007).

After genotoxic or non-genotoxic stresses, activation of p53 is a two steps process. First, p53 protein level is increased via the inhibition of its interaction with MDM2 and the other negative regulators. Secondly, a series of modulator (kinases, acetylases) will activate p53 transcriptional activity (Vousden, 2000, Vousden, 2002).

The MDM2 binds to mutant and wild-type TP53 proteins, thereby inhibiting the ability of wild-type TP53 to activate transcription from minimal promoter sequences (Momand et al., 1992, Oliner et al., 1992). Conversely, transcription of the *MDM2* gene is induced by wild-type TP53 (Barak et al., 1994, Zauberman et al., 1995). In normal cells, this autoregulatory feedback loop regulates both the activity of the TP53 protein and the expression of MDM2. The $p14^{ARF}$ gene product binds to MDM2 and inhibits MDM2-mediated p53 degradation and transactivational silencing. Conversely, $p14^{ARF}$ expression is negatively regulated by TP53 and inversely correlates with TP53 function in human tumor cell lines (Kamijo et al., 1998, Stott et al., 1998). Therefore, loss of normal TP53 function may also result from altered expression of *MDM2* and/or $p14^{ARF}$ gene [**Figure 2**].

$p16^{INK4a}$/RB1 pathway seems to be important in both, primary and secondary glioblastoma signaling [**Figure 2**]. RB1 protein controls progression through G1 to S phase of the cell cycle. The CDK4/cyclin D1 complex phosphorylates the RB1 protein, thereby inducing release of the E2F transcription factor that activates genes involved in the G1 to S transition. $p16^{INK4a}$ binds to CDK4, inhibits the CDK4/cyclin D1 complex, and thus inhibits the G1 to S transition. Therefore, loss of normal RB1 function may result from altered expression of either of the RB1, $p16^{INK4a}$, or CDK4 genes (Ohgaki and Kleihues, 2007).

1. Conventional glioma therapy

Despite several decades of ongoing neuro-physiopathology research as well as of clinical studies, neurooncologists are still lacking efficient therapy for brain tumors. The tumor environment is an extremely sensitive tissue with a limited capacity of self-repair and is enclosed in a strictly limited cranial space. These tumors tend to spread to brain parenchyma, which makes them hardly removable. They also often exhibit chemoresistance that has to be able to overcome the blood-brain barrier and exhibit low neurotoxicity as well. Taken together, successful therapy of brain tumors represents a great challenge for oncologists as

well as for molecular biologists to reveal the specificities of these neoplasms and propose well-targeted therapeutical approaches.

Nowadays, conventional treatment of brain tumors includes surgical resection (in 100%), and external-beam radiotherapy (87%) possibly combined with chemotherapy (54%). Eighty-eight percent patients receive anticonvulsant therapy, 29% used alternative medicine and 15% are included in clinical trials (Chamberlain, 2006).

Chemotherapy

Fifty percent of brain tumors represent gliomas, where 50% of them are glioblastomas. Nowadays, over half of all cases are treated by chemotherapy concomitantly with radiotherapy and adjuvantly. Conventionally, glioblastomas are treated with methylating agents, usually nitrosoureas, e.g. carmustine (BCNU), lomustine, or a triple combination of procarbazine, lomustine and vincristine [for structures see **Figure 3**]. During last decades, clinical trials phase II - IV emerged another promising methylating agent, temozolomide (Temodal, Temodar®, Schering-Plough), which became a reference drug for glioblastoma treatment.

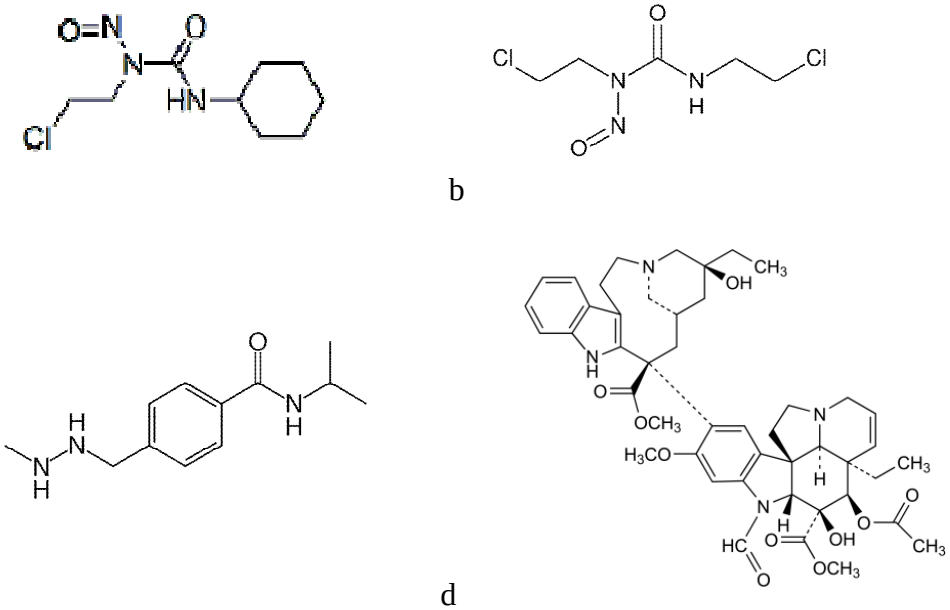

Figure 3: Lomustine (a), carmustine (b), procarbazine (c) and vincristine (d) structures.

1. *Temozolomide*

Temozolomide (TMZ), an imidazotetrazine derivative [**Figure 4**] containing three adjacent nitrogen atoms, spontaneously converts at physiologic pH into its metabolite MTIC (3-methyl-(triazen-1-yl)imidazole-4-carboxamide) and subsequently to a methyldiazonium cation, which transfers the methyl group to DNA, and degrading MTIC to the final degradation product [AIC in **Figure 4**] excreted by kidneys (Denny et al., 1994).

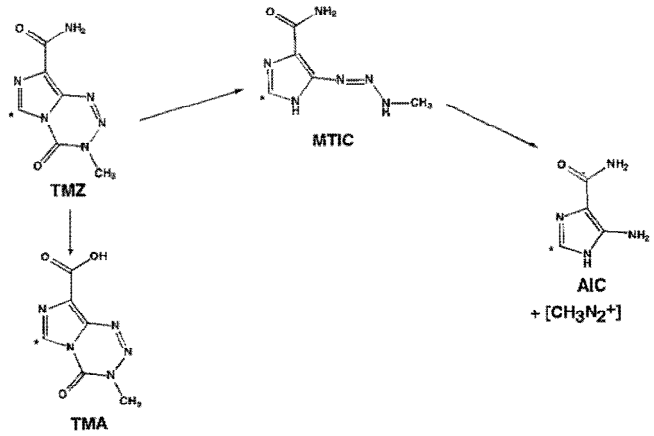

Figure 4: Temozolomide (TMZ) structure, its metabolic and degradation pathways (Baker et al., 1999).

The DNA methylation occurs most commonly at the N^7 position of guanine, followed by O^3 position of adenine and O^6 position of guanine. The O^6 guanin methylation represent only about 5% of the methylation reactions of MTIC, but seems to play a crucial role in antitumoral effects of temozolomide. This hypothesis is supported by the negative correlation between the sensitivity to temozolomide and the activity of O^6 methylguanine methyltransferase (MGMT), which specifically removes the methyl group from O^6 position of guanine (Friedman et al., 2000).

Temozolomide has been shown to be widely distributed in tissues including brain, thus overcrossing the blood-brain barrier (Stevens and Newlands, 1993). Moreover, it is 100% bioavailable after *per os* dosing.

According to recent studies, radiotherapy combined with temozolomide treatment, followed by postradiotherapy with TMZ for 6 months increased the median survival from 12 to 14.6 months with no negative impact on quality of life (Stupp et al., 2005). Consecutively, MGMT expression was evaluated, as it is a predominant DNA repair enzyme removing the alkyl

groups from DNA bases. MGMT gene silencing correlates with better responses to alkylating agents and higher survival rates (Hegi et al., 2005). Survival median of patients with methylated MGMT promoter, treated by temozolomide in combination with radiotherapy reached 21.7 months compared to 15.3 months of those expressing normal MGMT (Chamberlain, 2006).

2. *Ellipticine*

Ellipticine (5,11-Dimethyl-6H-pyrido(4,3-b)carbazole) and its derivatives are pyridocarbazoles which were found to possess significant anticancer and anti-HIV activity. Ellipticine was first identified in 1959 in the leaves of a small Australian tropical evergreen tree *Ochrosia elliptica Labill.* from the *Apocyanaceae* family (Garbett and Graves, 2004). Ellipticine's more soluble derivatives, 9-methoxyellipticine and 2-methyl-9-hydroxyellipticine in the form of acetate (NMHE), have been utilized pharmacologically since 1970s, especially in France (Le Pecq et al., 1974). Ellipticine derivatives entered clinical trials phase II for the chemotherapy of advanced breast cancer, metastatic adenoid carcinoma, lung carcinoma and and carcinoma of stomach (data NCI). They were also proved to be highly efficient against osteolytic breast cancer metastases, acute myeloblastic leukemia, kidney sarcoma and thyroid carcinoma (Acton et al., 1994). In 1994, ellipticines showed an increased cytotoxicity in the brain tumor cell line subpanel of the NCI-60 cell-line screening panel (Shi et al., 1998a, Shi et al., 1998b, Vistica et al., 1994).

Ellipticine pharmacokinetics

The physiological disposition of ellipticine was studied by Chadwick and co-workers in the mouse, rat, dog and monkey after administration of [1-^{14}C]ellipticine at 6 mg/kg intravenously (3 mg/kg to monkey). Ellipticine was widely, but not uniformly, distributed throughout the tissues including the brain, so it seems able to overcome the blood-brain barrier, either because of its lipid-solubility (Chadwick et al., 1978), or due to some form of active transport (Vistica et al. , 1994). Ellipticine is a weak base (pK_a = 5.8), it is ionized in acidic medium of the gastrointestinal tract (GIT) and could not be resorbed from the intestine.

The primary site of ellipticine metabolism is the liver, where it is predominantly metabolised to 9-hydroxyellipticine (rat). The 9-hydroxyellipticine does not accumulate here but is conjugated to its glucuronide and sulphate, which are secreted in bile (Chadwick et al. , 1978).

Hydroxylation at carbon C9 occurs approximately three times more intensively in animals treated by methylcholanthrene (an inductor of cytochrome P450 (CYP)1A and CYP1B1) and twice more intensively in animals treated by phenobarbital (an inductor of CYP2B) (Lesca et al., 1981). An overview of ellipticine metabolism by human CYP enzymes *in vitro* is shown in **Figure 5**.

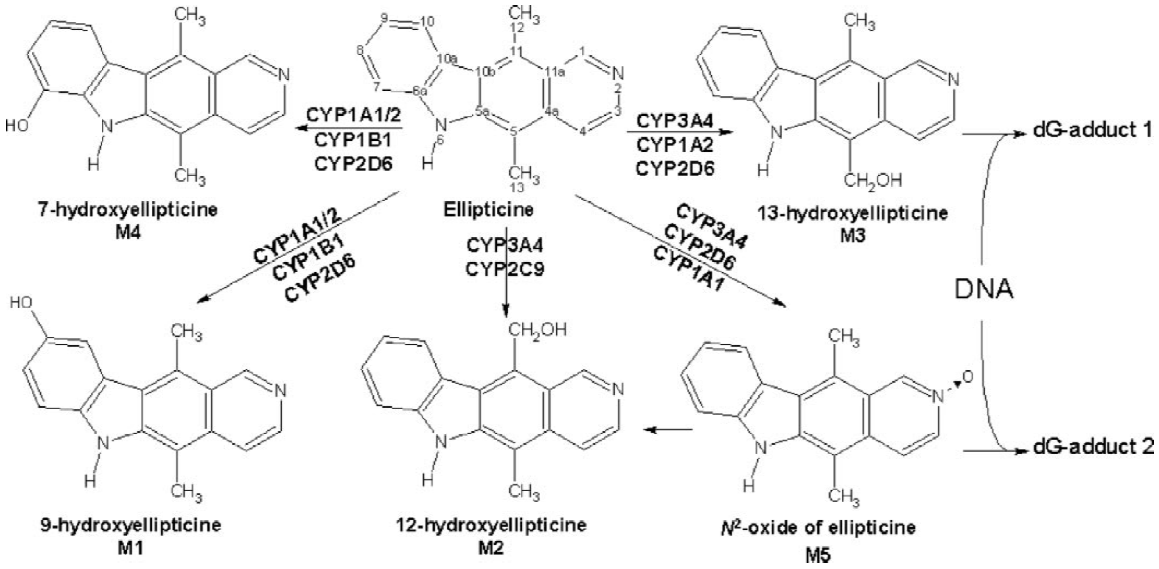

Figure 5: Scheme of ellipticine metabolism by cytochromes P450 (Stiborova et al., 2004).

Mechanisms of action of ellipticine

The mode of action of ellipticine is considered to be based mainly on:

- **DNA intercalation** caused by weak reversible hydrophobic interactions with DNA bases. Interaction of the methyl of ellipticine and the thymine in DNA is crucial to the ellipticine molecule's orientation at the intercalation site (Ashby et al., 1980, Bertrand and Giacomoni, 1985);
- **Inhibition of topoisomerase II**: ellipticines interact with DNA or topoisomerase II and form an inactive ternary complex. Thus, they stimulate double-strand breaks in DNA molecules and subsequent cell death (Froelich-Ammon et al., 1995, Stiborova et al., 2001);
- **Covalent DNA adducts formation** after enzymatic activation by CYPs ellipticine forms two major covalent DNA adducts through its metabolism to 13-hydroxyellipticine and 12-hydroxyellipticine. The latter one is formed by ellipticine oxidation by CYPs or spontaneously from ellipticine N^2-oxide (Stiborova et al. , 2001,

Stiborova et al., 2007a, Stiborova et al., 2007b, Stiborova et al., 2006, Stiborova et al. , 2004) [**Figure 6**];

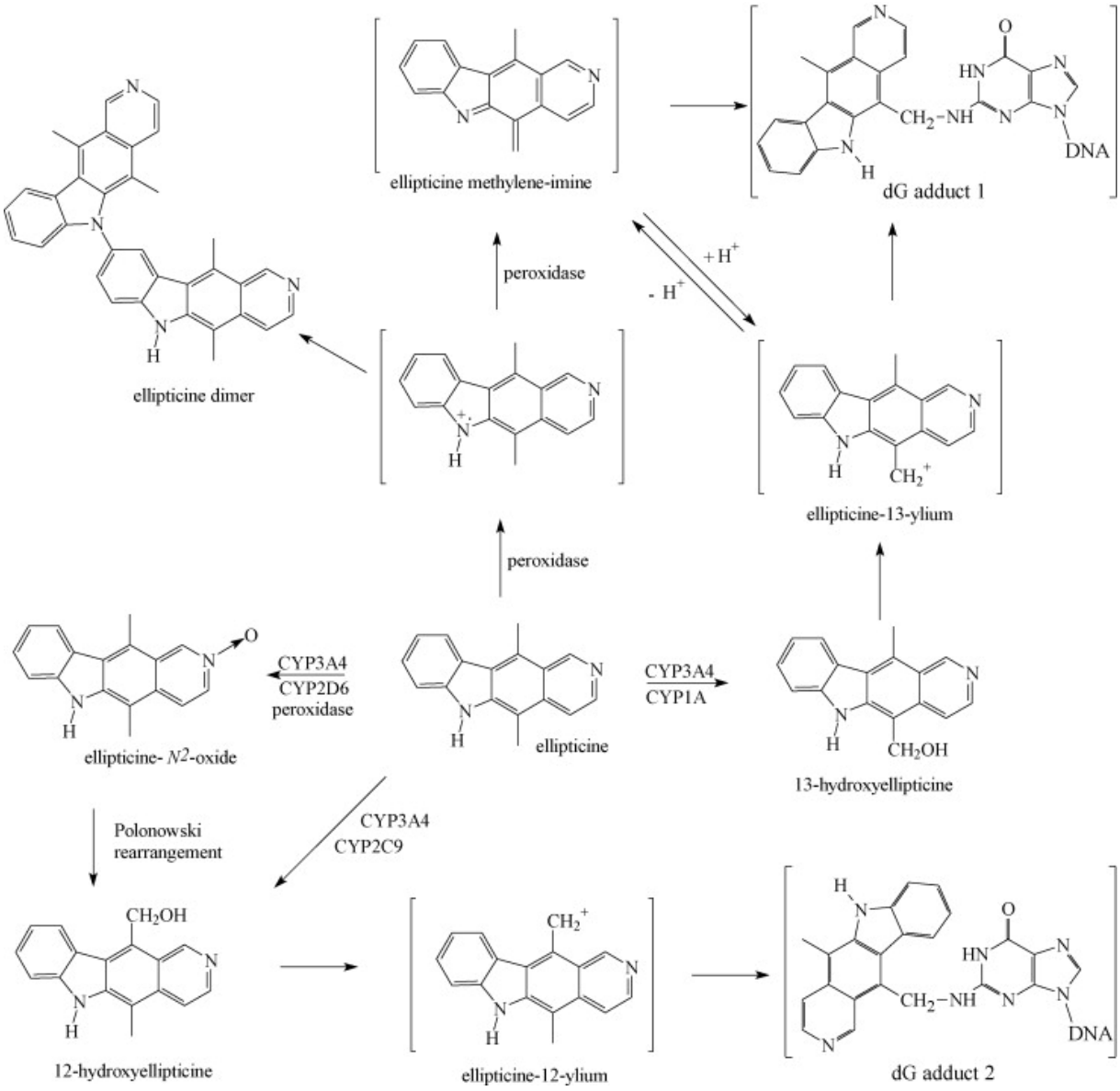

Figure 6: Scheme of ellipticine activation prior to covalent DNA adduct formation (Stiborova et al., 2008).

Other minor mechanisms of action are as follows:

§ **Selective inhibition of p53 phosphorylation:** protein p53 (product of the tumour suppressor gene *p53*) is present at very low concentrations in undamaged cells. DNA damage activates protein kinases that phosphorylate p53. This leads to a decrease in its degradation, resulting in the induction of apoptosis, which is the physiological function of p53. Mutations of the *p53* gene occur in at least half of all human cancers.

Ellipticines seem to be able to regenerate its physiological function probably via inhibition of a specific cyclin-dependent kinase (Ohashi et al., 1995, Sugikawa et al., 1999a, Sugikawa et al., 1999b).

- **Inhibition of oxidative phosphorylation,** which results in a lethal decrease of ATP concentration (Faddeeva and Beliaeva, 1997, Schwaller et al., 1995).
- **Inhibition of telomerase:** telomerase is a ribonucleoprotein enzyme that elongates and/or maintains telomeric DNA. It has been recognized as a potent diagnostic marker in a variety of human cancers because of its prevalence in most tumor cells (Sato et al., 1998).

Except the covalent DNA adduct formation most of the above mentioned mechanisms of antitumour activity of ellipticine are based on unspecific action. No discrimination between healthy tissues and tumour cells in ellipticine uptake is to be expected because ellipticines are highly hydrophobic and enter cell membranes by diffusion (Stiborova et al. , 2001). This fact contrasts with relatively specific antitumour activity of ellipticine against individual types of tumours. A cancer-specific cell-kill is known to be caused by several anticancer drugs, which are almost inactive until metabolised. Thereby, CYP/peroxidase-dependent formation of covalent DNA adducts could, at least partially, explain the antitumour specificity as well as the high efficiency of ellipticine. CYP isoenzymes known to be expressed in higher levels in tumours sensitive to ellipticine (*i.e.* breast cancer, renal cell cancer) than in peritumoral tissues, namely CYP3A4, CYP1A1 and CYP1B1 (Frei et al., 2002), are highly efficient in activating ellipticine to form covalent adducts *in vitro.* Hence, ellipticine is considered to act also as a pro-drug, whose pharmacological efficiency and/or genotoxic side effects are dependent on its enzymatic activation in target tissues (Stiborova et al. , 2004). There are significant inter-individual differences during the therapy with ellipticine, which is in accordance with different enzymatic equipment of human individuals.

2. Enzymatic systems biotransformating xenobiotics

Metabolic transformation of xenobiotics entering the organism is partially dependent on their solubility in water or fats. Lipophilic substances pass through membranes and can therefore cumulate in the organism. They cannot be eliminated directly, but they have to be transformed to more polar substances first. These more hydrophilic substances might be either non-toxic (biologically inert) or biologically active, depending on the structure of the xenobiotic and on

the enzymatic system transforming that substance. Hence, in spite of detoxification, metabolic activation may also occur. Numerous drugs require such metabolic activation. On the other hand, 98% of genotoxic carcinogens (those generating covalent adducts) are metabolically activated, too.

Biotransformation of xenobiotics is different in different species. Integrity and direction of biotransformation of the xenobiotic are important for defining the toxic level of the substance for individual organisms.

In animals, biotransformation of xenobiotics is a biphasic process. In the first phase, the derivatization phase, oxidative and reductive reactions occur to increase the polarity of a lipophilic xenobiotic. Hydrolytic reactions may also be applied to increase the hydrophilicity of some substances (***e.g.*** esters). In the second phase, the conjugation phase, these more polar molecules are conjugated with endogenous compounds (***e.g.*** glucuronic acid, glutathione, active sulphate, cysteine, acetate glycine, taurine).

Phase I of biotransformation

To increase the polarity of a xenobiotic, polar groups are introduced into the molecule or those already present are "demasked". The oxidative pathways of biotransformation are the most common ones (C-hydroxylation, N-hydroxylation, N-oxidation, S-oxidation, dealkylation, deamination, epoxidation, oxidation of alcohol and aldehydes, etc.); other reactions are hydrolytic (hydrolysis of esters and amides) or reductive (nitro- and azo-reductions). For example, aristolochic acids and 2-nitroanisole are carcinogens, which are activated by reductive mechanisms.

Enzymes catalysing the phase I reactions of xenobiotics are those located in the microsomal fraction (subcellular system formed from the endoplasmic reticulum during the homogenization), and in cytosol (cytoplasm diluted in an isolation buffer). A system of mixed function oxidases (MFO system) plays a crucial role in this phase of biotransformation. It catalyses most of the oxidative reactions. Other enzymes include flavin-containing monooxygenases (Ziegler's enzyme) (Ziegler, 2002), DT-diaphorase (Colucci et al., 2008), heme peroxidases (Ullrich and Hofrichter, 2007), alcohol- and aldehyde-dehydrogenases, and reductases (cytosolic xanthineoxidase) (Fang et al., 2007).

Phase II of biotransformation

Small hydrophilic endogenous molecules are bound to the functional groups created during the phase I. This results in further increase in the polarity of the xenobiotic and, therefore, its elimination from the organism is facilitated. Afterwards, it is usually excreted by urine or bile.

O- and N-glucuronosides are the most common conjugates excreted by urine. The conjugation of a derivatized xenobiotic with glucuronic acid is catalysed by an enzyme assignated as UDP-glucuronosyltransferase.

Glutathione-S-transferase is considered to play an important role in anti-carcinogenic processes, because it is able to bind reactive metabolites, especially epoxides, and catalyse their linkage to glutathione. In kidney, γ-glutamyl is split off; glycyl is split off in liver; cysteyl is then acetylated to form mercapturic acid, which is excreted by urine. Sometimes, xenobiotics form conjugates directly with cysteine. Hence, glutathione and cysteine are also considered as scavengers of xenobiotics.

The conjugates of phenolic substances with sulphate and those of carboxylic acids with glycine or taurine are usually excreted by faeces. Products of endogenous steroid compounds biodegradation (*i.e.* cholic acid) are excreted in the same way.

In the phase II of biotransformation, xenobiotics may also be converted into more toxic substances. For example, the conjugates of N-hydroxylated compounds, formed from aromatic amines, and active sulphate (PAPS = 2´-phosphoadenosine-5´-phosphosulphate) by sulphotransferases. Such conjugates are not stable in acidic conditions (*i.e.* urine) and form nitrene and/or carbenium ions. Such electrophiles then react with DNA and proteins.

Most enzymes of the phase I of biotransformation are inducible by carcinogens. This is also the case of the phase II enzymes, but these are inducible to a lower extent. Therefore, a certain imbalance between the rate of formation of reactive intermediates and the rate of their conjugation can be expected. On the other hand, there are also substances and complex factors (natural substances in vegetable diet), which predominantly induce enzymes of the phase II of biotransformation. It is obvious, that these factors are of extreme protective importance.

Mixed function oxidases system (MFO system)

Monooxygenation is on e of the most frequent reactions of phase I metabolism of xenobiotic molecules. The MFO system is composed of enzymes catalysing the monooxygenation (cytochromes P450 or CYPs) and enzyme which provides the reducing equivalents (NADPH:cytochrome P450 reductase) (Ertl and Winston, 1998). A membrane of endoplasmic reticulum or mitochondria is the third (and essential) part of the system. Membrane lipids, such as phosphatidylcholine, might cause conformational changes in the CYP structure to increase their affinity to the substrate. They also accumulate the substrates of CYPs, and stimulate the formation of the *cytochrome P450 - NADPH:CYP reductase* complex, which is essential for the CYP activity. The MFO system may also contain NADH:cytochrome b_5 reductase (EC 1.6.2.2) and/or cytochrome b_5, which may participate in a reaction cycle of these systems.

The MFO system is located either on the cytosolic side of smooth or rough endoplasmic reticulum (for example in organs highly exposed to xenobiotics - liver, kidney, lung, gastrointestinal tract, skin, brain, where it participates in phase I of biotransformation); or in the mitochondrial membrane (for example in adrenal cortex where it participates the metabolism of endogenous compounds - steroids, fatty acids).

Cytochrome P450 (EC 1.14.14.1)

The cytochrome P450 (CYP) is a multi-gene superfamily of constitutive and inducible heme-containing oxidative enzymes, which play an important role in the metabolism of a diverse range of xenobiotics (Gonzalez and Gelboin, 1994, Murray, 2000, Nelson et al., 1996, Wrighton and Stevens, 1992). These enzymes are also considered to play a central role in tumour development and progression and are also involved in tumor initiation and promotion, since they can activate or deactivate most carcinogens. Furthermore, CYPs can influence the response of tumor cells to anti-cancer drugs by metabolizing these drugs, both in normal tissues and in tumor cells (Kivisto et al., 1995, Murray, 2000).

The primary role of cytochromes P450 is the detoxification of a wide variety of chemicals. These enzymes play an important role in metabolism of xenobiotics; most of drugs,

environmental chemicals and carcinogens. Apart from the oxidative transformation of xenobiotics, cytochromes P450 are responsible for the oxidative phases of biosynthesis or biodegradation of several endogenous compounds – steroids, fatty acids or prostaglandins (Mansuy, 1998, Plewka et al., 2000).

Structurally, the CYP proteins consist of several domains: a hydrophobic N-terminal domain, which acts as a membrane anchor; a substrate-binding site; an oxygen-binding site; and a free hydrophilic C-terminal domain (Murray, 2000). Differential processing of the N-terminal peptide results in targeting of the CYP to either endoplasmic reticulum or mitochondria (Addya et al., 1997, Anandatheerthavarada et al., 1997). Cytochromes P450 contain a single heme b prosthetic group. The distal axial ligand of the heme iron is formed by a conserved cysteine residue belonging to the active site of the enzyme molecule. This thiolate anion determines the cytochrome P450 unusual properties. Since the heme is bound to cysteine via a coordination-covalent bond, CYP cannot be regarded as a real cytochrome; it would be more correct to assign it as a heme-thiolate protein. It usually forms clusters of a molecular weight of 500 kDa embedded in the membrane deeply.

Cytochromes P450 exist in two spin forms due to the transient character of the heme iron:

- High-spin form – the iron ion is pentacoordinated, all its valence electrons are unpaired (spin 5/2). This form exhibits an absorption maximum at 390 nm. The iron atom is placed upon the protoporphyrin IX ring plane.
- Low-spin form – the iron ion is hexacoordinated (spin 1/2); the sixth ligand may be, for example, an –OH, -COOH or –NH2 group of an amino acid from the apoprotein or an oxygen atom from a water molecule. The low-spin form exhibits an absorption maximum at 418 nm and the iron atom is placed inside the ring plane.

Both spin forms are balanced in the resting state. Binding of substrates in a protein site close to the heme generally shifts the equilibrium between the two forms towards the pentacoordinated complex, since the sixth ligand is forced out by the substrate molecule. The absorption increases at 390 nm and decreases at 418 nm – a so-called substrate spectrum is observed.

The substrate itself (or another substance not transformed by the enzyme) may become the sixth ligand of the iron ion. In this case, the absorption at 390 nm decreases and the

absorption maximum in the range of 418 - 460 nm (depending on the heteroatom) develops a so-called ligand spectrum.

Functionally, cytochrome P450 is the terminal oxidase in the system of mixed function oxidases that binds molecular oxygen and after its activation stereospecifically incorporates one atom of this molecular oxygen into the substrate. The second oxygen atom is reduced to form water. Cytochromes P450 catalyze many types of reactions besides oxidation of substrates also peroxidation and reduction. The typical reaction of the MFO system is the monooxygenation using NADPH as a cofactor (Murray, 2000). To these monooxygenation reactions belong C- and N-hydroxylation, epoxidation, N- and O-dealkylation, N- and S-oxidation and dehalogenation.

Cytochromes P450 also exhibit peroxidase activity if the second substrate is represented by an organic peroxide (or H_2O_2) instead of oxygen. For this type of reaction NADPH is not necessary as an electron donor. The product of the reaction is the same as in the case of the typical reaction mechanism – a hydroxylated substrate.

Cytochrome P450 enzyme families and subfamilies

The group of cytochromes P450 is one of the largest known mammalian gene families (over 1,000 genes). The CYPs are classified into families, sub-families and individual enzymes based on amino acid sequence homology (Nelson et al. , 1996). CYP family is marked with a number after the abbreviation "CYP": *e.g.* CYP**3**; CYPs from one family exhibit at least 40% sequence homology. After the number of a family, there is a letter representing the subfamily (at least 60% sequence homology): *e.g.* CYP3**A**. Afterwards, the number of an individual CYP enzyme follows, *e.g.* CYP3A**4**. Current CYP nomenclature has been introduced by Nebert and co-workers in 1996 (Nebert et al., 1996). Since the number of known CYPs and *CYP* genes continues to grow, there has been established an official website applied to the standardized CYP nomenclature, where newly discovered CYP forms are continuously added.

There are two broad groups of mammalian cytochromes P450 (57 known *CYP* genes and 58 pseudogenes in humans (Nelson et al. , 1996): a large group whose primary role is the

metabolism of xenobiotics (CYP1, CYP2, CYP3, and to a lesser extent CYP4), and much smaller group of CYPs which are constitutively expressed in endocrine glands, where they are specifically involved in steroid hormone synthesis (CYP11, CYP17, CYP19 and CYP21) (Murray, 2000).

There are great inter-individual differences among the activities of individual forms of cytochrome P450 caused predominantly by the two following factors:

- Genetic polymorphism (changes in genotype). Intrinsic changes in the DNA can result in the absence of some CYP forms, in the alteration of CYP inducibility or a CYP form with altered catalytic activity (Guengerich and Shimada, 1998).
- Changes in gene expression (changes in phenotype). The regulation of CYPs is complex and involves both transcriptional and post-transcriptional mechanisms (Morgan et al., 1998). The CYPs that are constitutively expressed are predominantly regulated by basal transcription factors, while other CYPs, which show inducible expression, are regulated by ligand-activated receptor-mediated mechanisms. Many of the receptor ligands are also substrates for CYPs. Post-trascriptional mechanisms include mRNA stabilization and protein stabilization (Murray, 2000).

CYP1A subfamily

Cytochromes P450 1A1 and 1A2 are the most important CYP enzymes involved in activation of procarcinogens. They can activate almost 90% of known carcinogens (Rendic and Di Carlo, 1997), especially chemicals of cigarette smoke. Both enzymes are very similar: they exhibit more than 70% homology in their amino acid sequences and they catalyse similar reactions (Guengerich and Shimada, 1991). Nevertheless, they differ in organ localization. CYP1A1 is present mainly in lung, GIT, kidney, placenta and skin. It is also expressed in human liver, but in much lower levels (<0.7% of the total hepatic CYP content) (Stiborova et al., 2002). CYP1A1 expression can be induced even 100-times by several compounds, *e.g.* TCDD, benzo[a]pyrene, 3-methylcholanthren, 5,6-benzoflavone or smoking. The major substrates of CYP1A1 are large planar molecules like polycyclic aromatic hydrocarbons (PAHs). It was shown that the genetic polymorphism of CYP1A1 might influence the development of tumours in lung, breast and skin (Guengerich and Shimada, 1991).

CYP1B1

Cytochrome P450 1B1 metabolizes many potential carcinogens and mutagens and is dioxin-inducible. It exhibits 40% homology to CYP1A subfamily. It has been reported to be expressed in astrocytic tumors but not in healthy brain tissue (Murray et al., 1997).

CYP3A4

CYP3A4 is the most abundant CYP enzyme in human liver (about 30% of total hepatic CYP content), and is also present in many other organs. Furthermore, it can be induced more than 30-times by barbiturates, erythromycin and rifampicin. Its substrate specificity is very wide. CYP3A4 metabolises carcinogenic xenobiotics as aflatoxins, PAHs or aromatic amines, as well as endogenous steroid compounds such as 17ß-estradiol, testosterone, progesterone and cortisol.

NADPH:cytochrome P450 oxidoreductase (EC 1.6.2.4)

NADPH:cytochrome P450 oxidoreductase (NADPH:CYP reductase) is a membrane protein which catalyses the electron transfer from NADPH to all known forms of CYPs (Schacter et al., 1972), to cytochrome c, cytochrome b_5, heme oxygenase, ferricyanide, etc. It is termed a "yellow protein" and is an unusual flavoprotein in that it contains both FMN and FAD.

Structurally, NADPH:CYP reductase consists of two functional domains: a hydrophobic N-terminal domain (6 kDa), which acts as a membrane anchor, and a hydrophilic C-terminal domain (72 kDa). A pancreatic protease trypsin is able to solubilize the C-terminal domain, which stays partially functional - it is able to transfer the electrons to cytochrome c and some other artificial electron acceptors, but it is no more capable to reduce cytochrome P450. The FAD-binding domain, which is a part of this functional C-terminus, is crucial for the non-covalent binding of the NADPH molecule. The FMN-binding domain is responsible for the electron transfer to the acceptor molecule – ***e.g.*** cytochrome P450.

The interactions between NADPH:CYP reductase and cytochrome P450 are predominantly electrostatic: the positively charged surface of CYP (lysines, arginines) interacts with the negatively charged surface of the NADPH:CYP reductase (aspartates, glutamates). In the surrounding of membrane domains, hydrophobic interactions among non-polar amino acids also play important roles.

Since the NADPH:CYP reductase contains two prosthetic groups (FAD and FMN) with different redox potentials, it acts as an electron pair divider. The FAD prosthetic group accepts the electrons (hydrogen atoms) from NADPH, which then transfers these to FMN. Finally, the reduced hydroquinone $FMNH_2$ reduces the CYP molecule.

The NADPH:CYP reductase activity is regulated hormonally, namely by triiodothyronine (T_3), which is a thyroid gland hormone.

Cytochrome b_5

Cytochrome b_5 is a small, cylindrical membrane protein (15 kDa) localized on the cytosolic side of a membrane of endoplasmic reticulum. It contains one or two heme *b* molecules. It participates in the electron transfer in a number of diverse reactions included in metabolism of, for example, lipids, steroids or xenobiotics.
Cytochrome b_5 consists of 6 α-helixes and 5 β-sheets. Its hydrophobic C-terminal domain acts as a membrane anchor, and its hydrophilic N-terminal domain contains the heme(s) molecule(s). The heme iron is coordinated by the side chains of two histidines (His[68] and His[44]). Mammalian cytochrome b_5 contains approximately 16% of negatively charged amino acids (aspartates, glutamates) in the catalytic domain. These amino acids participate in ionic interactions of cytochrome b_5 with other electron transporters and other proteins.

Since both the fifth and the sixth coordination positions of iron are occupied by the histidines, direct interaction of cytochrome b_5 with oxygen is not possible. Nevertheless, cytochrome b_5 may act as an intermediate electron transporter between reductase and CYP. For example, it is able to accept an electron from NADH:cytochrome b_5 reductase and deliver it to the cytochrome P450.

Cytochrome b_5 is also considered to stimulate many reactions catalysed by cytochromes P450 as it is another heme protein of the microsomal membrane. This fact is being explained by two interpretations: it directly transfers an electron to the CYP, or it mediates some conformational changes of the CYP.

3. Targeted therapy in gliomas

Due to identification of specific alterations of signaling pathways in glioblastoma cells reviewed in chapter 0.1.2, anti-tumoral treatment could be directly targeted specifically onto tumor cells. Although EGFR is widely overexpressed and truncated in glioblastomas and this results in strong activation of PI3K anti-apoptotic signaling pathway, EGFR (tyrosine kinase) inhibitors (gefitinib, erlotinib) exhibit only weak efficacy. Only about 10 - 15 % patients response to such therapy. This is caused mainly by high incidence of PTEN loss (in 50 %) in GBM. PTEN is an EGFR independent PI3K inhibitor. Therefore when non-functional, PI3K pathway is constitutively activated anyway and the cell does not answer to EGFR inhibition (Mellinghoff et al., 2005). Concurrent mTOR targeting (temsirolimus, everolimus) improves erlotinib treatment outcome. Similarly, effector molecules such as Ras, PI3K or PKC may be targeted, although they are hardly ever mutated themselves in glioblastoma. Their inhibition results in blocking the signal transfer from altered up-stream signaling receptor molecules. Ras membrane localization is regulated by farnesyl tranferases that provides the essential lipids. Their function is blocked by specific inhibitors tipifarnib or lonafarnib (Sathornsumetee and Rich, 2008). Perifosin, an Akt inhibitor, thus targeting PI3K and mTOR, entered phase II clinical trials. In addition, enzastaurin inhibiting the PKC-activated kinase, GSK3β, seems to have a high potential for GBM treatment (Omuro, 2008, Rieger et al., 2008).

Targeting p53 tumor suppressor represents multiple therapeutic strategies as it lies on the crossroad of the main regulation pathways determining cell fate and development. Firstly, *TP53* gene is mutated in about a half of all tumors. Therefore, therapeutic strategies must be aimed either on rescuing the p53 mutant, or enhancing functional p53 activity. Apart from the gene therapy, where a functional p53 is simply introduced into the tumor cell, p53 mutants` functionality may be rescued by other ways. Mutations of *TP53* gene are often temperature-sensitive and have only subtle effects on the stability of the DNA-binding domain of the p53 protein (Lane and Lain, 2002). In these cases, small molecules favorizing the correct p53 folding could reactivate the mutated p53 and thus reinduce the p53 response (Foster et al., 1999). However, such agents exhibit only low efficiencies. Peptides derived from some of well-known p53-binding proteins stabilizing the p53 protein core appear more promising in that way (Friedler et al., 2002). A particular need to rescue p53 can be evaded by mimicking its downstream genes - p21, Cdk inhibitors; or by inhibition of p53 in surrounding cells

(pifithrin-α) in combination with radio- or chemotherapy strongly inducing p53 (Komarov et al., 1999).

If p53 wildtype is expressed in the tumor cell, but the p53 signaling pathway is counteracted by some other alterations resulting from the tumoral context, its function may be enhanced either by protein stabilization, or by inhibiting p53 nuclear export (*e.g.* by Leptomycin B), which is regulating the p53 pathway (Lain et al., 1999). p53 protein stabilization could be increased by inhibiting the Mdm2 expression, or by blocking the Mdm2-p53 interaction, which is essential for p53 ubiquitinylation and subsequent degradation in proteasome. Indirect Mdm2-p53 interaction inhibitors represent those of $p14^{ARF}$, which binds to Mdm2 and thus prevents bnding of p53 (Xirodimas et al., 2001).

Table 5: An overview of anti-angiogenic therapy clinical trials in malignant glioma (modified from: (Tuettenberg et al., 2006). Clinical trials: (Baumann et al., 2004, Brandes et al., 1997, Buckner et al., 1995, Chang et al., 2004, Dillman et al., 2001, Fine et al., 2000, Fine et al., 1997, Herrlinger et al., 2005, Tuettenberg et al., 2005, Yung et al., 1991); GBM - glioblastoma multiforme, AA - anaplastic astrocytoma

Chemotherapeutic drug	No. patients	Status of disease	Median progression-free survival	Median overall survival
Thalidomide	36	Recurrent 25 GBM + 12 AA	10 weeks	28 weeks
Thalidomide + carmustine	40	Recurrent 38 GBM + 2 AA	100 days	~190 days
Thalidomide + temozolomide	67	Primary GBM	22 weeks	73 weeks
Thalidomide + temozolomide	25	Primary GBM	36 weeks	103 weeks
Interferon-α + BCNU	35	Recurrent glioma of any grade	9.9 months	13.3 months
Interferon-α + BCNU	21	Recurrent 12 GBM + 9 AA	4.5 months	7 months
Interferon-β	16	Recurrent 8 GBM + 8 AA	36 days	86 days
Interferon-α + 13-*cis*-retinoic acid + concurrent radiotherapy	40	Primary 36 GBM + 4 AA	n.g.	9.3 months
Interferon-β	65	Recurrent 41 GBM + 24 AA	23 weeks	n.g.
Low-dose temozolomide + COX-II inhibitor	13	Primary GBM	8 months	16 months
Metronomic methotrexate + cyclophosphamide	10	Recurrent GBM	2.5 months	6.9 months

Another therapeutic approach represents an anti-angiogenic therapy, as tumoral neovessels are essential to ensure oxygen as well as supply ofnutrients. Angiogenesis inhibitors include molecules targeted principally against VEGF (anti-VEGF antibody bevacizumab, Avastin®; thalidomide), PDGFR (imatinib, Gleevec®), FGF (interferon-β, thalidomide), HGF/SF (NK4), integrins (cilengitide against integrin $\alpha_v\beta_3$).

Although these agents are utilized specifically against tumor cells, the monotherapy remains usually not sufficient. Combinations of chemotherapy or radiotherapy with such targeted therapies tend to be used more and more commonly (**Table 5**).

4. Integrins

Integrins are transmembrane heterodimeric glycoproteins belonging to the cell adhesion molecule (CAM) superfamily, next to cadherins, selectins and immunoglobulin-cell adhesion family. They mediate dynamic interactions between cell and the extracellular matrix or another cell. Integrins anchor the cell physically to its microenvironment as well as act as signal transducers to and from the cell.

Binding integrin to its ligands is crucial for many physiological/pathophysiological processes such as cell attachment, differentiation, proliferation, migration, angiogenesis, embryogenesis, blood coagulation, tumoral metastasis, neoplasia, and immune dysfunctions (reviewed in (Hynes, 1992), which predestinate them as potential therapeutic targets for multiple pathologies including cancer.

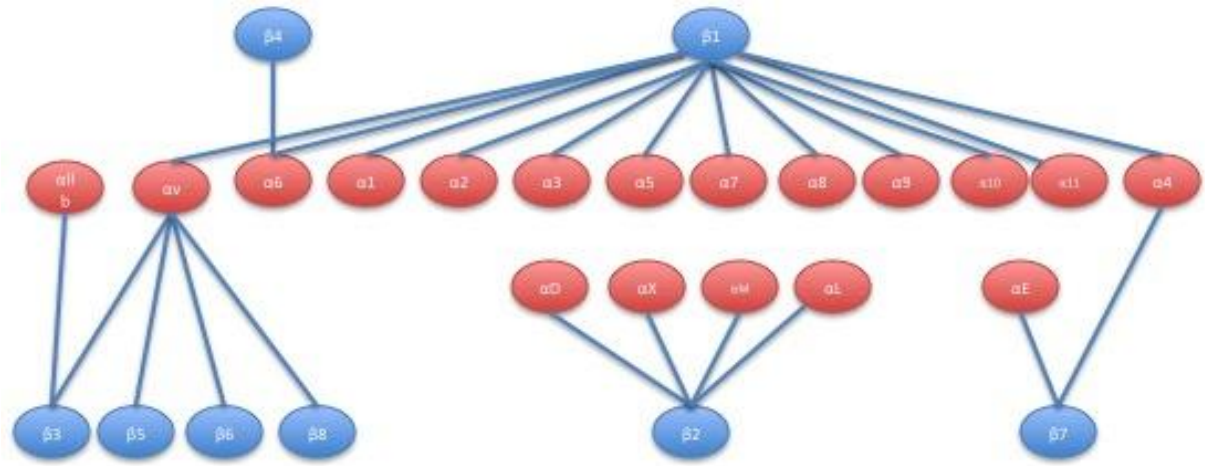

Figure 7: Various heterodimeric combinations of α and β integrin subunits representing ligand interactions.

Integrin heterodimers consist of one α and one β subunit that are bound by non-covalent interactions. Up to date, 24 α and 9 β subunits (including 6 novel α and 1 novel β subunit) have been identified. Various heterodimeric combinations are demonstrated in **Figure 7** and **Table 6**, which includes also their appropriate ligands. Although some subunits appear only in a single heterodimer, twelve integrin dimers contain β1 subunit and five five contain the αv subunit.

Each of the subunits has a large extracellular domain containing 700 - 1,000 amino acid residues, a single transmembrane domain, and a short cytoplasmic domain of 20 - 70 amino acid residues. The β4 subunit represents a sort of exception with its extra large cytoplasmic

domain (Lu et al., 2008). For schematic integrin dimer structure see FIG 9. The main inter-subunit interface lies within the head (N-terminal regions), between a seven-bladed β-propeller of the α-subunit and an A domain of the β-subunit. It exhibits a remarkable resemblance to the α-β interface in G proteins (Xiong et al., 2001). The remaining halves of the subunits form rod-shaped tails that span the plasma membrane.

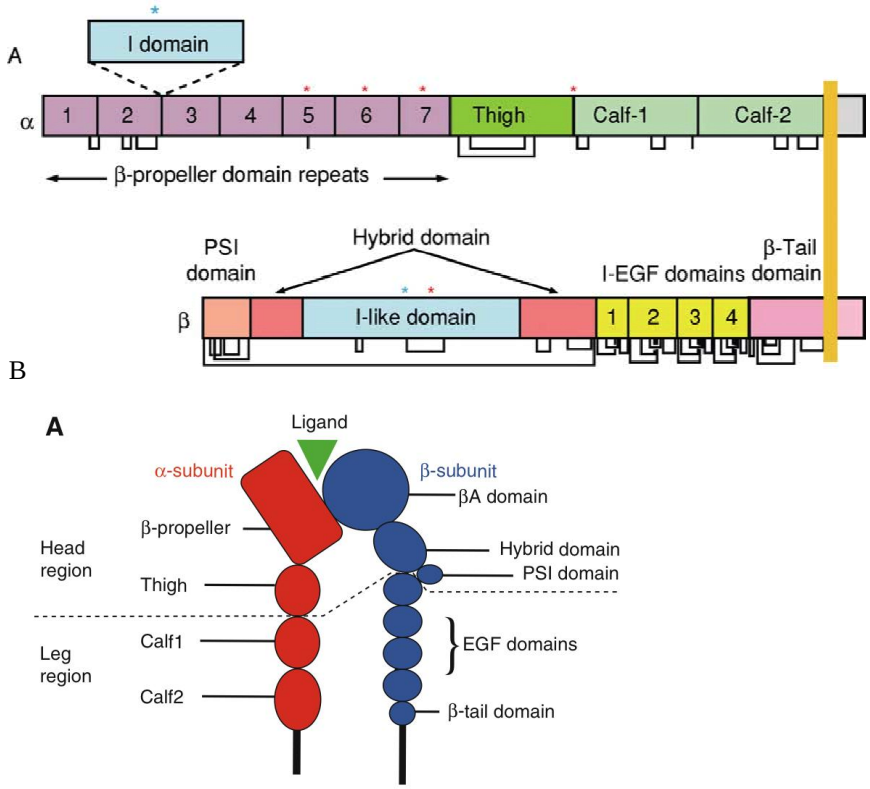

Figure 8: A. Integrin architecture. Organization of domains within the primary structure. Some α subunits contain an I domain inserted in the position denoted by the dotted lines. Cysteines and disulfide bonds are shown as lines below the stick figures. Red and blue asterisks denote Ca2+ and Mg2+ binding sites, respectively. (Adopted from: (Springer and Wang, 2004); B. Schematic integrin structure. (Adopted from: (Askari et al., 2009).

The α subunit

The α subunit is formed by 7 segments, each of about 60 amino acids. These segments forming N-terminal region of the integrin subunit are supposed to be folded to a seven-bladed β-propeller domain (Springer, 1997). The α subunits can be divided into two subgroups based on important structural differences: 1) those containing an I-domain (an inserted domain; a von Willebrand factor A domain) situated between the second and third β-sheet of the β-propeller; and 2) those not-containing the I-domain (e.g. α5β1). The I-domain in the first group of integrins harbors major ligand-binding sites including MIDAS (metal ion -dependent

adhesion site), which binds negatively charged residues in ligands. Arising from the name, its function is dependent on bivalent metal ions. The tail is composed of β-sandwich domais, so-called "thigh" Ig-like domain and two similar domains forming the "calf" module [**Figure 8**, p 39]. Between the thigh and the calf region, integrin tail folds back forming a V-shaped structure with a genu (Xiong et al. , 2001). Such bending is supposed to be crucial for conformation changes during the switch between high- and low-affinity integrin states [**Figure 9**, p 43]. The α integrin subunit can be post-translationally cleaved into two polypeptide segments bound together by disuphide bridges (e.g. α5β1) (Hynes, 1992).

The β subunit

The head of β integrin subunit is formed by a βA domain inserted into the loop of a hybrid domain. The βA domain consists of a central six-stranded β-sheet surrounded by eight helices. At the top of the central β-strand, a MIDAS motif is placed in a small slot. Nearby, another Ca^{2+} ion binding site (ADMIDAS) is present.

The tail consists of a PSI domain, same as other membrane proteins, plexins and semaphorins (PSI from plexin, semaphorine, integrin) (Bork et al., 1999), four EGF domains and a β-tail domain.

The PSI region has about 50 residues in size and contains seven cysteines, from which the first one forms a long-distance disulphide bond to the C-terminal Cys-rich region. Cooperation of these Cys-rich regions plays a key role in preventing the integrin to shift from the high to low-affinity conformation (Zang and Springer, 2001).

The EGF-like domains are also Cys-rich and have unique structural properties enabling structural motion while signaling (Tan et al., 2001).

The β-tail domain consists of a four-stranded β-sheet and faces an N-terminus of an α-helix (Xiong et al. , 2001).

Table 6: Ligands of the integrin family. (Adopted from: (Lu et al. , 2008)

β_1		
	α_1	Colls, laminins
	α_2	Colls, laminins, chondroadherin
	α_3	Laminins (such as laminin-1, -5, -8, -10, and -11), Fn, thrombospondin, TIMP-2, uPAR, collagen, epiligrin, entactin
	α_4	Fn, VCAM
	α_5	Fn, Fg, uPAR
	α_6	Laminins, merosin (laminin α2 chain), kalinin
	α_7	Laminins, merosin (laminin α2 chain),
	α_8	Fn, vitronectin, Tn-C, osteopontin, and nephronectin
	α_9	angiostatin, Tn-C, osteopontin, and ADAMs, VCAM-1, tTG,
	α_{10}	Colls
	α_{11}	Colls
	α_V	Fn, vitronectin
β_2		
	α_L	ICAM-1, -2 and -3
	α_M	Fg, ICAMs, iC3b, factor-Xa, denatured ovalbumin
	α_X	Fg, iC3b
	α_D	VCAM, ICAMs
β_3		
	α_{IIb}	Coll, Fn, vitronectin, Fg, vWF, thrombospondin
	α_V	Fn, vitronectin, Fg, vWf, thrombospondin, FGF-2, MMP-2 and some ADAM proteins
β_4		
	α_6	Laminins
β_5		
	α_V	Vitronectin, uPAR
β_6		
	α_V	Fn, Tn
β_7		
	α_4	Fn, VCAM, MAdCAM
	α_E	E-cadherin
	α_V	Colls, laminins, Fn
β_N		
	α_V	Fn, Colls
β_8		
	α_V	Vitronectin, Fn

Integrin ligands

A characteristic feature of most integrins is their ability to bind a wide variety of ligands and ECM proteins bind to multiple integrins. According to the ligand specificity, integrins can be

classed into four groups: RDG-recognizing integrins (αv integrins, α5β1, α8β1...), collagen-binding integrins (α10β1, α1β1, α2β1...), laminin-binding integrins (α3β1, α3β1, α6β1...) and leucocyte integrins (β2 integrins).

Structurally, RDG-recognizing integrins bind to RDG tripeptide of the ligand, which interacts with an interface between the α and β subunits. The **R** residue fits to the β-propeller module of the α subunit, whereas the **D** residue coordinates a cation bound to the I-domain of the β subunit. The β2 integrin subfamily and some other integrins recognize an acidic LDV motif that is functionally related to RGD. A-domain containing β1 integrins (α1, α2, α10 and α11) form a collagen/laminin binding integrin subfamily, where the glutamate within the collagenous GFOGER peptide provides the key cation-coordinating residue. The laminin-selective receptors (α3β1, α6β1, α7β1 and α64) that do not contain the A-domain bind to different laminin regions without targeting any particular sequence (Humphries et al., 2006). Integrin ligands are overviewed in **Table 6**.

Integrin conformations

Integrin conformations and their linkage to integrin functionality are still being a subject of extensive studies. In the current model, which is generally accepted, integrins are known to adopt three principal conformations: 1) inactive (low-affinity) bent; 2) active (high-affinity) extended; and 3) ligand binding conformation, which corresponds to an extended conformation with an opened headpiece (Takagi and Springer, 2002).

When integrin activated from inside out [**Figure 9**, A-C], the process is believed to be initiated by binding of the talin phosphotyrosine-binding (PTB) domain with the membrane-proximal region of the cytoplasmic tail of the β integrin subunit. This is a key convergence point that controls integrin inside-out activation (Askari et al. , 2009, Tadokoro et al., 2003). Such talin/β-integrin interaction then leads to the separation of the α- and β- cytoplasmic tails and transmembrane regions. This results in subsequent swinging out of the β-hybrid domain away from the α subunit resulting in pulling the α7 helix of the βA domain down and upward movement of the α1 helix (Xiao et al., 2004).

Outside-in integrin activation [**Figure 9**, D-E] upon ligand binding stabilizes an extended integrin conformation, which again leads to prolonged separation of the cytoplasmic tails of the subunits (Askari et al. , 2009, Luo and Springer, 2006). Binding of talin and ligand initiates focal adhesion formation. As the cytoskeleton matures, tension is generated on the

integrin across the cell membrane. Such force triggers further outward movement of the β hybrid domain, strengthening integrin-ligand interaction and enabling stable focal adhesions formation and triggering signaling cascades (Askari et al. , 2009).

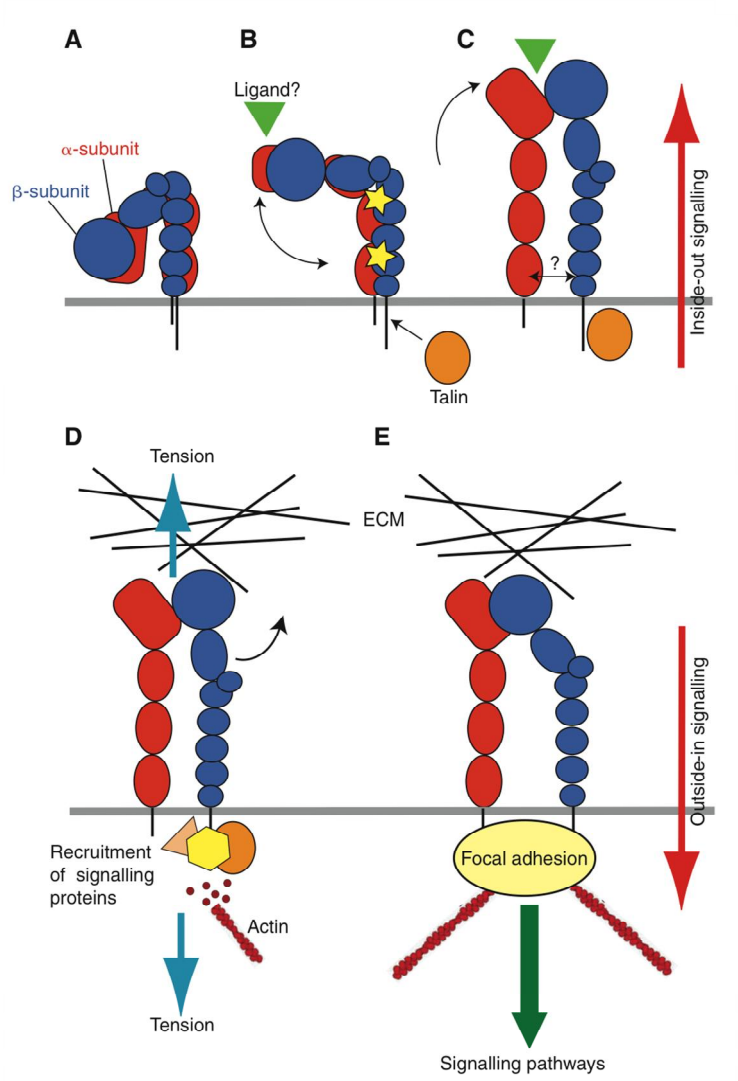

Figure 9: Model of relationships between integrin conformation and its function. (Adapted from: (Askari et al. , 2009)

The question that remains to be answered is whether the three conformations described are the only possible integrin states or if some intermediate forms are possible. Recently, number of evidences outline that the conformation changes may not be all-or-nothing functional responses and it is suggested that different agonists may induce specific shape changes that then result in multiple signaling responses. Electron microscopy images revealed integrin molecules exhibiting varying degrees of bending from 135° to 90°. When integrin is locked in the 135° angle conformation, the ligand is not able to bind to the integrin due to the binding

site inaccessibility. When integrin is in the right-angled conformation, the ligand-binding pocket may be positioned away from the cell membrane and thus accessible for the ligand even when integrin is not in a fully extended state (Beglova et al., 2002, Takagi et al., 2002).

Integrin signaling

Integrins act as important signal transducers by associating with proteins that interconnect them with cytoplasmic kinases, cytoskeleton and transmembrane receptors for growth factors. When integrins are bound to their ECM ligands, they become clustered in the membrane and form so called focal adhesions (FA) and associate with a cytoskeletal and signaling complex. This results in actin filaments reorganization, which in turn promotes integrin clustering, thus providing a positive feedback (Giancotti and Ruoslahti, 1999). Some integrins associate with a small scaffolding protein caveolin-1 that helps integrins to cluster (Bray et al., 1998). When Fyn activated through Shc by some αv and β1 integrins, caveolin-1 functions as a membrane adapter. It couples the α integrin subunit to Fyn. This is consistent with caveolin`s ability to bind cholesterol and glycosphingolipids to create membrane rafts enriched in Src kinases that carry myristoyl and palmytoyl lipid groups, including Fyn (Harder and Simons, 1997).

Integrins activate various protein kinases, among the most important ones belong focal adhesion kinase (FAK), Src kinase family, serine-threonine kinase, and integrin-linked kinase (ILK).

The FAK activation is coupled to focal adhesion formation. It is linked to the cytoplasmic tail of the β integrin subunit either directly, or via talin or paxillin (Lewis and Schwartz, 1995). Activated FAK autophosphorylates at Tyr397, creating a binding site for the SH2 domain either of Src, or of Fyn (Schlaepfer et al., 1994). The Src kinase then phosphorylates number of FA components. The FAK also activates PI3K cascade, either directly, or via Src (Giancotti and Ruoslahti, 1999). A cytoplasmic phosphatase PTEN encoded by a tumor suppressor gene dephosphorylates the PIP2 and PIP3 lipids as well as FAK and Shc, and thus counteracts integrin signaling when overexpressed (Gu et al., 1999).

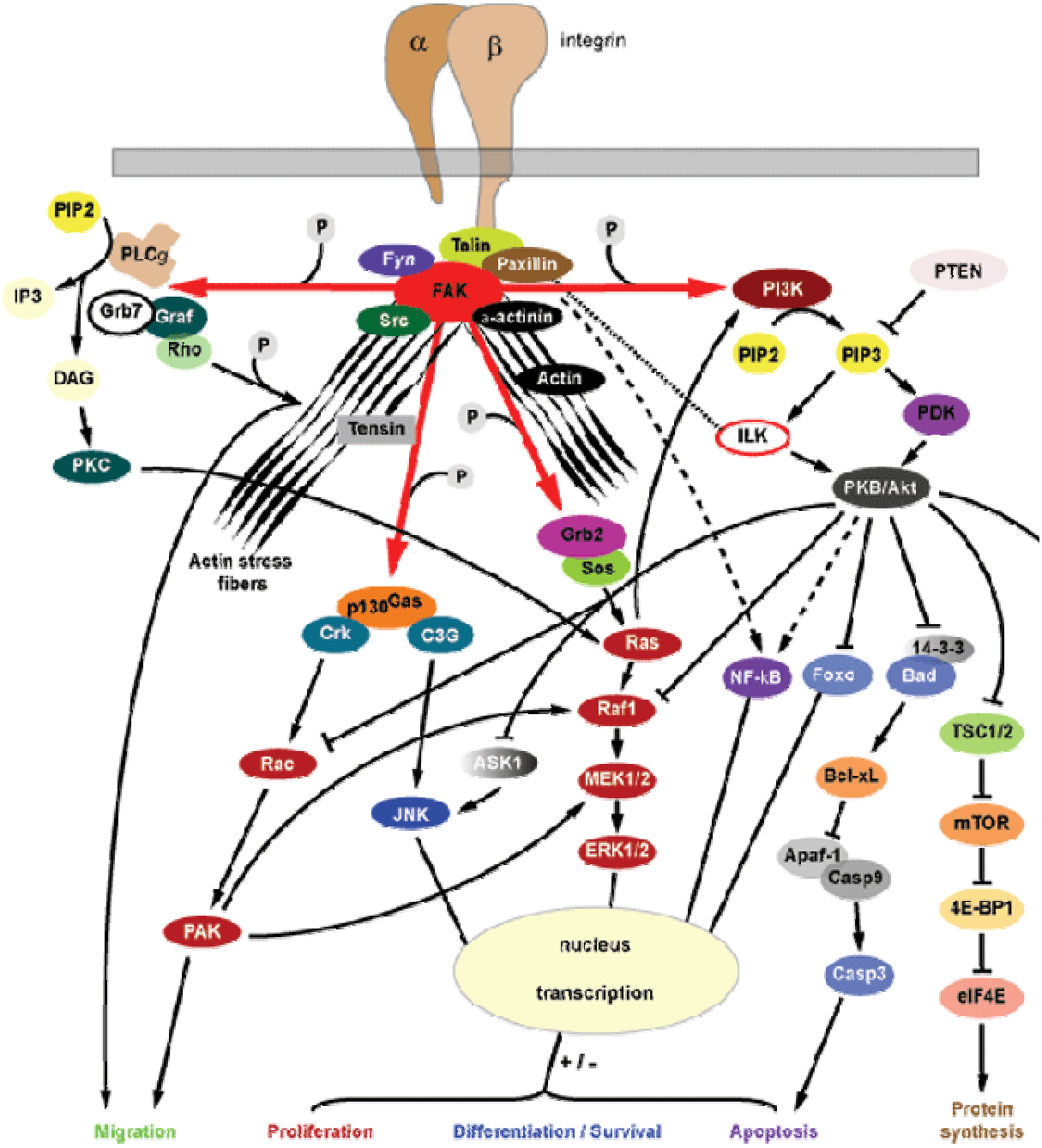

Figure 10: Overview of integrin-initiated signaling pathways. The 4 major signaling pathways activated by integrin engagement in adhesion complexes are shown. The key element in all these pathways is FAK which becomes activated through autophosphorylation at Y397 and thereby allow binding of Src and Fyn for further phosphorylation and full activation. Phosphorylation of FAK at specific sites dictates its subsequent interactions with other proteins (i.e. Grb2, p130Cas, PI3K, Graf) which in turn elicit a cascade of events that lead to cell proliferation, migration or survival. FAK can also be activated by cell surface receptors for growth factors, hormones and chemokines. Plain lines, direct activation or inhibition; dashed line, indirect functional interaction; red lines, FAK-mediated events mediated by specific phosphorylation events. (Adopted from http://www2.unil.ch/cepo_research/introduction.html; cached 17.12.2009)

During mitosis, FAK becomes phosphorylated on Serine and dissociates from Src and $p130^{CAS}$, which results in loss of cell substrate contact and allows the cell to divide and move (Yamakita et al., 1999).

In many cell types, proliferation is likely to require co-stimulation of growth factor receptors, and of the MAPK/ERK pathway via integrins. The ERK activation occurs when Shc-linked integrins bind to the ECM. In contrast, integrins that do not activate Shc are weak ERK activators (Pozzi et al., 1998). In some cells, ERK-Ras signaling is blocked when cell is not attached. If cell is linked to the ECM, integrins remove this block by activation Rac or PI3K and thus enable cell proliferation (Frost et al., 1997).

Moreover, cell attachment via integrins is essential for appropriate activation of growth factor receptors by their ligands PDGF (platelet-derived growth factor), EGF (epidermal growth factor) and VEGF (vascular endothelial growth factor). Integrin clustering and association with the cytoskeleton appear to give rise to integrin-growth factor complexes (Miyamoto et al., 1996).

Furthermore, integrins activate the MAPK c-Jun NH2 kinase (JNK), which regulates progression through the G1 cell cycle phase, via association of FAK with Src and $p130^{CAS}$. Generally, cell cycle progression is regulated by cyclin-dependent kinases. The activation of some of them (Cdk4/6, Cdk2) is mediated by integrins upon cell attachment to ECM (Giancotti and Ruoslahti, 1999). Moreover, anchorage to the ECM is essential for p27 and p21 inhibition, both inhibitors of Cdk2.

On the contrary, cell attachment by integrins also facilitates exit from the cell cycle and provides signal for subsequent differentiation. However, such integrin signals are only additional, as differentiation requires both, integrin signals and soluble differentiation factors (Giancotti and Ruoslahti, 1999).

Loss of cell attachment to the ECM causes an apoptosis-like cell death called anoikis. This phenomenon contributes to tissue integrity. Again, FAK seems to play a crucial role in mediating survival signals upon cell attachment, as it binds PI3K and thus activates protein kinase B/Akt. Akt promotes survival by phosphorylating/inactivating the pro-apoptotic proteins: Bad and caspase-9 (Datta et al., 1997). The integrin $\alpha 5\beta 1$ induces expression of an

anti-apoptotic protein Bcl-2 protecting cells from apoptotic stimuli mediated by lack of growth factors (Zhang et al., 1995).

As most cells are not actively dividing after differentiation, other proteins such as cadherins override growth-promoting integrin effects. However, integrins keep the ability to promote cell survival. Such contact inhibition ensures the cell survival of differentiated cells well positioned in tissues. Tumor cells are generally resistant to anoikis and are able to proliferate even in absence of ECM anchorage (Giancotti and Ruoslahti, 1999).

The association of integrins with other transmembrane proteins provides additional coordinate signals to cells that are also specific for individual integrins (Giancotti and Ruoslahti, 1999).

Integrins in anti-cancer therapy

It has been well established that there is an association between the regulation of integrin expression and cancer. Changes in the integrin pattern during malignant transformation are highly dependent on the type of the cancer as well as on cancer stage. Integrins are involved in cell migration, invasion, intra- and extra-vasation, and platelet interactions. Therefore, their role in tumorigenesis is obvious. Malignant transformation is characterized by disruption of cytoskeletal organization, suppressed adhesion and altered adhesion-dependent processes. Thus appropriate integrin expression pattern as well as their function is crucial to maintain a normal cell phenotype.

Tumor cell entrance into vascular system during metastasis involves the loss of adhesion and a release of proteolytic enzymes digesting tissue membrane barriers through the way. The metastatic process involves making and breaking contacts with different components of the ECM, which may require alterations of integrin expression pattern (Mizejewski, 1999).

Tumor angiogenesis, the initiation and control of capillary growth, is another crucial process during tumor growth, as the solid tumoral mass requires continuous supply of oxygen and nutrients. When exceeding 1 mm^3 in size, pre-existing vessels become insufficient and tumoral neoangiogenesis is inevitable. The role of integrins in this process can be demonstrated by αvβ3 in melanoma, where differential integrin expression was found on newly formed blood vessels compared to the pre-existing ones (Danen et al., 1995,

Mizejewski, 1999). Apart from integrins, many other factors regulate this process: growth factor receptors (VEGF), adhesion molecules (cadherins), ECM components (fibronectine, collagen), proteases (MMPs), signaling molecules (Raf, MAPKs, PKA), and transcription factors (HIF, NFκB) (Guo and Giancotti, 2004). Since recently, anti-angiogenic therapy targeted against integrins has emerged interest. Historically, integrins αvβ3 and αvβ5 were the most studied ones regarding their role in angiogenesis and possible clinical exploitation. They bind to vitronectine and fibronectine, respectively, and are strongly overexpressed on tumoral neovessels. Blocking them by their antagonists results in suppressed tumor progression. Similarly, integrin α5β1 is markedly overexpressed in novel blood vessels and antagonizing it leads to the block of angiogenesis as well as of tumor growth (Serini et al., 2006).

As integrins are largely implicated in the regulation of cell cycle, survival, proliferation etc. They are obviously supposed to play a role also in the resistance of cancer cells to anti-cancer therapy. It has been proven that some integrins are able to modulate cytotoxic effects of chemotherapeutic agents *in vitro* (Hazlehurst et al., 2000, Hazlehurst et al., 2001, Lewis et al., 2002).

Hoyt et al. (1996) have shown that specific activation of α5, β1 and β3 integrins by appropriate antibodies protected cells from DNA damaged induced by etoposide, a topoisomerase II inhibitor. (Hoyt et al., 1996)

In gliomas, the αv integrin and its ligand vitronectine were proved to play an important role in tumor invasion, as margins strongly expressing this integrin were often sites responsible for recidivation. The mechanism passed through an increased Bcl/Bax ratio, independently on p53 (Uhm et al., 1999a). Similarly, β1 integrin signaling inhibits paclitaxel and vincristine induced apoptosis in breast carcinoma via increased Bcl-2 expression (Aoudjit and Vuori, 2001). In some melanomas and sarcomas, integrins repress DNA damage-induced apoptosis by modulation of p53 expression (Lewis et al. , 2002).

However, cellular response to chemotherapeutic agents depends also on cell attachment, especially in carcinomas, gliomas and some hematopoietic cell types. Altered adhesion abilities of tumoral cells to specific matrices may confer a *de novo* phenotype resistant to chemotherapy (Hazlehurst et al. , 2000). Therefore, integrin-mediated cell adhesion has a protective effect against drug-induced apoptosis.

Integrin αvβ3

In integrin-targeted therapy, particular emphasis has been given to αvβ3/β5 integrins, which are overexpressed in tumoral neovessels and their role in angiogenesis has been proven (Brooks et al., 1994). Primarily, αvβ3 integrin has attracted a particular interest and became a main target of anti-angiogenic therapy (Tucker, 2002).

A cyclic synthetic peptide cilengitide [**Figure 11**] (Merck KGaA, Darmstadt, Germany), an αvβ3/β5 antagonist, is currently undergoing clinical trials to target neoangiogenesis in malignant glioma (Nabors et al., 2007, Reardon et al., 2008a, Reardon et al., 2008b).

A small non-peptidic αvβ3/β5 antagonist, S247 [**Figure 11**] inhibits adhesion on vitronectine as well as vessel formation, migration and clonogenicity of endothelial cells *in vitro* (Reinmuth et al., 2003).

Similarly, a humanized monoclonal antibody LM609 against αvβ3 known as vitaxin (Scripps Research Institute, La Jolla, CA, USA) is now being tested for metastatic melanoma.

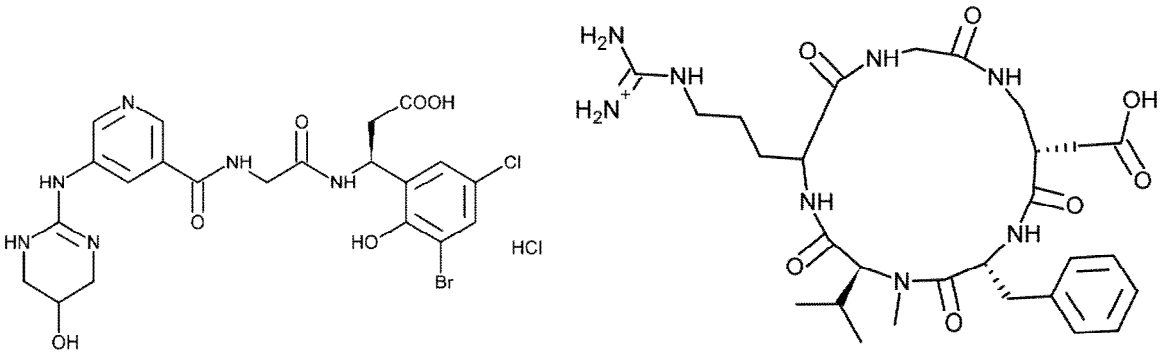

Figure 11: Structure of a non-peptidic antagonist, S247 (LEFT) and a peptidic antagonist, cilengitide (RIGHT) of the αvβ3/β5 integrin.

Integrin α5β1

More recently, integrin α5β1 has attracted a lot of interest as a potential therapeutic target for glioblastomas (Farber et al., 2008, Li et al., 2009a, Maier et al., 2007), as its expression correlates with tumor aggressiveness and invasiveness (Mattern et al., 2005, Paulus et al., 1993). In contrast, it is very poorly expressed in healthy brain tissue [**Figure 12**].

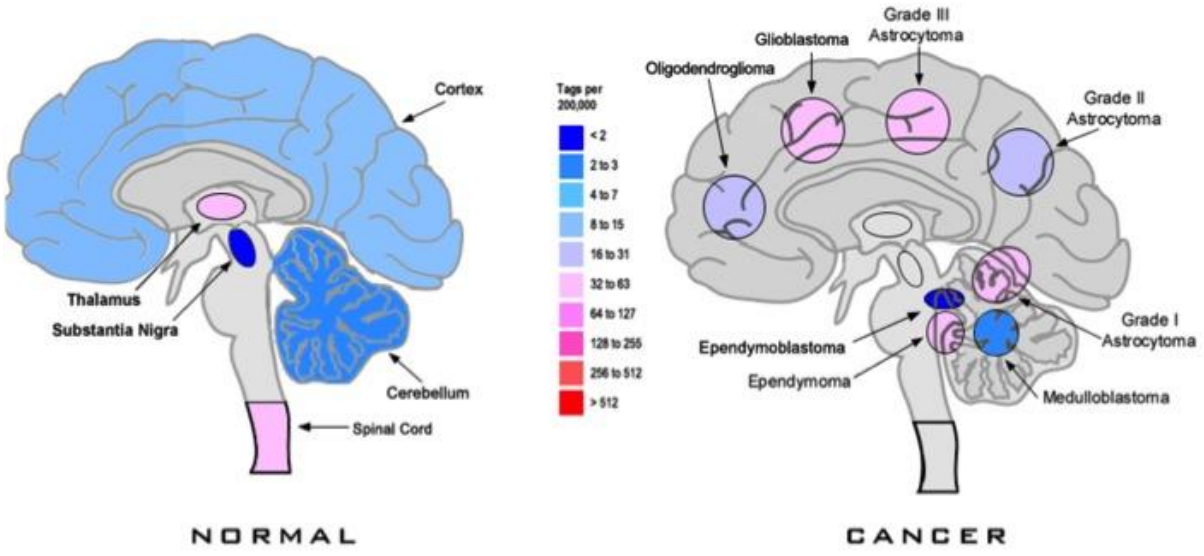

Figure 12: Expression of the α5 integrin in brain tissue and brain tumors (http://cgap.nci.nih.gov/; cached 16.12.1009)

Integrin α5β1 is primarily specific for one ECM component, fibronectin, thus is also called a fibronectin receptor. Its β1 subunit recognizes the RGD sequence and a synergy region PHSRN in fibronectin, which is responsible for its specificity (Mould et al., 1997). The α5 subunit binds exclusively to the β1.

The α5β1 integrin plays a role in angiogenesis (Alghisi and Ruegg, 2006), and is implicated in multiple signalization cascades including PI3K/Akt pathway. It is strongly overexpressed on tumoral neovessels but not in preexisting ones (Kim et al., 2000a). Its expression is regulated transcriptionally by angiogenic factors such as bFGF, IL-8 and TNF-α, but not VEGF (Boudreau and Varner, 2004, Kim et al. , 2000a). Among its other partners belong FAK, ILK or PKA.

The α5β1 integrin is also employed in processes such as migration, invasion or cell survival regulation via its interactions with caspases or Bcl-2 protein family (Stupack et al., 2001, Zhang et al. , 1995).

Antagonists of the α5β1 integrin

Integrin antagonists may be divided into three classes: antibodies, peptides and peptidomimetics, and non-peptidic molecules.

A humanized monoclonal antibody against integrin α5β1, Volociximab (M200), has entered clinical trials (Kuwada, 2007, Ricart et al., 2008). It is a humanized antibody IIA1 (PDL BioPharma) specifically recognizing the α5 integrin subunit. It has been tested *in vitro* and

found to be able to counteract angiogenesis induced by VEGF and bFGF. It has also been shown to inhibit adhesion to fibronectin, cell proliferation and invasion of ovarian cancer cells (Sawada et al., 2008).

Peptidic antagonists mimick the binding region of the ECM components recognized by the integrin of interest. In the case of the α5β1, RGD and PHSRN sequences may be targeted. The RGD mimetics are the most frequent ones, but these are very unspecific as multiple integrins recognize this motif.

A small peptide Ac-PHSCN-NH_2, ATN-161 (Attenuon LLC, San Diego, CA, USA) [**Figure 13**] is a non-competitive inhibitor of the PHSRN synergy sequence, where the arginine was substitued by cysteine to yield a product with acceptable pharmaceutical properties. It entered clinical trials phase I/II in 2003 against solid tumors (Cianfrocca et al., 2006). The ATN-161 does not block cell adhesion to fibronectin, but is supposed to inhibit integrin signaling. It has been shown that it does not bind exclusively the β1 subunit, but all β integrin subunits (Donate et al., 2008). It has been proven to bind also to αvβ3 and αvβ5 integrins. ATN-161 seems to be a promising anti-cancer agent as it has been shown to exhibit synergy with conventional chemotherapy (Stoeltzing et al., 2003).

Pramanik et al. (2008) have tested a lipopeptide RGDK, specific to α5β1 due to the lysine following the RDG sequence, to be used for treatment of melanoma. Thus liposomal RGDK inhibited tumor growth due to the blockade of vascularization development. (Pramanik et al., 2008)

A small non-peptidic integrin α5β1 antagonist, SJ749 [**Figure 13**], is an RGD mimetic, but is specific for this integrin due to the conformation constraints (Smallheer et al., 2004). Indeed, the IC_{50} for α5β1-fibronectin is 1.8 nM, whereas for αvβ3-vitronectine it is 1 μM. SJ749 has been shown to inhibit migration of endothelial cells and adhesion of tumor cells (Kim et al. , 2000a, Kim et al., 2000b, Maglott et al., 2006). SJ749 also blocked angiogenesis in the chick chorioallantoic membrane model (Kim et al. , 2000a, Maglott et al. , 2006).

Another α5β1 non-peptidic antagonist, JSM6427 (Jerini AG Pharma, Berlin, Germany) blocked angiogenesis in a mouse model of choroidal neovascularization, induced apoptosis in endothelial cells and inhibited ERK phosphorylation upon fibronectin binding (Umeda et al., 2006). It entered clinical trials phase I in 2007 and is being also tested for glioma treatment (Farber et al. , 2008).

Very recently, Pr Kessler`s team (Heckmann et al., 2008) synthetized another α5β1 integrin antagonist here assigned as K34c, which have not entered any detailed biological studies, yet.

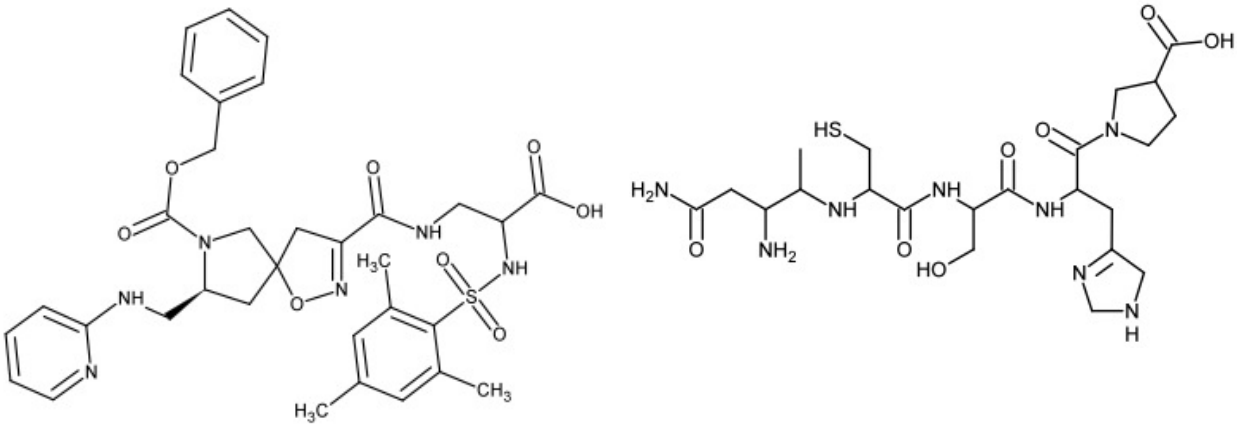

Figure 13: Structures of integrin α5β1 antagonists: SJ749 (LEFT); ATN-161 (RIGHT).

5. Combination therapy

In recent years, integrins have attracted a lot of interest as potential therapeutic targets for various cancers including glioblastomas. We have identified integrin α5β1 as a promising target as it is overexpressed in tumoral neovessels as well as in various cancer cells (Sawada et al. , 2008) including brain tumors. A specific non-peptidic antagonist of α5β1 integrin, SJ749, has been shown to inhibit glioblastoma cell lines, U87MG and A172, proliferation and clonogenicity (Maglott et al. , 2006). Tentori and Graziani reviewed possible approaches how to improve chemotherapy effects. Such novel approaches include inhibition of tumoral neoangiogenesis, e.g. via integrins (Tentori et al., 2008, Tentori and Graziani, 2002). Integrins regulate various physiological as well as pathological processes and they are known to be able to confer chemo- and radioresistance of various cancer types. Therefore, their inhibition in combination with chemotherapeutic drugs, e.g. DNA damaging compounds, could improve the therapy outcome.

Part II. Aims of the study

Glioblastomas are the most abundant and most aggressive type of CNS tumors in adults with a survival median of less than one year. Current therapeutic approaches remain inefficient enough, since these tumors are often chemo- and/or radioresistant and they recur easily. Ellipticine has been shown to be a brain-tumor-specific anti-cancer drug when screening the NCI-60 cell line panel, but very few studies were performed in glioblastomas using this drug.

Therefore, the principal aims of the first part of the study were as follows:

- to describe ellipticine`s cytotoxicity in model glioblastoma cell lines U87 and U373
- to investigate ellipticine`s metabolism/activation in glioblastoma cell lines U87 and U373

Since ellipticine is currently not used in clinical practice due to its cardiotoxicity, its potential re-utilisation would necessarily be linked with dose-depression or with targeting it directly to tumor tissue. Here, we propose a use of combination therapy of ellipticine and an α5β1 integrin antagonist. Such novel therapeutic approach to glioblastoma treatment could lead to ellipticine dose-depression while final therapy outcome improves.

The principal aim of the second part of the study was to design a combination therapy of integrin α5β1 antagonist and ellipticine for glioblastoma treatment and elucidate its mechanisms.

Part III. Experimental

Material

1. Celular models

U87MG cell line	human glioblastoma cell line, WHO grade IV; p53 wild-type	ATCC (LGC Standards Sarl, Molsheim, France)
U373 cell line	human glioblastoma cell line, WHO grade IV; p53 mutated (R273H)	ECACC (Sigma, Lyon, France**)**
HCT116 p53+/+ cells **HCT116** p53-/- cells	isogenic human colon carcinoma cell lines	generous gift from B. Vogelstein (Baltimore, USA)

2. Treatment agents

Ellipticine: 5,11-dimethyl-6H-pyrido[4,3-b]carbazole	Sigma (Lyon, France)
Temozolomide: 8-carbamoyl-3-methylimidazo[5,1-d]-1,2,3,5-tetrazin-4-(3H)- one	gift of Schering-Plough (Levallois Perret, France)
SJ749: (S)-2-[(2,4,6-trimethylphenyl) sulfonyl] amino-3-[7-benzyloxycarbonyl-8-(2-pyridinylaminomethyl)-1-oxa-2,7-diazaspiro-(4,4)-non-2-en-3-yl]carbonylamino] propionic acid	synthesized in our laboratory according to the procedure described in the patent WO 97/33887
K34c: 2-(S)-2,6-dimethylbenzamido)-3-[4-(3-pyridin-2-ylaminoprooxy)-phenyl] propionic acid	first synthesized and characterized by the group of Pr Kessler (Munchen, Germany); here synthesized in our laboratory according to the procedure described in (Heckmann et al. , 2008)
Ke34a: 2-(R)-(benzamido)-3-[4[3-(pyridine-2-ylamino)propoxy]phenyl]-propionic acid	first synthesized and characterized by the group of Pr Kessler (Munchen, Germany); here synthesized in our laboratory according to the procedure described in (Heckmann et al. , 2008)

3. *Antibodies*

Mouse monoclonal anti-**p53** antibody	BD Pharmingen	San Jose, CA, USA
Rabbit anti-**phospho(**Ser15**)p53** antibody	Cell Signaling Technology	Danvers, MA, USA
Mouse monoclonal anti-**p21** antibody	Cell Signaling Technology	Danvers, MA, USA
Mouse anti-**mdm2** antibody	Santa Cruz Biotechnology	Heidelberg, Germany
Rabbit anti-**Fas** antibody	Santa Cruz Biotechnology	Heidelberg, Germany
Mouse monoclonal anti-**GAPDH** antibody	Millipore	Molsheim, France
Mouse anti-**β-actin** antibody	Sigma	St. Louis, MO, USA
Rabbit anti-α5 **AB1928** antibody (recognizes cytoplasmic α5 integrin part)	Chemicon International	Molsheim, France
Rabbit anti-β1 **AB1952** antibody (recognizing cytoplasmic β1 integrin part)	Chemicon International	Molsheim, France
TS2/16 antibody recognizing extracellular part of β1 integrin	Dr E Georges-Labouesse	IGBMC, Illkirch, France
snaka51 antibody recognizing extracellular part of α5 integrin	Dr M Humphries	Manchester, UK
Rabbit anti-**CYP1A1** antibody	Millipore	Billerica, MA, USA
Rabbit anti-**CYP1B1** antibody	Abcam	Cambridge, MA, USA
Rabbit anti-**CYP3A4** antibody	AbD Serotec	Oxford, UK
Mouse monoclonal anti-**COX-1** antibody	Abcam	Cambridge, MA, USA
Rabbit polyclonal anti-**LPO** antibody	Abcam	Cambridge, MA, USA
HRP-conjugated secondary antibodies (Rabbit, Mouse)	BioRad *or* Promega	Herkules, CA, USA Madison, WI, USA

Methods

1. *Cell culture*

Cells were routinely cultured in Eagle's MEM supplemented with 10% heat-inactivated FBS, 0.6 mg/mL glutamine, 200 IU/mL penicillin/streptomycin, and 0.1 mg/mL gentamicin in

humidified 5% CO2 at 37°C. All experiments were performed in 2% FBS containing medium if not indicated otherwise.

2. *siRNA transfection*

U87MG cells (5,000 cells/cm^2) were plated onto 6-well plates in 10% heat-inactivated FBS containing medium without antibiotics. The day after, attached cells were covered with fresh medium and transfected either with control non-targeting (siNON) siRNA (Dharmacon, Thermo Fisher Scientific, Waltham, USA), either with siRNA targeted against p53 (siTP53) (Dharmacon) at a concentration 50 nM using INTERFERin^{TM} (Polyplus Transfection, Illkirch, France) as a transfection reagent following the manufacturer`s instructions. p53 expression was examined and subsequent experiments were launched 72 hours after the transfection.

3. *pcDNA transfection*

U373 cells (5,000 cells/cm^2) were plated onto 6-well plates in 10% heat-inactivated FBS containing medium without antibiotics. The day after, attached cells were covered with fresh medium and transfected with 1 µg pcDNA3.1 plasmid comporting p53 sequence a kind gift of C. Blattner, Karlsruhe, Germany) in 10 µl Lipofectamine 2000 (Sigma) as a transfection reagent in OptiMEM® (Invitrogen, Carlsbad, CA, USA) following the manufacturer`s instructions. The plasmid pcDNA3.1 (Invitrogen) was used as a transfection control. Cells were covered with fresh medium 6 hours after the transfection. The pcDNA3.1 plasmid comports a sequence of resistance to geneticine G418 enabling subsequent selection of successfully transfected cells.

4. *Proliferation assay*

Cells were plated onto 96-well plates and treated with respective solvents (50% methanol/50% H_2O for SJ749, temozolomide; and DMSO for ellipticine, K34c), SJ749 (5 µM), K34c (20 µM), ellipticine (1 µM), temozolomide (200 µM), or combination of drugs at the time of plating. Cell viability was determined using CellTiter 96 Aqueous One Solution Cell Proliferation Assay (Promega) which quantifies the tetrazolium salt degradation into formazan product by the respiratory chain enzymes in mitochondria. Manufacturer's

instructions were followed. Briefly: at the indicated time periods, MTS reagent (10 µL per well) was added and the plate was incubated at 37°C for 3 hours. Living (metabolically active) cells were quantified by measuring absorbance at 492 nm. Wells of the plating controls were quantified directly following plating on day 0. The relative number of living cells (as the combined effect of proliferation and survival) represents the portion of living cells at the given time point expressed as a multiple of the number of cells plated at day 0. IC_{50} were determined using the GraphPad software.

5. Clonogenicity

Cells were plated onto 6-well plates in very low densities and treated as indicated in 2% serum containing medium. When treatment completed, cell were covered with fresh 10% serum containing medium and grown for 7 days without drug. Cells were then fixed by 4% paraformaldehyde and stained by 0.1% crystal violet in ethanol. Results represent number of colonies formed by treated cells compared to colony numbers of non-treated cells.

6. RT PCR assay.

RNA was extracted with Trizol (Sigma) and was transcribed into cDNA using high capacity cDNA kit (Applied Biosystems, Foster City, CA, USA). Real-time quantitative PCR was performed using the ABI7000 SYBRGreen PCR detector with the probes purchased from Invitrogen (cyclophilin, p53, p21, human mdm-2, Apaf-1, Fas, E2F1, ATM, Bad, Bax) or Generi Biotech, Hradec Králové, Czech Republic (CYP1A1, CYP1B1, CYP3A4, POLR2A).

Relative levels of mRNA gene expression were calculated using the $2^{-\Delta\Delta Ct}$ method as previously described (Livak and Schmittgen, 2001).

7. Western blot.

Detached cells were washed with PBS and lysed in ice-cold lysis buffer (1% Triton X-100, 100 mM NaF, 10 mM NaPPi, 1 mM Na_3VO_4 in PBS supplemented with Complete anti-protease cocktail; Roche, Meylan, France) for 1 hour at 4°C. Suspension was sonicated (10 sec) and centrifugated at 12,000g for 15 min at 4°C. Protein concentration in the supernatant was assessed by *DC* Protein Assay (BioRad, Hercules, CA, USA). Proteins

were electrophoresed by SDS-PAGE (8-15% acrylamide gels according to protein of interest) and transferred to PVDF membranes (Amersham Bioscience, Fairfield, CT, USA). For p53, p21, AB1952, and AB1928, non-specific binding sites were saturated by casein (I-Block™ Tropix/Applied Biosystems) in PBS for 1 hour at room temperature. For phospho-p53, CYP1A1, CYP1B1, CYP3A4, LPO, and COX-1, non-specific binding sites were saturated using 5 % Blotting Grade Blocker Non-Fat Dry Milk (BioRad) in TBS for 1 hour at room temperature. Afterwards, membranes were incubated with appropriate primary antibodies overnight at 4°C, washed and incubated for 1 hour with HRP–conjugated secondary antibodies (Promega/BioRad) at room temperature. Immun-Star™ HRP Substrate Kit (BioRad) with chemiluminescence reaction followed by exposure to CL-Xposure films (Sigma) was used to visualize proteins. Equal protein quantities in all samples were verified by GAPDH or β-actin markage. Band intensities were quantified using the GeneTools or Elfoman software.

8. Senescence assay

The β-galactosidase activity at pH 6 was determined using the Senescence β-Galactosidase Staining Kit (Cell Signaling Technology) according to the manufacturer's instructions. Briefly, cells were plated onto 6-well plates. After completion of the treatment, cell were washed with PBS and fixed using the Fixative Solution for 15 minutes at room temperature. After washing, cells were covered with Staining Solution overnight at 37°C. The day after, percentage of positively perinuclearly blue stained cells indicating β-galactosidase activity at pH 6 was quantified under microscope (Leica, magnification 200x). At least 200 cells were counted per condition.

9. Apoptosis assays

Apoptotic programmed cell death was assesed by several techniques:

a) subG1 cell cycle phase

Cells were plated onto 24- or 6-well plates and treated as indicated. After the treatment completion, medium and trypsinized cells were harvested, washed with PBS and resuspended in hypotonic buffer containing 3.4 mM sodium citrate and 0.1 % Triton X-100 in PBS and stained by 50 µg/mL propidium iodide. SubG1 cell population was determined by flow cytometry (*FACS*Calibur, BD Biosciences) analysis after propidium iodide staining. Ten

thousand events per sample were acquired and the percentage of cells in the subG1 phase was quantified by the CellQuest computer software.

b) Annexin V/PI staining

Cells were plated onto 6-well plates. After the treatment, trypsinized cells and medium were harvested and washed with PBS. Apoptosis was assessed using the Annexin V-FITC Kit (MACS Miltenyi Biotec, Bergish Gladbach, Germany). Briefly, cells were plated onto 6-well plates and treated as indicated. When treatment completed, medium was harvested together with cells detached by trypsine. Cells were washed with Binding Buffer and stained with Annexin V-FITC in Binding Buffer for 15 minutes at room temperature. After washing the cells, propidium iodide was added and cells were analysed by flow cytometry (*FACS*Calibur, BD Biosciences). Apoptotic cell populations positively stained with Annexin V, but not with propidium iodide, were quantified using the CellQuest software.

c) Hoechst 33342 nuclear staining

Cells were plated onto cover glasses placed at the bottom of 24-well plates and treated as indicated. Culture medium was discarded and cells were fixed by 4% paraformaldehyde for 15 min. After washing with PBS, Hoechst 33342 dye (1/1,000 in PBS, Sigma) staining was performed. Abundant dye was washed out, cover slips were transferred onto microscopic slides and nuclei morphology was analyzed by fluorescence microscopy. Results are represented as a percentage of cells with fragmented nuclei. At least 200 cells were counted per condition.

10. Cell cycle analysis

Cells were plated onto 24- or 6-well plates and treated as indicated. After the treatment completion, medium and trypsinized cells were harvested, washed with PBS and resuspended in hypotonic buffer containing 3.4 mM sodium citrate and 0.1 % Triton X-100 in PBS and stained by 50 µg/ml propidium iodide. The DNA content of the cells was quantified by flow cytometry (*FACS*Calibur, BD Biosciences, San Jose, CA, USA). Cell cycle analysis was perfomed using the ModFit software.

11. Oxidation of ellipticine by human recombinant cytochromes P450 in Supersomes™

Incubations, where the efficiency of human recombinant CYPs was investigated, contained in a final volume of 250 µl: 100 mM potassium phosphate buffer (pH 7.4), NADPH-generating system (1 mM $NADP^+$, 10 mM D-glucose 6-phosphate, 1 unit/mL D- glucose 6-phosphate dehydrogenase, 10 mM $MgCl_2$), 10 µM ellipticine dissolved in 1 µl methanol and from 10 to 200 nM CYP in Supersomes™ (Gentest Corp., Woburn, MA, USA). The reaction was started by adding NADPH-generating system. After the incubation (37°C, 30 min), the reaction was terminated by adding 750 µl ethyl acetate and 2.5 µl phenacetin (1 mM solution in methanol) was added as an internal standard. Ellipticine and its metabolites were extracted and separated by HPLC as described below (see § 12. HPLC, p 62).

12. HPLC (High-performance liquid chromatography)

Cells were treated with ellipticine for indicated times, detached by trypsine and harvested. After washing with PBS, they were stored at -80°C overnight. Defrosted cell pellets were resuspended in PBS and sonicated for 15 sec. Ellipticine and its metabolites were extracted with equal volume (750 µl) of ethyl acetate. After centrifugation (7 min at 13,000 RPM centrifuge MSE Micro Centaur, Sanyo, UK), organic phase was collected and evaporated to dryness, then resuspended in 20 µl methanol and separated by HPLC (Stiborova et al. , 2004). The column used was a 5-µm Ultrasphere ODS (4.6 x 250 mm; Beckman, Fullerton, CA), the eluent was 64% methanol plus 36% of 5 mM heptane sulfonic acid containing 32 mM acetic acid in water with flow rate of 0.8 mL/minute, and detection was at 296 nm (Stiborova et al. , 2004).

13. ^{32}P-postlabeling assay

Procedures for analysis of ellipticine-derived DNA adducts by the ^{32}P-postlabeling assay were performed with nuclease P1 enrichment, the procedure found to be appropriate to detect and quantify ellipticine-derived DNA adducts (Stiborova et al. , 2001, Stiborova et al. , 2004). Briefly, DNA samples (12.5 µg) were digested with micrococcal nuclease (750 mU) and spleen phosphodiesterase (12.5 mU) in digestion buffer (20 mM sodium succinate, 8 mM $CaCl_2$, pH 6.0) for 3 h at 37°C in a total volume of 12.5 µl. Here, 2.5 µL of the digests were removed and diluted 1:1500 to determine the amount of normal nucleotides. The digests

(10 µL) were enriched for adducts by incubating with 5 µg (5 U) of nuclease P1 in 3 µL of a buffer containing 0.8 M sodium acetate, pH 5.0, and 2 mM $ZnCl_2$ for 30 min at 37°C. The reaction was stopped by adding 3 µl of 427 mM Tris base. Four microliters of labeling mix consisting of 400 mM bicine, pH 9.5, 300 mM dithiothreitol, 200 mM $MgCl_2$, 10 mM spermidine, 100 µCi [γ-32P]ATP (15 pmol) (ICN Biochemicals, Costa Mesa, CA, USA), 0.5 µl 90 µM ATP, and 10 U T4 polynucleotide kinase were added. After incubation for 30 min at room temperature, 20 µl were applied to a polyethylenimine (PEI)-coated cellulose TLC plate (Macherey-Nagel, Duren, Germany) and were chromatographed as described previously (Stiborova et al. , 2001, Stiborova et al., 1994), except that D3 and D4 were adjusted to pH 4.0 and 9.1, respectively, for better resolution. To determine the amount of normal nucleotides 5 µl of the 1:1500 dilution of digests were mixed with 2.5 µL of Tris buffer (10 mM, pH 9.0) and 2.5 µL of labeling mix (see above) and incubated for 30 min at room temperature. The samples were then diluted by mixing 4 µL with 750 µL of 10 mM Tris buffer, pH 9.0. Five microliters of this solution were applied to a PEI-cellulose TLC plate and run in 0.28 M $(NH_4)_2SO_4$, 50 mM NaH_2PO_4, pH 6.5. Adducts and normal nucleotides were detected and quantified by storage phosphor imaging on a Packard Instant Imager. Count rates of adducted fractions were determined from triplicate maps after subtraction of count rates from adjacent blank areas. Excess [γ-^{32}P]ATP after the postlabeling reaction was confirmed. Adduct levels were calculated in units of relative adduct labeling (RAL), which is the ratio of cpm of adducted nucleotides to cpm of total nucleotides in the assay (Stiborova et al. , 2001)

14. Statistical analysis

Data are represented as mean ± SEM. In all cases, n refers to the number of independent experiments. Statistical analyses were performed by the Student's t test. $P < 0.05$ was considered significant (*, $P < 0.05$; **, $P < 0.01$, ***, $P < 0.001$).

Part IV. Results & Discussion

Part IV.A: Ellipticine chemotherapy

Glioblastoma is a hardly treatable tumor type, often chemo- and radio-resistant (Penas-Prado and Gilbert, 2007, Sathornsumetee et al., 2007). Ellipticine is highly cytotoxic for various cancer cell types (for review see (Garbett and Graves, 2004, Stiborova et al. , 2006) and it has been evaluated as a brain tumor-specific drug when screening the cell lines in NCI database (Shi et al. , 1998a, Shi et al. , 1998b). In the 80`s and 90`s, ellipticine was extensively studied as a promising chemotherapy drug for diverse cancers such as breast cancer, hepatocarcinomas, acute myeloblastic leukemia etc. Nevertheless, very few studies were performed with brain tumors.

1. Ellipticine effects on U87MG glioblastoma cell line

Firstly, we evaluated the cytotoxicity of ellipticine to U87MG glioblastoma cell line using the MTS proliferation assay. Ellipticine inhibited U87MG cell proliferation with IC_{50} of 1.48 ± 0.08 μM after 72 hours of ellipticine treatment in reduced serum conditions

[

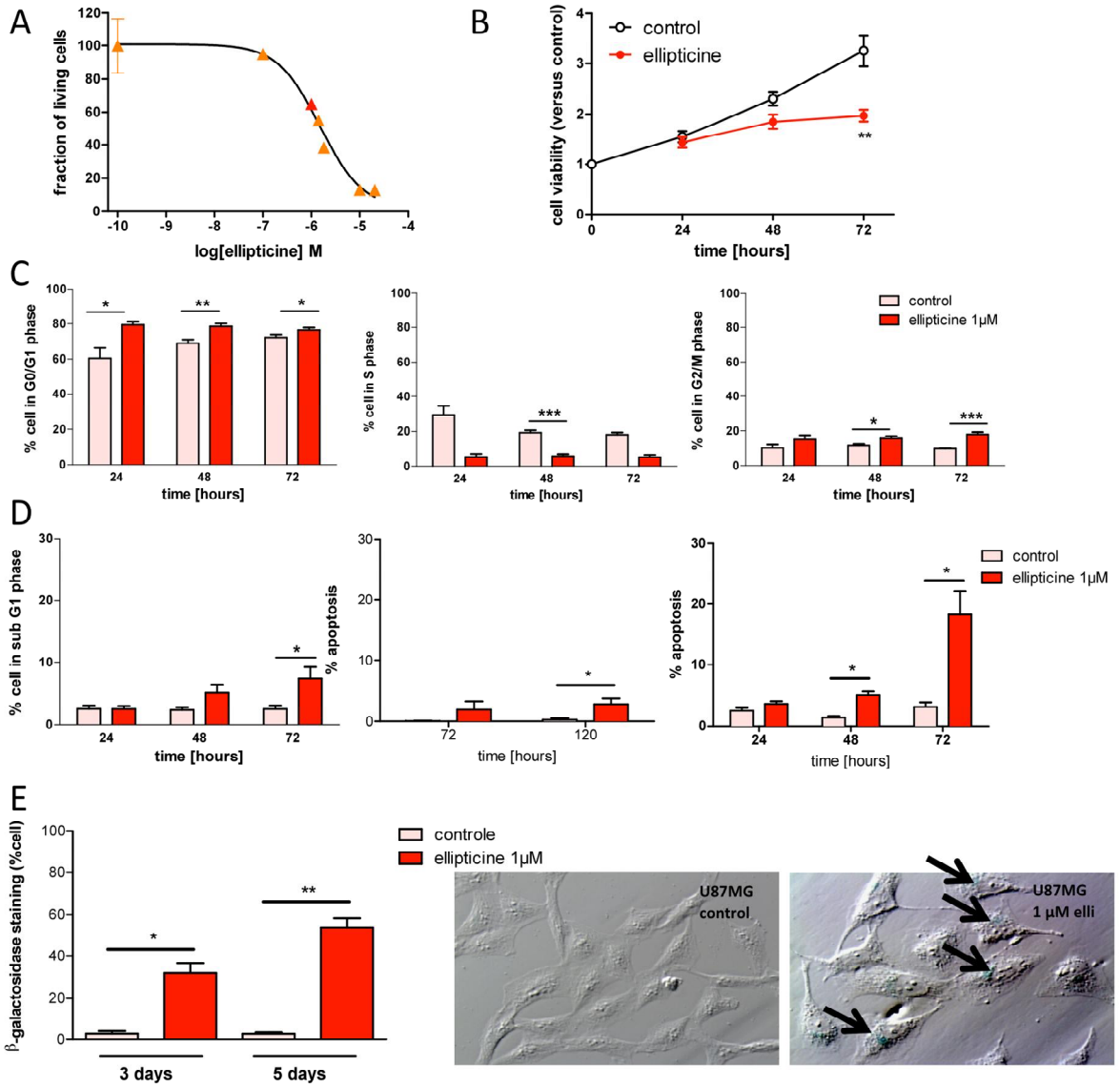

Figure 14a]. For the majority of further experiments, 1 µM ellipticine concentration was used. Various treatment times indicated gradual increase in cytotoxic effect of ellipticine starting at 21.5 % after 24 hours and raising to up to 56.8 % growth inhibition after 72 hours of ellipticine treatment

[

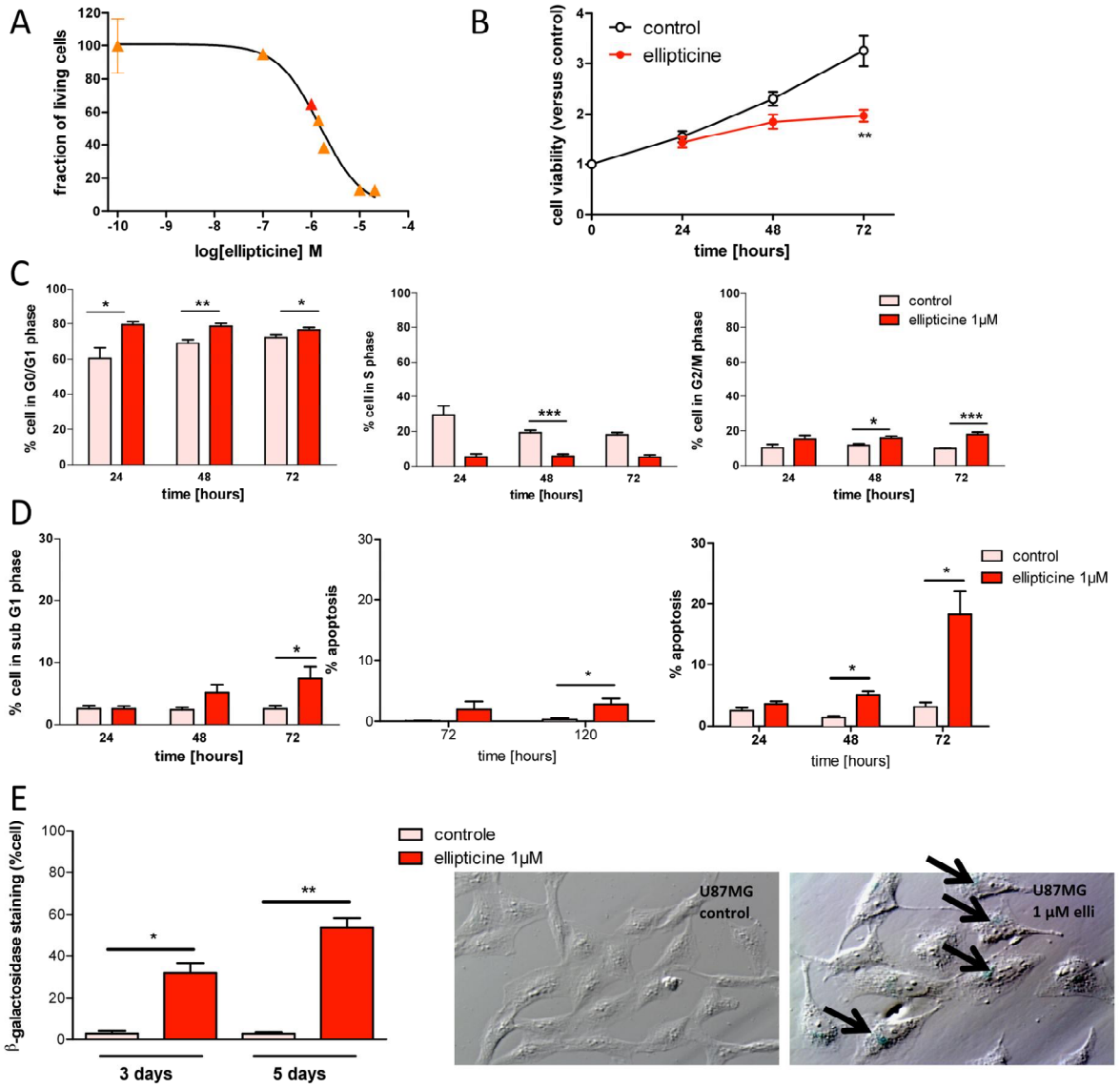

Figure 14b].

Next, mechanisms implicated in ellipticine cytotoxic effect were investigated in more detail. Ellipticine has been reported to arrest cell cycle progression by regulating the expression of cyclin B1 and Cdc2 as well as phosphorylation of Cdc2 in breast cancer cell lines (Kuo et al., 2005a, Kuo et al., 2005b), to induce apoptotic cell death by the generation of cytotoxic free radicals, the activation of Fas/Fas ligand system, the regulation of Bcl-2 family proteins (Kuo et al. , 2005a, Kuo et al. , 2005b, Kuo et al., 2006), an increase of wild-type p53, the rescue of mutant p53 activity and the initiation of the mitochondrial apoptosis pathway (Garbett and Graves, 2004, Kuo et al. , 2005a, Kuo et al. , 2005b, Kuo et al. , 2006).

Chemotherapy-induced cell cycle arrest was shown to result from DNA damages caused by a variety of chemotherapeutics. In the case of ellipticine, it was suggested that the prevalent DNA-mediated mechanisms of its antitumor, mutagenic and cytotoxic activities are 1. intercalation into DNA, 2. inhibition of DNA topoisomerase II activity (Garbett and Graves, 2004, Stiborova et al. , 2006), and 3. covalent DNA adduct formation after its metabolic activation. Ellipticine chemotherapy induces DNA damage and results in cell cycle arrest predominantly at the G1/S and G2/M checkpoints.

We therefore examined the progression of U87MG through the cell cycle in presence of ellipticine [

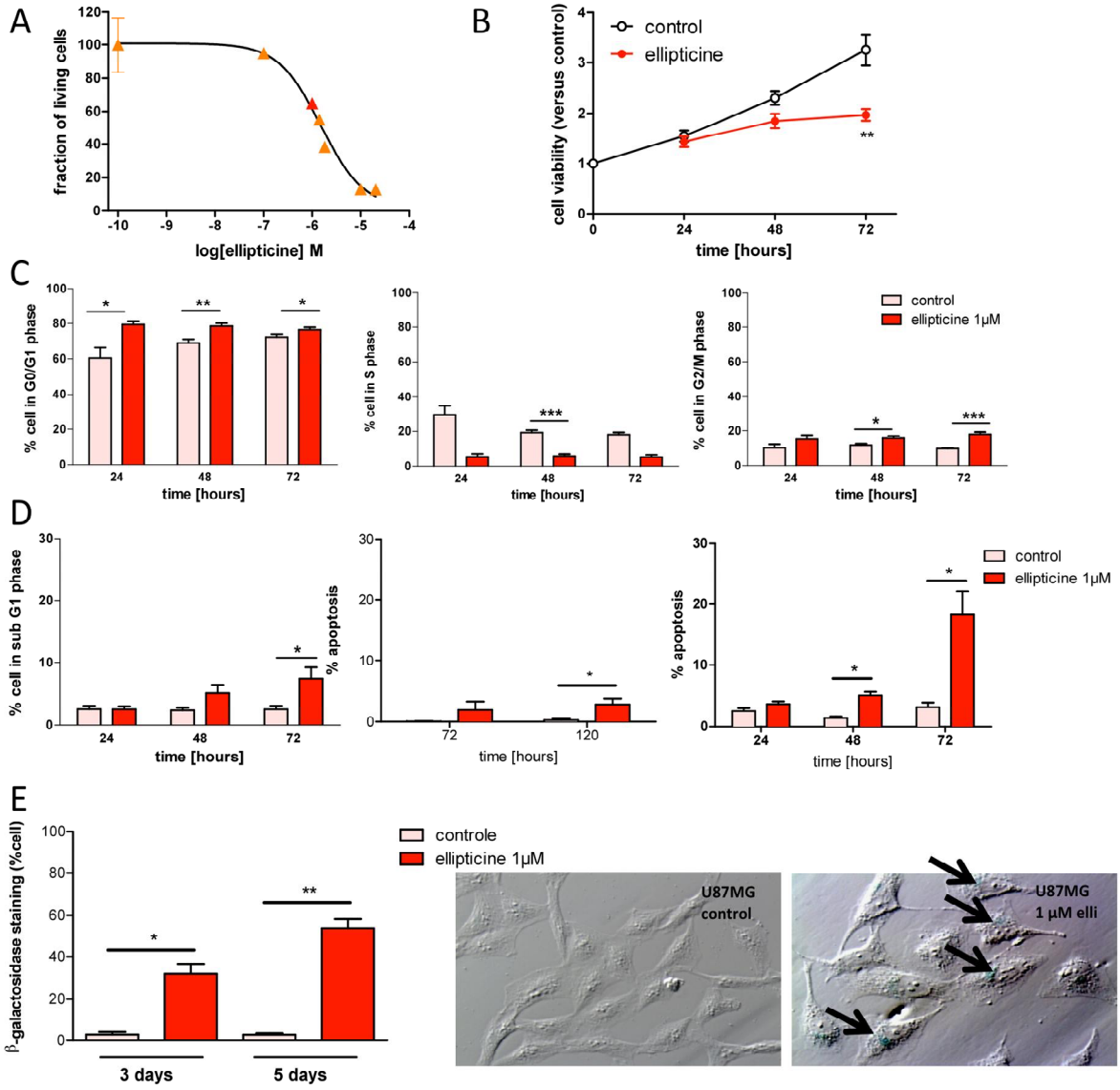

Figure 14c]. Ellipticine arrested the U87MG cells in G0/G1 phase and slightly also in G2/M phase, accompanied by a decrease of synthetic S phase. G0/G1 cell cycle arrest appeared as

soon as after 24 hours of treatment blocking cycle progression of almost 80% of cells compared to 60% of non-treated cells present in G0/G1 phase. In contrast, G2/M cycle arrest became significant much later, reaching maximum 18% of cell population after 72 hours of ellipticine treatment compared to 9.8% of control cells.

In additional work, we examined what were the consequences of genotoxic ellipticine`s action regarding programmed cell death induction in U87MG cells. Although high ellipticine concentrations (5-10 μM) induce cell death, 1 μM ellipticine did not provoke apoptotic cell death as late as after 72 hours of treatment and still not exceeding 18% as assessed by any of the three experimental approaches: propidium iodide-stained cells in subG1 cell cycle phase, Annexin V staining combined with propidium iodide staining, both analyzed by flow cytometry, and Hoechst 33342 nuclear staining and subsequent nuclei morphology analysis using fluorescent microscopy [

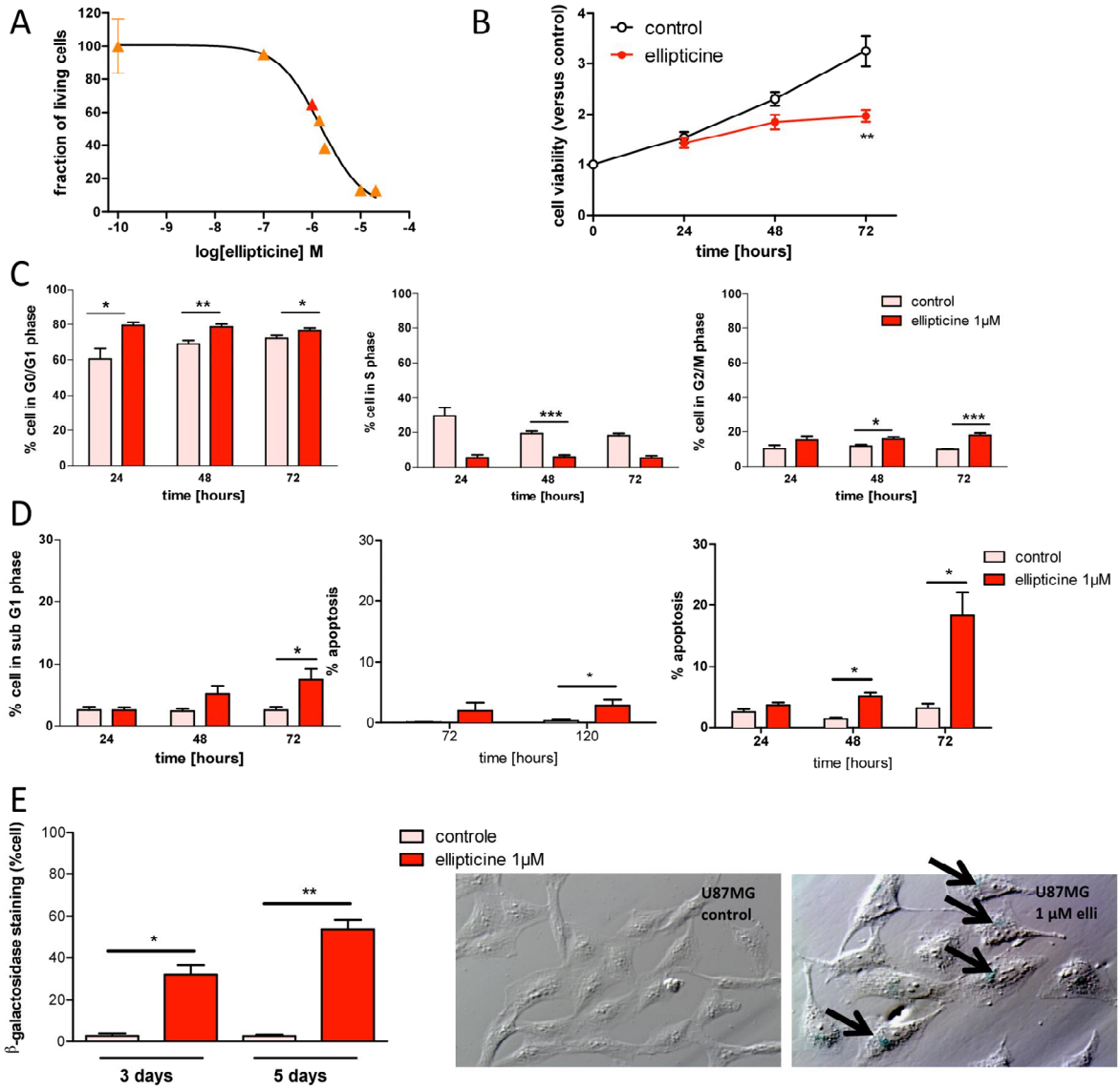

Figure 14d].

Since such a low percentage of apoptotic population could not clarify the U87MG proliferation inhibition induced by 1 µM ellipticine treatment, we regarded cellular senescence as it is another common cellular answer to chemotherapy resulting in irreversible cell cycle arrest accompanied by typical morphological changes such as platitude or large perinuclear cellular regions.

The expression of the senescence–associated acidic β-galactosidase (SA-β-Gal) was therefore determined in ellipticine-treated cells. Blue perinuclear positive staining for SA-β-Gal activity was detected in 32.3 ± 4.6 and 53.7 ± 4.6 of ellipticine-treated U87MG cells after 3 and 5 days, respectively
[

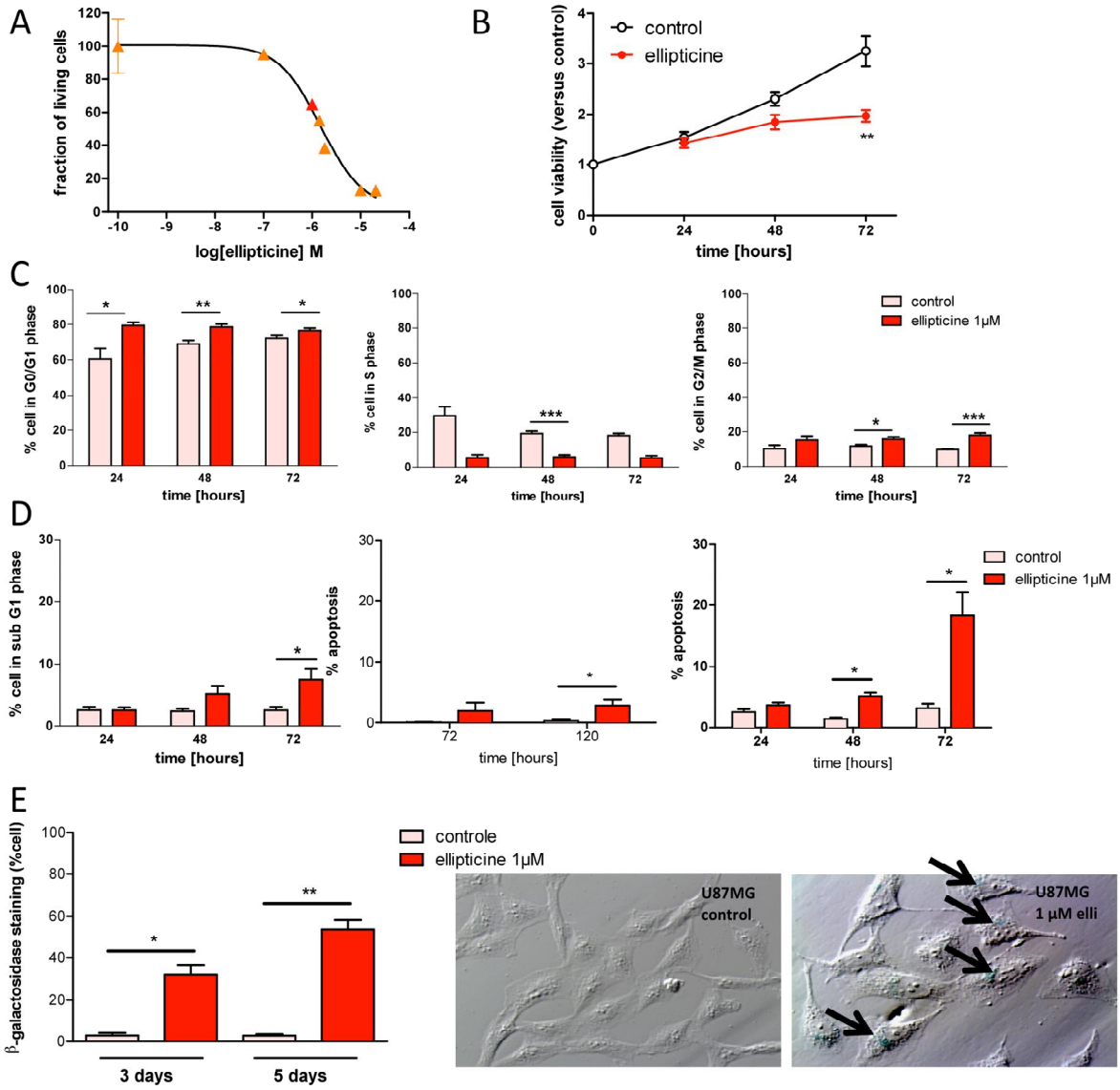

Figure 14e]. U87MG cells exhibited also morphological changes characteristic to senescence, as they appeared more flattened compared to control cells

[

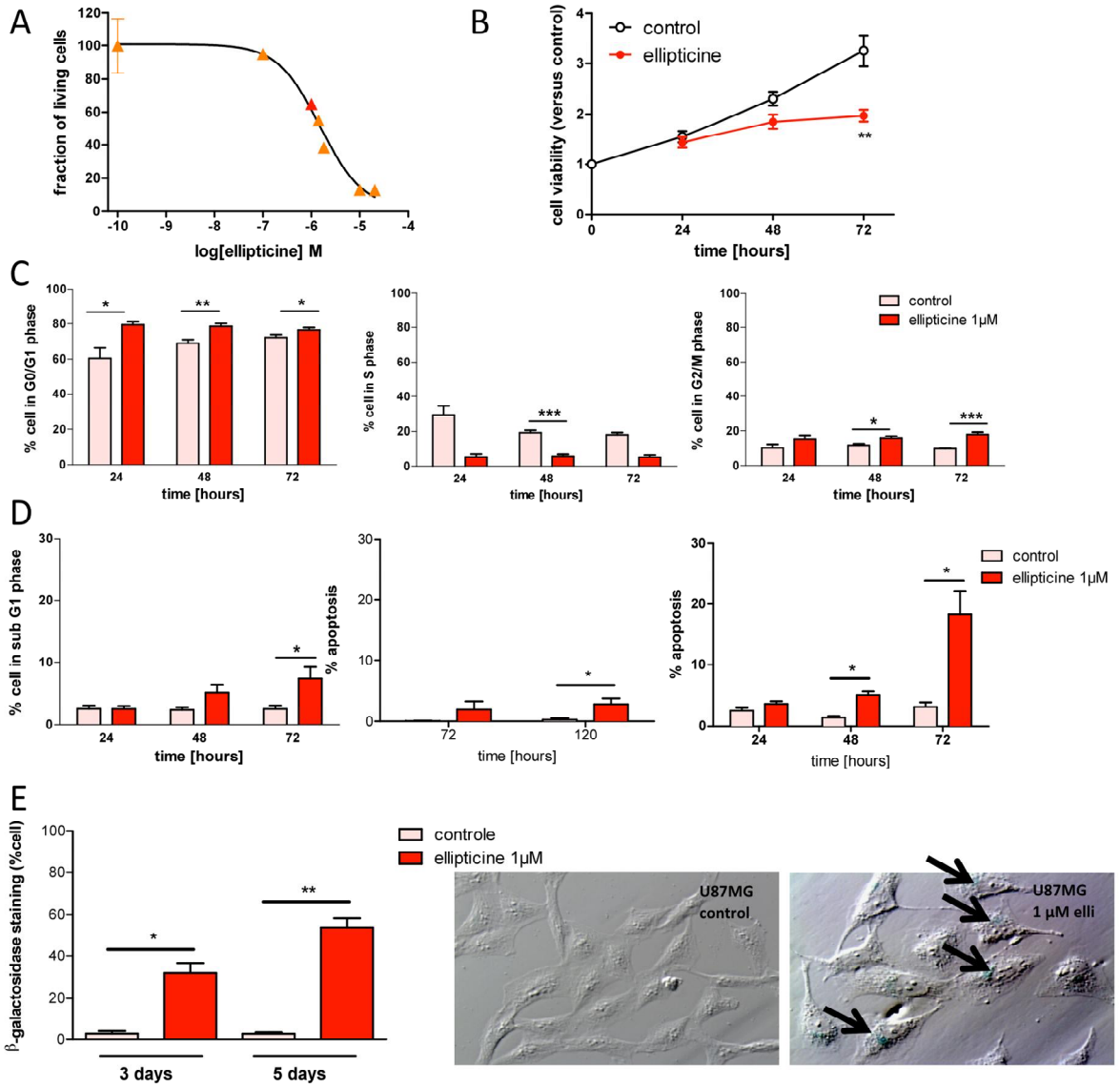
A
fraction of living cells
log[ellipticine] M
B
control
ellipticine
cell viability (versus control)
time [hours]
C
% cell in G0/G1 phase
% cell in S phase
% cell in G2/M phase
control
ellipticine 1µM
time [hours]
D
% cell in sub G1 phase
% apoptosis
control
ellipticine 1µM
time [hours]
E
β-galactosidase staining (%cell)
controle
ellipticine 1µM
3 days
5 days
U87MG
control
U87MG
1 µM elli

Figure 14e].

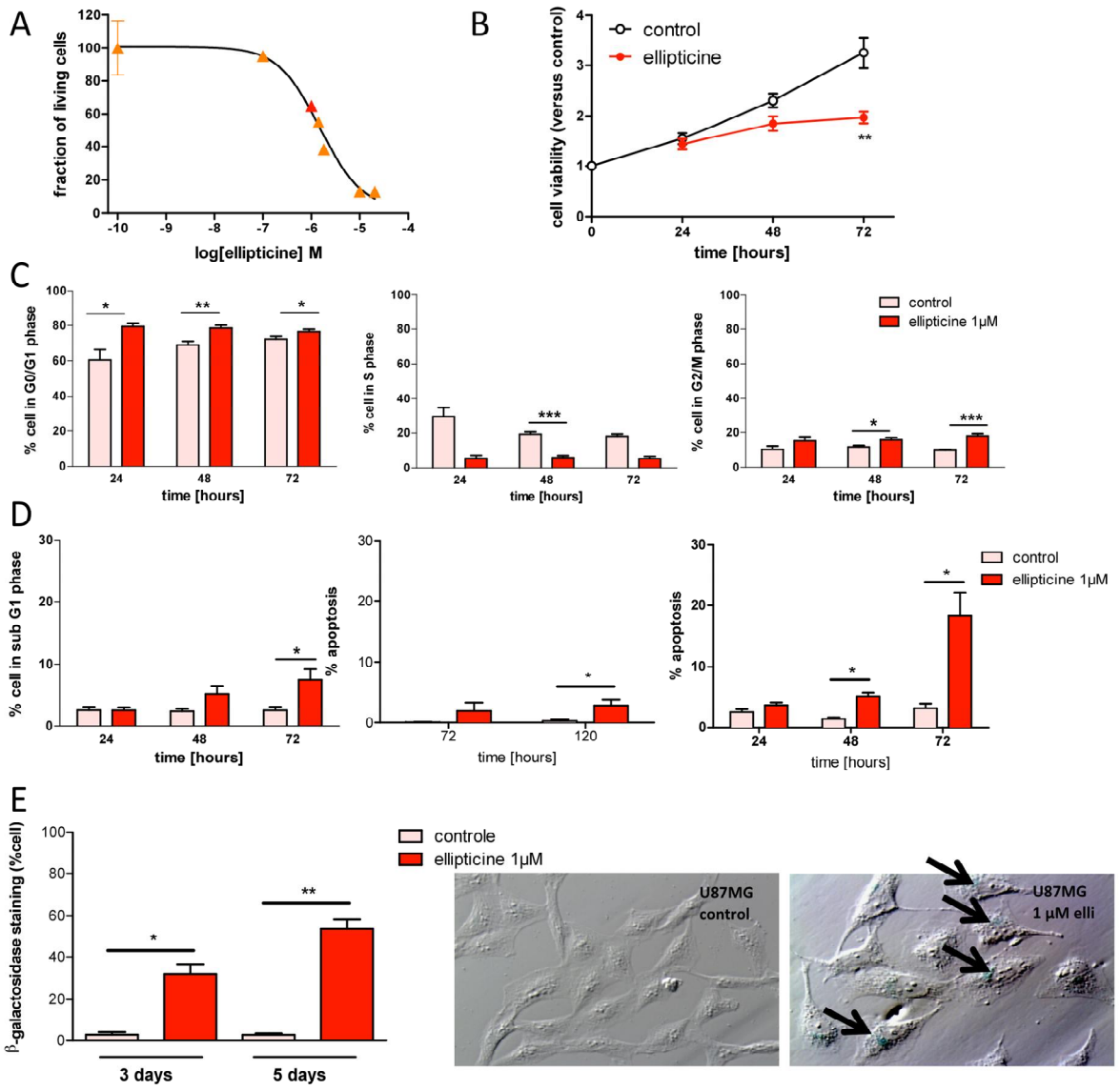

Figure 14: A. Proliferation assay. U87MG cells were treated 72 hours in 2% FBS containing medium with either solvent (DMSO) or ellipticine (0.1 - 20 µM). Proliferation is expressed as the percentage of living cells after ellipticine treatment compared to untreated cells grown in the presence of solvent considered as 100%. IC_{50} were determined using GraphPad Prism software, non-linear sigmoidal dose-response regression. **B.** U87MG cells were treated 24, 48 or 72 hours in 2% FBS medium with either solvent (DMSO), or 1 µM ellipticine. **C.** Cell cycle analysis. U87MG and U373 cells were treated for 24, 48, and 72 hours in 2% serum medium with DMSO or ellipticine (1 µM) before propidium iodide staining and cell cycle analysis by flow cytometry. Data represent the percentage of cells in G0/G1, S, G2/M cycle phases. **D.** Apoptosis. U87MG cells were treated with 1 µM ellipticine for the times as indicated and percentage of apoptotic cells was assessed using different techniques: PI-stained cells in subG1 cell cycle phase were quantified by FACS (LEFT); cell were fixed and stained by Hoechst 33342 dye. Percentage of cells with fragmented nuclei (apoptotic) was determined using fluorescent microscopy. At least 200 cells were analyzed per condition (CENTER); apoptosis was assessed using Annexin-V and PI staining (RIGHT). **E**. Senescence. U87MG cells plated in 6-well plates and left untreated or treated for 3 or 5 days in 2% FBS medium with 1 µM ellipticine before the detection of β-galactosidase activity at pH 6. Data represent positive cells percentage of at least 200 total cell number per condition (n=3). Representative photographs are shown on the right.

2. Ellipticine effects on U373 glioblastoma cell line

To confirm our results, we used another glioblastoma cell line U373. We examined cytotoxicity of ellipticine on U373 cells. Ellipticine inhibited cellular proliferation of these cells with IC_{50} of 1.92 ± 0.64 µM after 72 hours of treatment
[

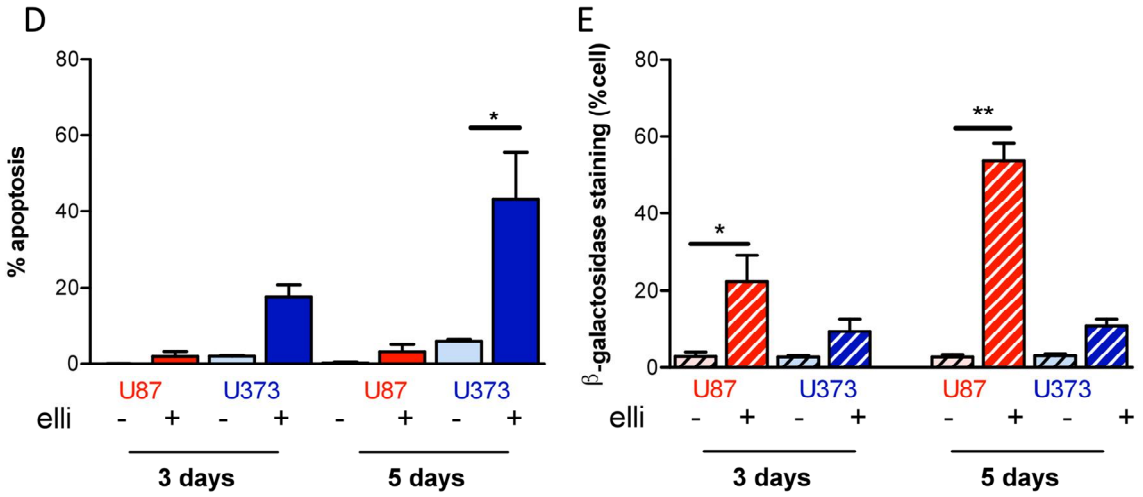

Figure 15a]. As contrasted to U87MG cells, U373 cells did not recover so easily after 48 hours of ellipticine treatment. Six days after the completion of 48-hours ellipticine treatment U87MG proliferation was inhibited by 23% compared to 54% in U373
[

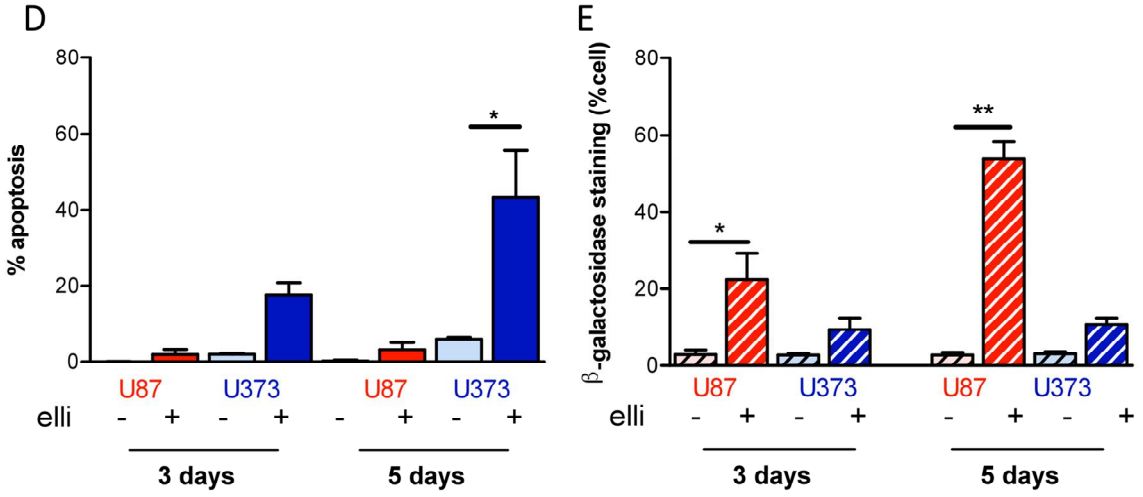

Figure 15b].

The proliferation inhibition could be partially explained by cell cycle arrest in G2/M phase provoked as soon as after 24 hours of ellipticine treatment reaching 19.9 % and even increasing to up to 39.8 % after 72 hours of ellipticine treatment. In contrast to U87MG cell cycle, population of U373 cells present in G0/G1 cycle phase was reduced by half starting at 48 hours of ellipticine treatment

[

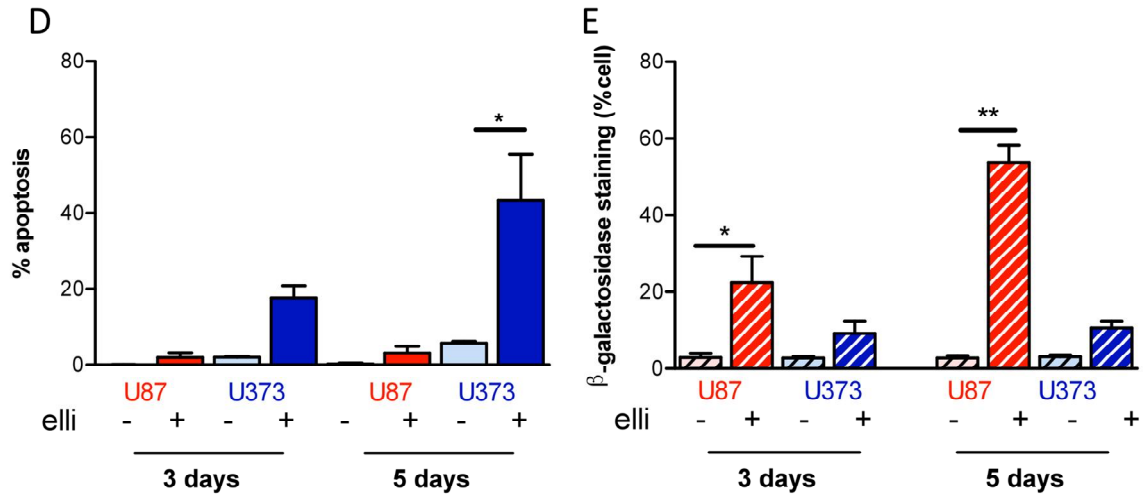

Figure 15c].

Ellipticine induced apoptotic cell death in nearly 44% of U373 cells after 5 days of ellipticine treatment as assessed by Hoechst 33342 dye staining and subsequent nuclei morphology analysis by fluorescence microscopy

[

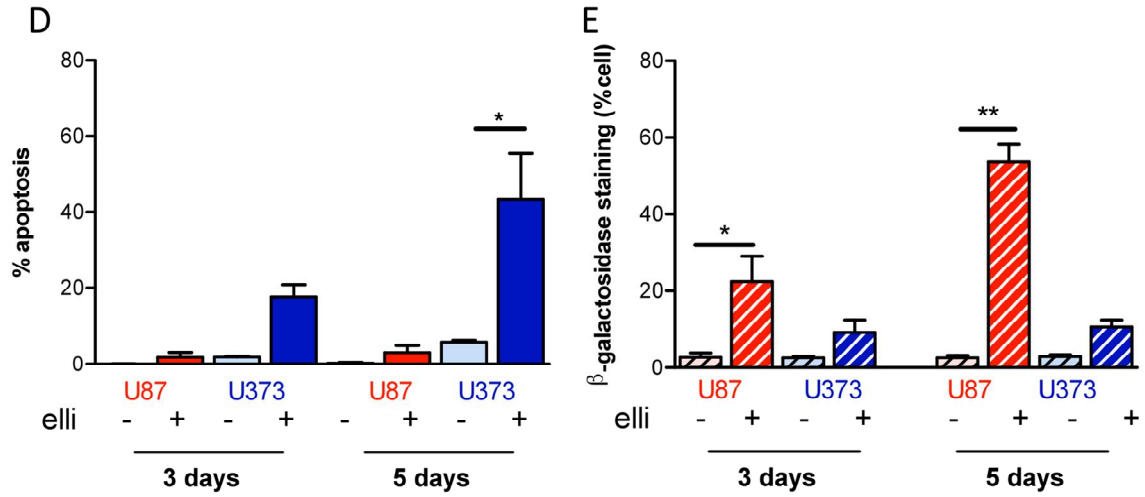

Figure 15d]. As contrasted to U87MG cell line, U373 cells hardly senesced, not exceeding 11% of cells expressing senescence–associated acidic β-galactosidase (SA-β-Gal) after 5 days of ellipticine treatment

[

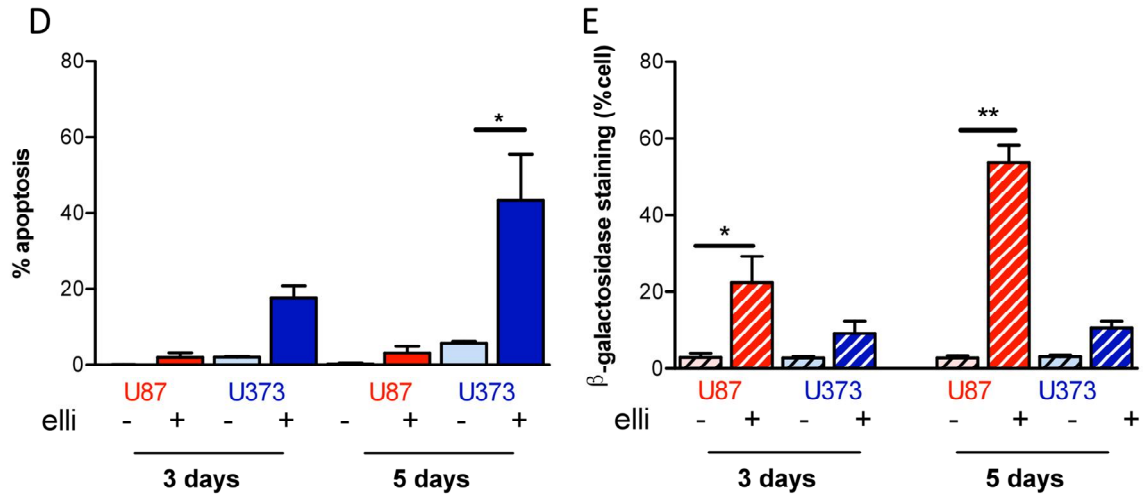
D
% apoptosis
80
60
40
20
0
*
U87
U373
U87
U373
elli
- + - + - + - +
3 days
5 days
E
β-galactosidase staining (%cell)
80
60
40
20
0
*
**
U87
U373
U87
U373
elli
- + - + - + - +
3 days
5 days

Figure 15e].

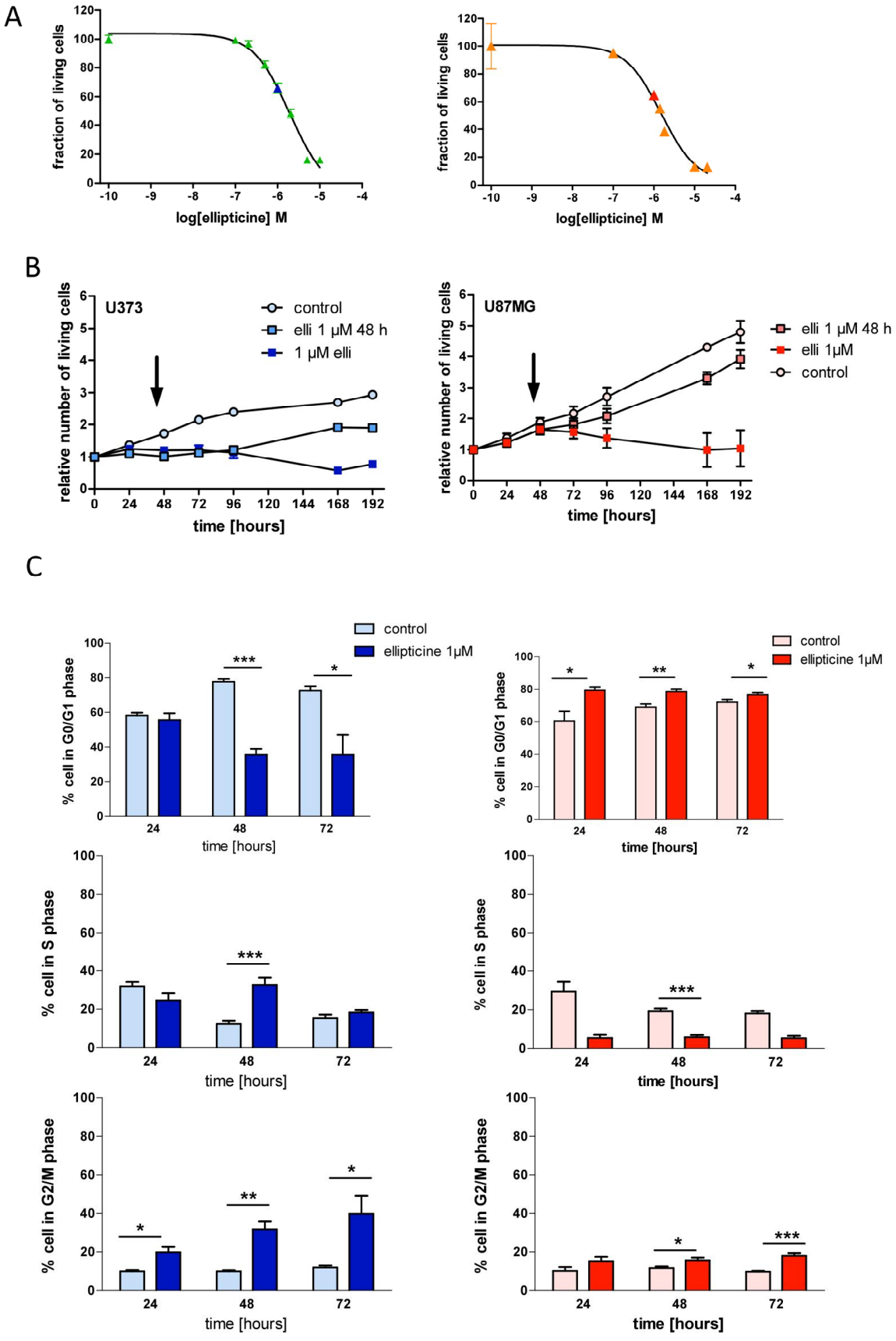
A
fraction of living cells
log[ellipticine] M
B
U373
control
elli 1 µM 48 h
1 µM elli
relative number of living cells
time [hours]
U87MG
elli 1 µM 48 h
elli 1µM
control
C
control
ellipticine 1µM
% cell in G0/G1 phase
% cell in S phase
% cell in G2/M phase
time [hours]

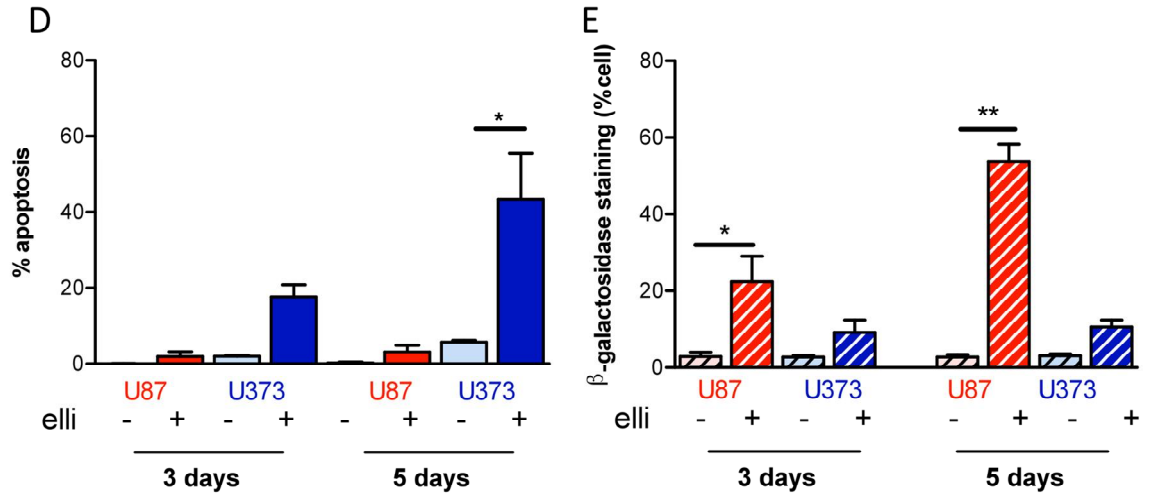

Figure 15: Comparison of ellipticine effects on U373 (LEFT) and U87MG (RIGHT) glioblastoma cell lines. **A.** Proliferation assay. U87MG cells were treated 72 hours in 2% FBS containing medium with either solvent (DMSO) or ellipticine (0.1 - 20 µM). Proliferation was expressed as the percentage of living cells after ellipticine treatment compared to untreated cells grown in the presence of solvent considered as 100%. IC_{50} were determined using GraphPad Prism software, non-linear sigmoidal dose-response regression. **B.** Proliferation assay. U87MG cells were treated 24, 48, 72, 96, 168 or 192 hours in 2% FBS medium with either solvent (DMSO) or 1 µM ellipticine. Alternatively, medium was replaced after 48 hours of ellipticine treatment (elli 1 µM 48h) and cells were then grown in ellipticine-free medium. **C**. Cell cycle analysis of U373 (LEFT) and U87MG (RIGHT) cells. Cells were treated 24, 48 or 72 hours with solvent, or ellipticine (1 µM), stained with propidium iodide and cell populations detected by FACS analysis (n=5-10). **D**. Induction of apoptosis in U373 and U87MG cell lines. Cells were treated with 1 µM ellipticine for the times as indicated and fixed and stained by Hoechst 33342 dye. Percentage of cells with fragmented nuclei (apoptotic) was determined using fluorescent microscopy. At least 200 cells were analyzed per condition. **E**. Induction of senescence in U373 and U87MG cell lines. Cells plated in 6-well plates and left untreated or treated for 3 or 5 days in 2% FBS medium with 1 µM ellipticine before the detection of β-galactosidase activity at pH 6. Data represent positive cells percentage of at least 200 total cell number per condition (n=3).

Taken together, both glioblastoma cell lines, U87MG and U373, are sensitive to ellipticine. However, the mechanisms how ellipticine inhibits their proliferation are different. In U87MG cell line ellipticine induces G0/G1 cell cycle arrest, whereas U373 cells are blocked in S and G2/M cycle phase after ellipticine treatment. Ellipticine induces senescence but not apoptosis in U87MG cells, while U373 cells die from apoptosis and hardly senesce.

3. Role of the p53 pathway in ellipticine effects on human glioblastoma cell lines

To elucidate the molecular background of these ellipticine`s effects on U87MG and U373 cells, we investigated the effect of ellipticine on the regulatory proteins and genes

implemented in cell cycle and cellular survival regulation. We focused on the p53 signaling pathway, as the p53 is a key regulator of cell cycle and apoptotic processes and as it is known to be affected by ellipticine in diverse cell types (Kuo et al. , 2006, Peng et al., 2003). Moreover, U373 glioblastoma cell line expresses mutated (R273H) and non-functional p53.

In U87MG cells, p53 signaling pathway was strongly activated by ellipticine treatment, resulting in a very fast increase in p53 protein quantity present in the cell. As soon as after 3 hours of ellipticine treatment, the p53 protein level increased 2.6 times [**Figure 16**a]. The p53 activity is known to be regulated predominantly by two phenomena: i) stabilization of the protein, and ii) preservation against its ubiquitination. Therefore, such a protein quantity increase should indicate also p53 signaling pathway activation. This phenomenon was confirmed via quantification of the mRNA levels of some of the p53 downstream and upstream targets such as p21 (He et al., 2005), Fas (O'Connor et al., 1999), Mdm-2 (Moll and Petrenko, 2003), E2F1 (Wunderlich and Berberich, 2002), and ATM (Morgan and Kastan, 1997) [**Figure 16**b].

p21 is a cyclin-dependent kinase inhibitor blocking cell cycle progression in G1 phase due to inhibition of cyclin CDK-2 or -CDK4 complexes.

Mdm-2 indirectly participates at p53`s proteasomal degradation, whereas it acts as an E3 ubiquitin ligase recognizing the N-terminal trans-activation domain (TAD) of the p53. Moreover, it functions as an inhibitor of p53 transcriptional activation.

Fas is an important pro-apoptotic protein, which plays a central role in extrinsic apoptotic pathway initiation due to DISC (Death Inducing Signaling Complex) assembly and subsequent caspase-8 activation.

Ellipticine treatment apparently selectively activates the p53 signaling pathway, as the mRNA expression levels of the three p53 target proteins mentioned above (Mdm-2, p21 and Fas) were potentiated after 12 and 24 hours of ellipticine treatment while others remained unchanged or even inhibited. p21 induction by ellipticine was also confirmed at protein level [**Figure 16**c].

ATM is a specific serine/threonine kinase that is recruited and activated by DNA double-strand breaks. It phosphorylates p53 as well as other key proteins that initiate activation of the DNA damage checkpoint, leading to cell cycle arrest, DNA repair or apoptosis.

Messenger RNA level of p53 itself remained at the basal level after ellipticine treatment compared to un-treated cells, suggesting that the p53 expression occured at the protein level [**Figure 16**b].

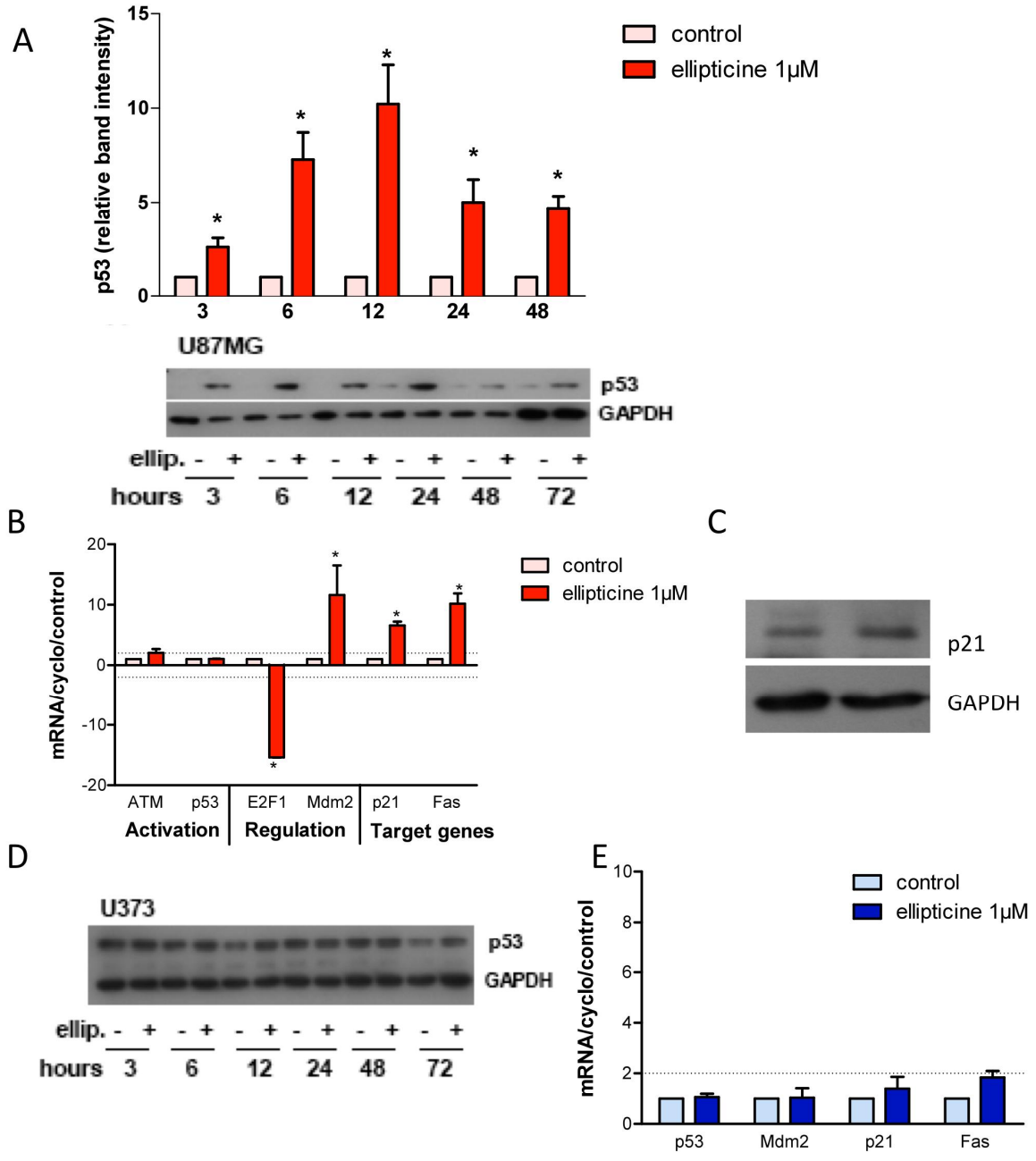

Figure 16: p53 pathway activation by ellipticine in U87MG and U373 cells. **A**. p53 protein expression in U87MG cells. Western blot analysis of U87MG cells treated with 1 µM ellipticine in 2% FBS containing medium for indicated times. GAPDH was used as a loading control. **B**. ATM, p53, E2F1, human mdm2, p21, and Fas mRNA levels in U87MG were determined by qPCR. Scattergrams represent the fold increase of mRNA in U87MG cells treated during 12 hours as compared to control cells and normalised with the reporter gene, cyclophilin (n=3). **C**. p21 protein expression. Western blot analysis of U87MG cells treated with 1 µM ellipticine in 2% FBS containing medium for 12 hours.

D. p53 protein expression in U373 cells. Western blot analysis of U373 cells treated with 1 µM ellipticine in 2% FBS containing medium for indicated times. GAPDH was used as a loading control. **E**. p53, human mdm2, p21, and Fas mRNA levels in U87MG were determined by qPCR. Scattergrams represent the fold increase of mRNA in U373 cells treated during 12 hours as compared to control cells and normalised with the reporter gene, cyclophilin (n=3).

In U373 glioblastoma cell line expressing mutated (R273H) and non-functional p53, the situation is different. Mutated p53 was reported to be expressed usually at high levels even in non-stimulated cells as its expression cannot be regulated by binding to Mdm-2 (Blandino et al., 1999). Therefore, we compared the p53 protein level in untreated U87MG (p53 wild type expressing) and in U373 (p53 mutated R273H) cell lines. At the basal level, U373 (p53mt) expressed much more p53 protein compared to U87MG (p53wt) cells. Moreover, the mutated p53 expressed in U373 seemed to be non-inducible by ellipticine by contrast to the wild type p53 in U87MG cell line [**Figure 16**d]. To confirm the malfunction of the p53mt (R273H), downstream targets of p53 were examined at the mRNA level. Ellipticine induced neither p21, nor Fas mRNA expression in U373 cells. Similarly, p53 mRNA level remained unaffected after ellipticine treatment [**Figure 16**e].

To summarize the results obtained in this very first part of our study, the functional p53 pathway is strongly activated by ellipticine treatment. Upon p53 activation, ellipticine induces senescence rather than apoptosis, whereas in the context of non-functional p53, ellipticine induces apoptosis, but not senescence. These data suggest that different responses of U87MG and U373 cells to ellipticine treatment originate from the different p53 status.

4. Ellipticine metabolism by human recombinant cytochromes P450

Oxidation of ellipticine by human recombinant cytochrome P450 1A1 (CYP1A1)

Human recombinant CYP1A1 in Supersomes® oxidized ellipticine mainly to 9-hydroxyellipticine, while other ellipticine metabolites were formed only in a minority [**Figure 17**a]. The peak of 12-hydroxyellipticine was not detected in this system. Nevertheless, its formation could not be excluded because it could have been covered by the great peak area of 9-hydroxyellipticine.

Formation of 13-hydroxyellipticine and 7-hydroxyellipticine was not quantified separately as they were eluted with similar retention times showing only shoulders in one broad peak.

Covalent DNA adducts 1 and 2 were generated in comparable amounts [**Figure 17**b].

Oxidation of ellipticine by human recombinant cytochrome P450 1B1 (CYP1B1)

Similarly to CYP1A1, 9-hydroxyellipticine was the major metabolite formed by human recombinant Supersomal CYP1B1 [**Figure 17**a]. Other ellipticine metabolites were formed only in a minority, similar to the case of CYP enzymes of the 1A subfamily. Formation of 12-hydroxyellipticine was not quantified.

Covalent DNA adducts 1 and 2 were generated in comparable amounts [**Figure 17**b].

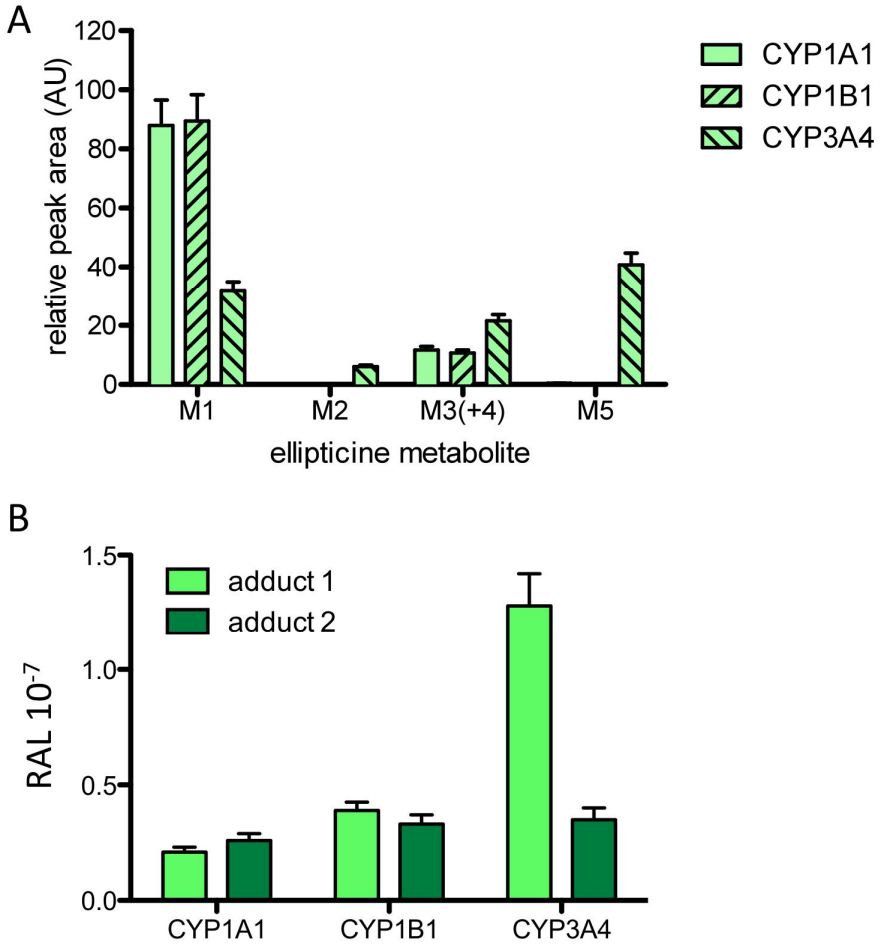

Figure 17: A. Quantification of formation of ellipticine metabolites by human recombinant CYP1A1, 1B1 and 3A4 enzymes in Supersomes. Ellipticine metabolites were separated by HPLC with UV detection. HPLC column: C18, 250 x 4.6 mm, 5 µm (Beckman, Fullerton, CA, USA), mobile phase: 64% methanol and 36% of 0.005 M heptane sulfonic acid and 0.032 M acetic acid in distilled water, detection wavelength: 296 nm. **B**. Quantification of the ellipticine-DNA adduct levels generated by human recombinant CYP1A1, 1B1 and 3A4 enzymes in Supersomes. Analyses were performed by the nuclease P1 version of the ^{32}P-postlabeling assay. Film exposure was 4 hr at -80°C. Origins are located at the bottom left corners (D3 from bottom to top and D4 from left to right) (n = 3).

Oxidation of ellipticine by human recombinant cytochrome P450 3A4 (CYP3A4)

CYP3A4 is the most abundant CYP isoform in human liver. Human recombinant CYP3A4 in Supersomes generated from ellipticine four metabolites: ellipticine N^2-oxide, 9-hydroxyellipticine, 13-hydroxyellipticine and 12-hydroxyellipticine [**Figure 17**a]. CYP3A4 was the only CYP enzyme metabolizing ellipticine primarily to DNA adducts-forming metabolites.

CYP3A4 generated high amounts of DNA adduct 1, while adduct 2 was formed to a lower extent, comparable to other CYPs tested [**Figure 17**b].

Among the CYPs tested, human recombinant CYP3A4 activates ellipticine most efficiently, as this enzyme generates high amounts of ellipticine metabolites responsible for covalent DNA adduct formation, which was confirmed by the ^{32}P-postlabeling technique.

5. Expression of ellipticine-metabolizing enzymes in U87MG and U373

Ellipticine has been shown to act *via* several mechanisms of action (Stiborova et al. , 2006). We are focusing at covalent DNA modifications - formation of DNA adducts, as it is a mechanism, which can at least partially explain ellipticine`s selectivity to tumor tissues. Such DNA adducts are not formed by ellipticine itself, but it needs to be metabolically activated. It has been reported to be metabolized by cytochromes P450 and/or peroxidases (Stiborova et al. , 2008, Stiborova et al. , 2007a) [see **Figure 5**]. Therefore, cell lines U87MG and U373 employed in the study were analyzed for the expression of biotransformation enzymes known to activate ellipticine: CYP1A1, 1B1, 3A4, cyclooxygenase 1 (COX-1), and lactoperoxidase (LPO) [**Figure 18**].

Expression of cytochrome P450 1A1 (CYP1A1)

CYP1A1 expression was tested at both, mRNA and protein levels. U87MG cells expressed 8 times more CYP1A1 mRNA and 1.5 times more CYP1A1 protein than U373 [**Figure 18**a]. Ellipticine induced CYP1A1 protein expression in U87MG cells in concentration dependent manner. Similarly, CYP1A1 mRNA level increased 6.5 times after 72 hours of 1 μM ellipticine treatment in U87MG cells [**Figure 18**b]. However, in U373 such treatment resulted in no significant change regarding both, mRNA and protein levels [**Figure 18**a,b].

Expression of cytochrome P450 1B1 (CYP1B1)

CYP1B1 expression in U87MG cell line was very strong at both, mRNA and protein levels. Expression of the CYP1B1 mRNA in U87MG exceeded that in U373 8.2 fold. One micromolar ellipticine treatment slightly induced CYP1B1 mRNA in U87MG (1.7 fold) but not in U373 [**Figure 18**a]. At the protein level, ellipticine treatment led to an outstanding induction of CYP1B1 expression. Further substantial increase of CYP1B1 level was not observed when higher (10 µM) ellipticine used [**Figure 18**c]. In contrast, in U373 cells, CYP1B1 protein was expressed in much lower levels and no induction was observed [**Figure 18**b].

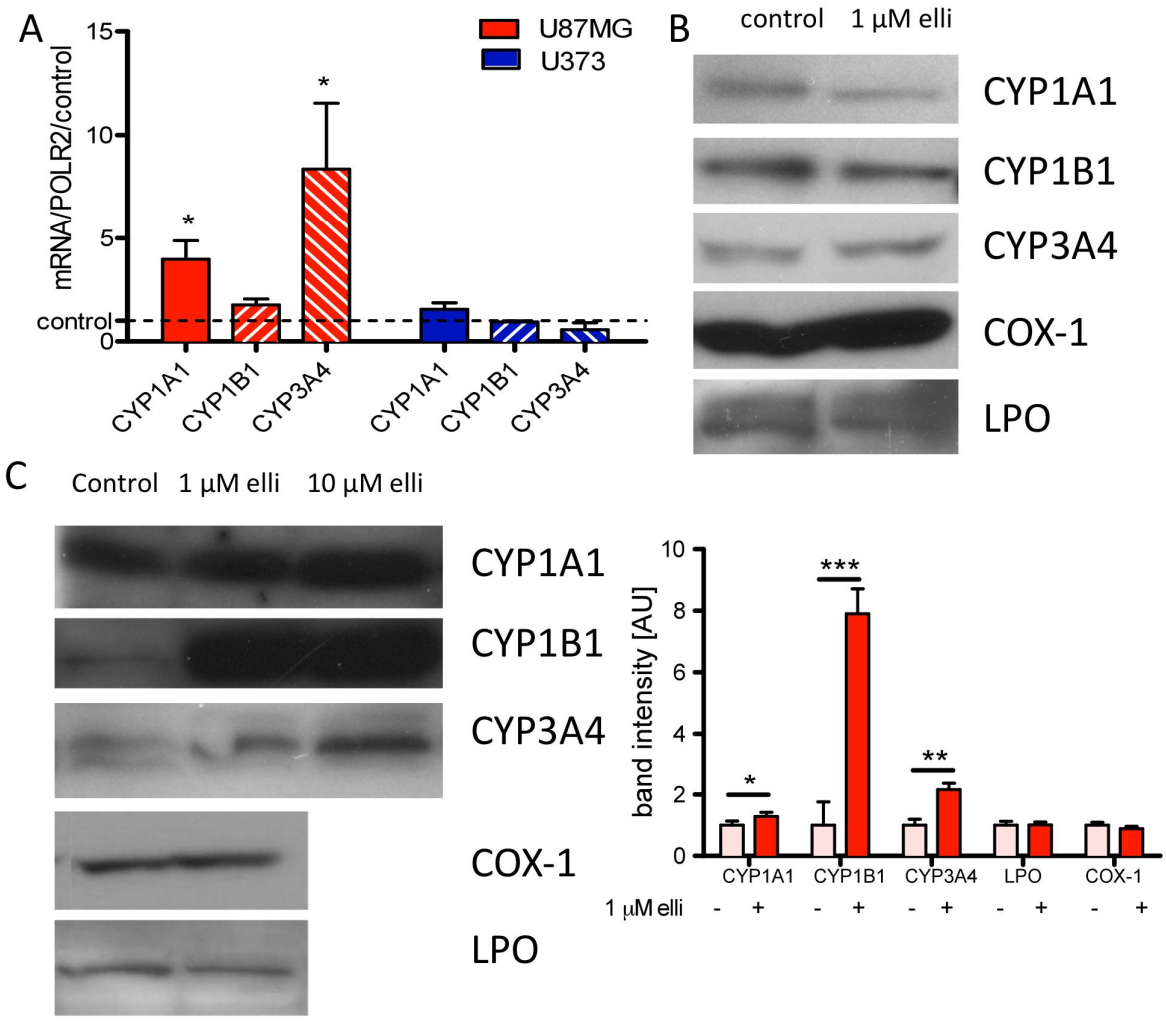

Figure 18: A. *CYP1A1, 1B1* and *3A4* mRNA levels were determined by qPCR. Scattergrams represent the fold increase of mRNA in U87MG cells treated during 72 hours in 2 % FBS containing EMEM medium as compared to control cells and normalized with the reporter gene, POLR2 (n=3). **B**. The CYP1A1, 1B1, 3A4, LPO and COX-1 protein expression in U87MG cells treated with 1 µM (and

10 μM) ellipticine in 2% FBS medium for 72 hours. Total protein extracts were resolved by SDS-PAGE, transferred to PVDF membranes and probed with anti-CYP antibodies. GAPDH was used as a loading control. A representative blot is shown and the graph on the right displays means relative band intensities quantified using Elfoman software (n=3, S.E.M. < 10%). **C.** The CYP1A1, 1B1, 3A4, LPO and COX-1 protein expression in U373 cells treated with 1 μM ellipticine in 2% FBS medium for 72 hours. Total protein extracts were resolved by SDS-PAGE, transferred to PVDF membranes and probed with anti-CYP antibodies. GAPDH was used as a loading control. A representative blot is shown.

Expression of cytochrome P450 3A4 (CYP3A4)

We detected small amounts of CYP3A4 mRNA in U87MG glioblastoma cells as well as apparent amounts of CYP3A4 protein. The mRNA content was slightly lower in U373 compared to U87MG cells [**Figure 18**a]. Ellipticine treatment (1 μM, 72 hours) induced CYP3A4 in U87MG 7-fold at the mRNA level. Likewise, CYP3A4 protein expression in U87MG was induced by ellipticine in concentration-dependent manner [**Figure 18**c].

Expression of lactoperoxidase (LPO)

LPO expression was examined at the protein level and indispensable amounts of this enzyme were detected in both cell lines tested. Ellipticine treatment (1 and 10 μM for 48 hours) did not affect the LPO expression in either of the cell types [**Figure 18** b,c].

Expression of cyclooxygenase 1 (COX-1)

COX-1 protein was also found to be expressed in both cell lines, U87 and U373. However, ellipticine treatment did not induce or inhibit its protein expression [**Figure 18** b,c].

6. Ellipticine metabolism in U87MG and U373

In additional part of our work, ellipticine metabolism in U87MG and U373 cells was studied. HPLC was used to separate and detect them. Interestingly, ellipticine metabolite profiles differed significantly according to the cell type as well as to ellipticine concentration [**Figure 19**a,b].

Treatment of U373 cells with ellipticine, both its concentrations used (1 and 10 μM) resulted in predominant generation of 13-hydroxyellipticine (M3) and ellipticine-*N2*-oxide (M5). Their amount was ellipticine concentration-dependent [**Figure 19**b].

In contrast, when low concentrations (1 μM) of ellipticine were used for the U87MG treatment, detoxifying metabolite 9-hydroxyellipticine (M1) was formed predominantly. However, when 10 μM ellipticine was administered to U87MG cells, detoxification/activation

metabolites ratio inversed completely resulting in predominant formation of 13-hydroxyellipticine (M3) and ellipticine-*N2*-oxide (M5), which are ellipticine metabolites responsible for covalent DNA modifications [**Figure 19**a].

Therefore, we examined whether ellipticine modifies covalently DNA in glioblastoma cell line U87MG as it occurs *in vivo* in rat brain [**Figure 19**c]. We proved ellipticine dose-dependent covalent DNA adduct formation using the technique of ^{32}P-postlabeling. The amounts of adduct 2, which is generated from ellipticine-12-ylium, were 2.2 times higher than those of adduct 1, formed from ellipticine-13-ylium [**Figure 19**d,e].

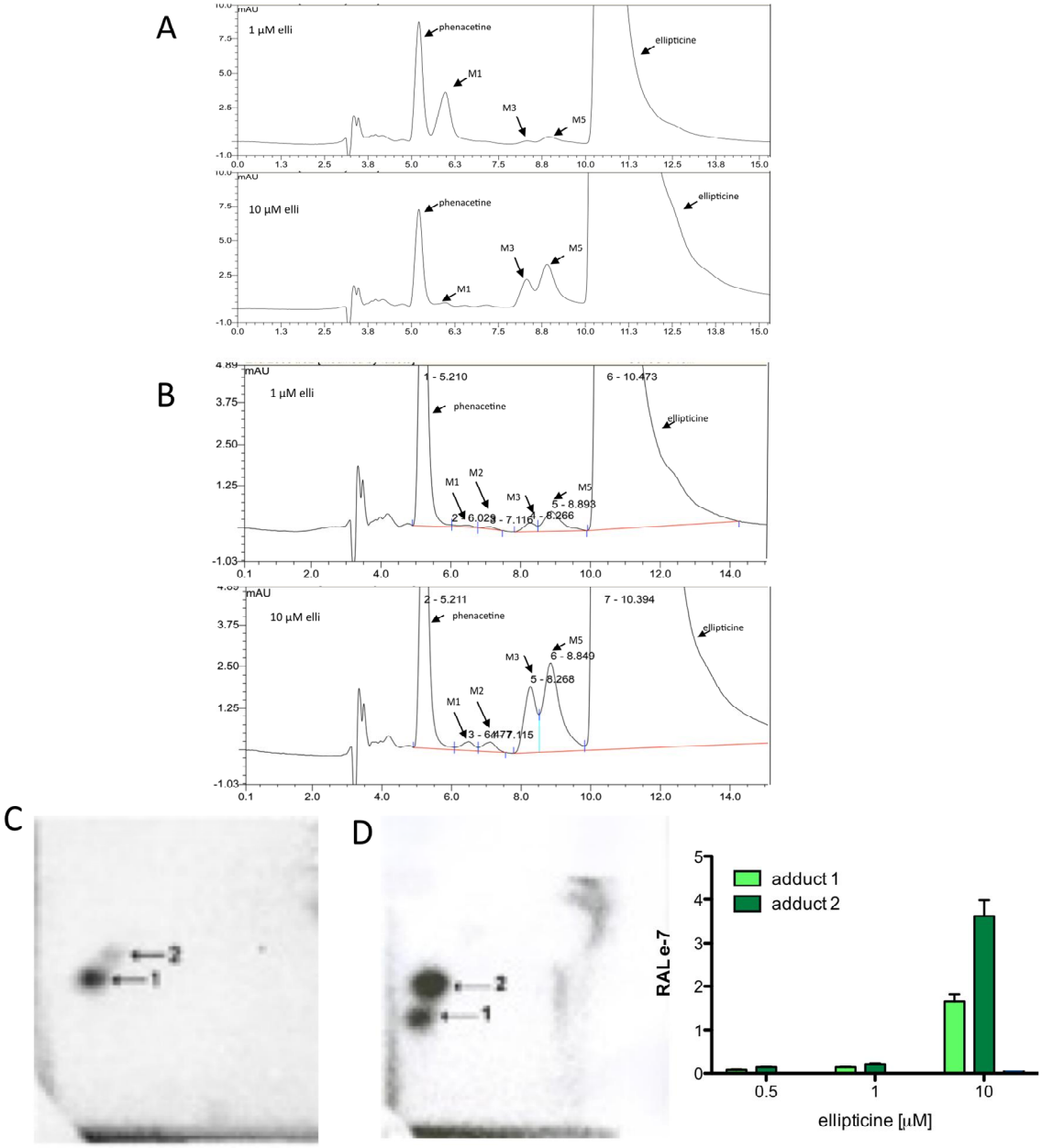

Figure 19: A. HPLC separation of ellipticine metabolites formed in U87MG cells, and **B**. U373 cells. Cells were treated with 1 μM (A) and 10 μM (B) ellipticine for 72 hours in 2 % FBS containing EMEM. HPLC column: C18, 250 x 4.6 mm, 5 μm (Beckman, Fullerton, CA, USA), mobile phase: 64% methanol and 36% of 0.005 M heptane sulfonic acid and 0.032 M acetic acid in distilled water, detection wavelength: 296 nm. **C.** Autoradiograph of PEI-cellulose TLC maps of ^{32}P-labeled digests of DNA isolated from brain of rats treated with 40 mg ellipticine per kg body weight (Stiborová et al., 2003a), **D**. U87MG cells treated with 1 μM ellipticine. **E.** Quantification of the ellipticine-DNA adduct levels generated in U87MG cells treated with ellipticine for 72 hours. Analyses were performed by the nuclease P1 version of the assay (Stiborova et al. , 2001, Stiborova et al., 2003). Film exposure was 4 hr at -80°C. Origins are located at the bottom left corners (D3 from bottom to top and D4 from left to right) (n = 3).

Ellipticine chemotherapy : Conclusions and discussion

In the first part of this work, we investigated ellipticine effects on two glioblastoma cell lines varying in the p53 status, U87MG and U373.

Ellipticine was chosen as a model chemotherapeutic drug known to act via multiple mechanisms of action. It was used in clinical medicine, primarily against advanced breast cancer. Moreover, it exhibits a high potential to reduce growth of diverse other cancers and it has been proven to exhibit a certain specificity to brain tumors (Acton et al. , 1994). Although the former study of Gouyette et al. claimed low distribution of ellipticine salts into brain parenchyma (Gouyette et al., 1982), our recent work has proven ellipticine covalent DNA-adduct formation in rat brain (Stiborova et al., 2007b). These findings together with ellipticine`s hydrophobic character suggest it to be able to overcome the blood-brain barrier.

Ellipticine derivatives have been studied for the glioma therapy in combination with topoisomerase I inhibitors (Ciesielski and Fenstermaker, 1999), or alone *in vitro*. The 9-chloro-2-methylellipticinium acetate (NMHE) was studied *in vivo* on human brain tumor xenografts in combination with carmustine, but these studies did not give encouraging results (Arguello et al., 1998).

Here we evaluated ellipticine`s cytotoxic effects showing it inhibited U87MG and U373 cell proliferation with IC_{50} in micromolar ranges, which is comparable to other ellipticine-sensitive cancer cell lines. However, regarding these effects in more detail, we found that the response to ellipticine treatment was completely different comparing these two cellular models.

In p53wt expressing U87MG cells, ellipticine provoked an early G0/G1 cell cycle arrest, whereas in U373 (p53mt) cells were blocked in S and G2/M phase. It has been previously reported, that the p53 mutation sensitizes some cancer cells to chemotherapy (Yamasaki et al.,

2009). Here, ellipticine therapy induced premature senescence but not apoptosis in U87MG cells, while U373 cells reacted inversely. Since the functional p53 pathway is strongly activated by ellipticine treatment, we hypothesize that different answers of U87MG and U373 cells to ellipticine treatment originate from their different p53 status. The p21 is supposed to be primarily responsible for senescence regulation. Since p21 is a p53`s downstream target, our results suggest, that it is due the p53 non-functionality, why U373 cells hardly senesced when treated with ellipticine. Senescent cells remain alive and may even stimulate their environment by secretion of pro-proliferative factors. Therefore, ellipticine treatment of U373 cells expressing p53 mutant is more efficient than that of U87MG p53-wt expressing cells, since non-functional p53 results in ellipticine-induced apoptosis.

The mode of antitumor, cytotoxic and mutagenic action of ellipticine is considered to be based mainly on DNA damage such as intercalation into DNA, inhibition of topoisomerase II and formation of covalent DNA adducts. Intercalation of ellipticine into DNA and inhibition of topoisomerase II occur in all cell types irrespective of their metabolic capacity, because of the general chemical properties of this drug and its affinity to DNA and topoisomerase II protein (Garbett and Graves, 2004). In contrast, the formation of ellipticine-DNA adducts is dependent on ellipticine activation by CYPs and peroxidases. Therefore, this anticancer agent should be considered a drug, whose pharmacological efficiency and/or genotoxic side effects are dependent on its cytochrome P450 (CYP) and/or peroxidase-mediated activation (Stiborova et al., 2004).

We were thus investigating, whether our model glioblastoma cell lines U87MG and U373 express such biotransformation enzymes. Both cell lines were found to express enzymes metabolizing ellipticine, namely CYP1A1, CYP1B1, CYP3A4, lactoperoxidase (LPO) and cyclooxygenase-1 (COX-1). Moreover, ellipticine induced expression of the CYP enzymes in U87MG suggesting that it is regulating its own metabolism. On the contrary, the pattern of expression of biotransformation enzymes in U373 was much poorer. Moreover, neither of the enzymes exhibited inducibility by ellipticine.

These results were in accordance with ellipticine metabolites profiles generated in both cell lines employed in the study. In U87MG cells, ellipticine concentration dictated the ratio between the detoxifying and activating metabolites. At higher concentrations, ellipticine metabolites responsible for DNA adducts formation became predominant. However, in U373 cells, ellipticine generated its metabolites also in a concentration-dependent manner but

without affecting the relative metabolite pattern. Such results may be explained by different extends of inductions of individual CYPs in U87MG.

We observed certain discrepancies between ellipticine-mediated CYP induction at protein and mRNA level. Similar differences between induction of mRNA of several CYPs and protein levels were found also for other compounds by other authors in rats treated with ellipticine (Aimova et al., 2007) and for other compounds as found by several authors (Chen et al., 1998, Dickins, 2004). This might be due to the fact that some inducers might prolong half-lives of mRNAs, whereas others increase their transcription.

Human recombinant CYP3A4 generated primarily 12-, 13-hydroxyellipticine and ellipticine N2-oxide (all three metabolites that are responsible for covalent DNA modifications). CYP1A1 metabolized ellipticine mainly to 9-hydroxyellipticine and in a minority also to 13-hydroellipticine. Likewise, CYP1B1 generated primarily detoxifying 9-hydroxyellipticine. Since CYP1A1 and CYP3A4 enzymes were inducible by ellipticine in a concentration-dependent manner, whereas low ellipticine concentrations already led to CYP1B1 expression saturation, we hypothesize, that this could at least partially explain inverse ratio between detoxifying and activating ellipticine metabolites when changing the drug concentration.
However, the systems containing human recombinant CYPs (Supersomes®) are only approximate models of the situation in human tissues. Other CYP forms may be involved in ellipticine metabolis in brain tumoral tissue. Furthermore, the enzymatic activity of the CYPs is known to be influenced by presence of cytochrome b_5 widely expressed in all tissues (Porter, 2002).

Taken together, we confirmed that U87MG cell line expressed biotransformation enzymes generating ellipticine metabolites known to covalently bind to deoxyguanosine in DNA as well as formation of these ellipticine metabolites: 13-hydroxyellipticine and ellipticine N2-oxide. Subsequently, we found indispensable amounts of two major ellipticine-DNA adducts formed in U87MG cells. Their levels were comparable to those found in neuroblastoma or leukemia cells (Poljakova et al., 2009, Poljakova et al., 2007). Because the covalent ellipticine-derived DNA adducts are also generated in brain tissues in vivo, in rats treated with ellipticine [see **Figure 19**c], ellipticine and/or its metabolites probably overcome the blood-brain barrier, which is an important criteria in brain tumor chemotherapy.

Part **IV.**B: Combination therapy of chemotherapeutics and **α**5**β**1 integrin antagonists

Currently, ellipticine is not being used in clinic, as it exhibits important toxicity *in vivo*. Since it seems to be highly efficient and rather selective against glioblastoma, it is worth to reduce its toxic side effects by reducing the dose ***e.g.*** by combining it with α5β1 integrin-targeted therapy. In this study, we were searching whether such combination therapy would be profitable for the final therapy outcome in glioblastomas.

Recent results from our laboratory showed the effects of a specific non-peptidic α5β1 integrin antagonist, SJ749, on glioblastoma cell lines U87MG and A172 *in vitro* (Maglott et al. , 2006). In the first part of this work we were investigating ellipticine`s effects on U87MG and U373 glioblastoma cell lines. Based on these data, here we study the effects of the combination therapy (ellipticine chemotherapy with α5β1 integrin antagonists, SJ749 or K34c) on human glioblastoma cell lines U87MG and U373 *in vitro*. To confirm the most important results, we used temozolomide, which is a reference chemotherapeutic drug used currently in clinical practice against glioblastoma.

1. Analysis of different experimental conditions of drug combinations

<u>Combination therapy of glioblastoma: ellipticine with SJ749;</u>

Three different treatment schedules were tested:

1. Cells were treated concomitantly with ellipticine and SJ749 at the time of plating, thus both drugs were administered to non-attached cells. In 10 % serum containing medium, SJ749 had no effect on U87MG cell proliferation. Ellipticine effect reached up to 26.2% inhibition of cell proliferation at 72 hours of treatment. Addition of integrin antagonist did not significantly increase the proliferation inhibition compared to single ellipticine treatment [**Figure 20**a LEFT]. More promising results were reached, when we performed similar experiments under reduced serum conditions (2% serum containing medium). Despite non-treated cells proliferated normally, efficacy of SJ749 seemed to be dependent on serum concentration as it was able to inhibit cell proliferation to up to 33.6%. Ellipticine was also more efficient under reduced serum conditions inhibiting U87MG cell proliferation by 56.8% compared to 26.2%. Combination of both drugs resulted in 85.2% proliferation inhibition [**Figure 20**a RIGHT].

2. Cells were treated with the first drug (SJ749 or ellipticine) at the time of plating and 24 hours later, the second drug was added. Here, the first drug was administered to non-attached cells, whereas the second one to already attached cells. When SJ749 administered prior to ellipticine, it had weak but significant inhibitory effect on U87MG cell proliferation in 10% FBS containing medium, which increased under reduced serum conditions [**Figure 20**b LEFT in 10% FBS; RIGHT in 2% FBS]. When ellipticine administered prior to SJ749 [**Figure 20**c LEFT in 10% FBS; RIGHT in 2% FBS], SJ749 had no significant effect on cell proliferation either in 10%, or in 2% FBS containing medium. Combination therapy resulted in same inhibitory effects as the single ellipticine treatment.

3. To avoid drug interferences, we tried to withdraw the first drug before the second treatment launch. Non-attached cells were treated with the first drug. Twenty-four hours later, drug-containing medium was replaced for the fresh one, which was containing the second drug. Nevertheless, it did not improve the result compared to the second treatment schedule without media change. When 5 μM SJ749 administered prior to **1** μM ellipticine treatment, 72 hours after the addition of the second drug, inhibition of proliferation reached 37.2% [**Figure 20**d LEFT]. The reverse treatment order resulted in 45.4% inhibition of proliferation (5 μM SJ749 + **2** μM ellipticine) [**Figure 20**d RIGHT].

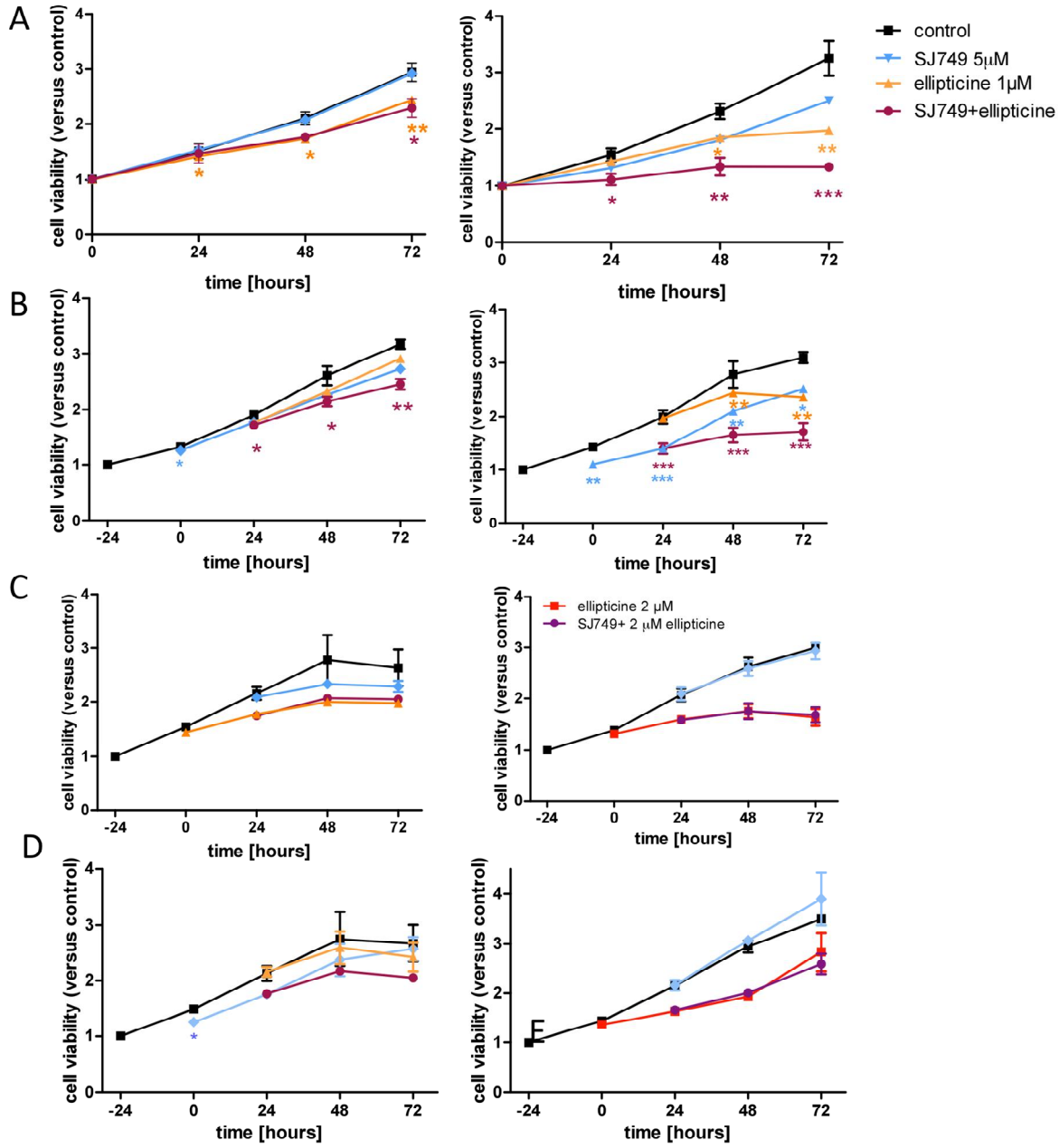

Figure 20: Effect of an α5β1 integrin antagonist SJ749, ellipticine and their combination on glioblastoma cell viability under various experimental conditions. Viability was measured every 24 hours using the MTS assay. Results are expressed as the relative number of living cells versus cells at the time of plating (n=3 in sextuplates). **A.** U87MG cells were treated either with solvent (black), 5 µM SJ749 (blue), 1 µM ellipticine (orange) or with a combination of both drugs (violet) at the time of plating. LEFT: in 10% FBS; RIGHT: in 2% FBS. **B**. U87MG cells were treated either with solvent (black) or 5 µM SJ749 (blue) at the time of plating. 1 µM ellipticine was added to solvent-treated (orange) or to SJ749-treated (violet) cells 24 hours after plating. LEFT: in 10% FBS; RIGHT: in 2% FBS. **C**. U87MG cells were treated either with solvent (black) or 1 µM (orange) / 2 µM (red) ellipticine at the time of plating. 5 µM SJ749 was added to solvent-treated (blue) or to ellipticine-treated (violet) cells 24 hours after plating. LEFT: in 10% FBS; RIGHT: in 2% FBS. **D**. U87MG cells were treated either with solvent (black) or 5 µM SJ749 (blue) at the time of plating. 1 µM ellipticine was added to solvent-treated (orange) or to SJ749-treated (violet) cells 24 hours after plating. Before

ellipticine addition, medium was replaced. Experiment performed in 10% FBS containing medium. **E**. U87MG cells were treated either with solvent (black) or 2 µM ellipticine (red) at the time of plating. 5 µM SJ749 was added to solvent-treated (blue) or to ellipticine-treated (violet) cells 24 hours after plating. Before SJ749 addition, medium was replaced. Experiment performed in 10% FBS containing medium.

These results revealed that SJ749 was more potent to inhibit proliferation when it acts before the adhesion of cells. No floating cells corresponding to unattached cells could be observed during the experiment. Results also show that inhibition of cell proliferation by SJ749 was sensitive to the level of serum in the medium possibly related to the integrin-growth factor receptors interactions. Similarly, ellipticine efficiency was also dependent on serum level, possibly due to its interactions with serum proteins that are decreasing the free drug concentration. Taken together, both drugs were most efficient when used under reduced serum conditions and on non-attached cells. Therefore, immediate co-treatment with 5 µM SJ749 and 1 µM ellipticine in 2 % serum was evaluated as the optimal combination therapy protocol and was used in all subsequent experiments.

2. Effects of chemotherapy combined with an integrin antagonist on the U87MG cell cycle

Combination therapy of glioblastoma: ellipticine with SJ749

Using the optimized treatment protocol of combination therapy of 5 µM SJ749 with 1 µM ellipticine, we analyzed cell cycle using flow cytometry 12, 24, 48, and 72 hours of treatment. Previous results of our laboratory showed that SJ749 transiently blocked the cell cycle progression in G0/G1 phase persisting for 48 hours without affecting other phases markedly (Maglott et al. , 2006). As stated in the first part of this work, single ellipticine treatment resulted in a transient G0/G1 cycle arrest and slight G2/M cycle block starting at 72 hours of treatment

[

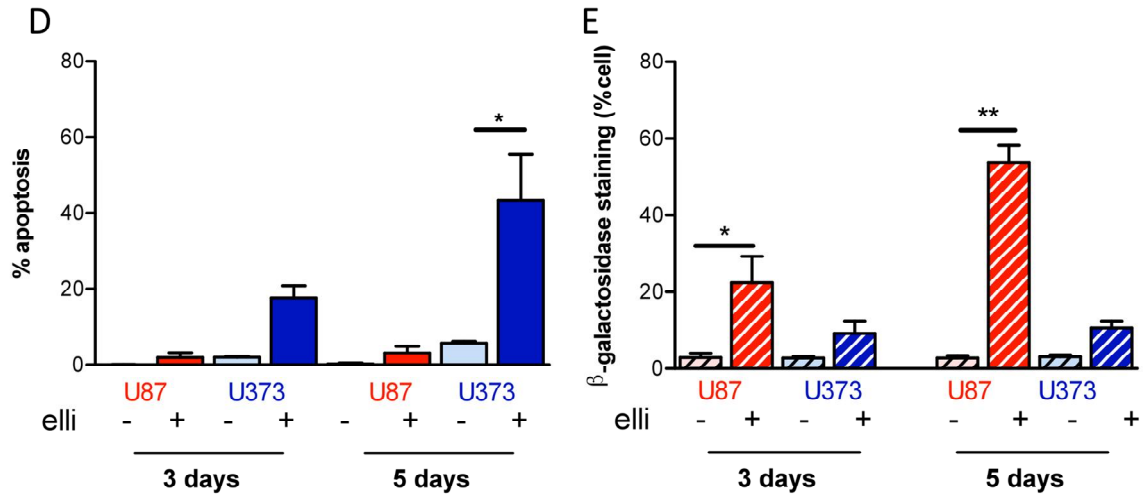

Figure 15c, p 71].

Combination of both agents resulted in persisting G0/G1 cell cycle arrest reaching 90.4 % compared to 76.7 % for single ellipticine treatment. Ellipticine-induced depression of the synthetic phase (18.1 % to 5.3 %) was even more pronounced when integrin antagonist added reaching only 2.5 % after 72 hours of treatment. G2/M phase was not affected compared to non-treated cells, counteracting the ellipticine-induced G2/M cell cycle arrest [**Figure 21**a].

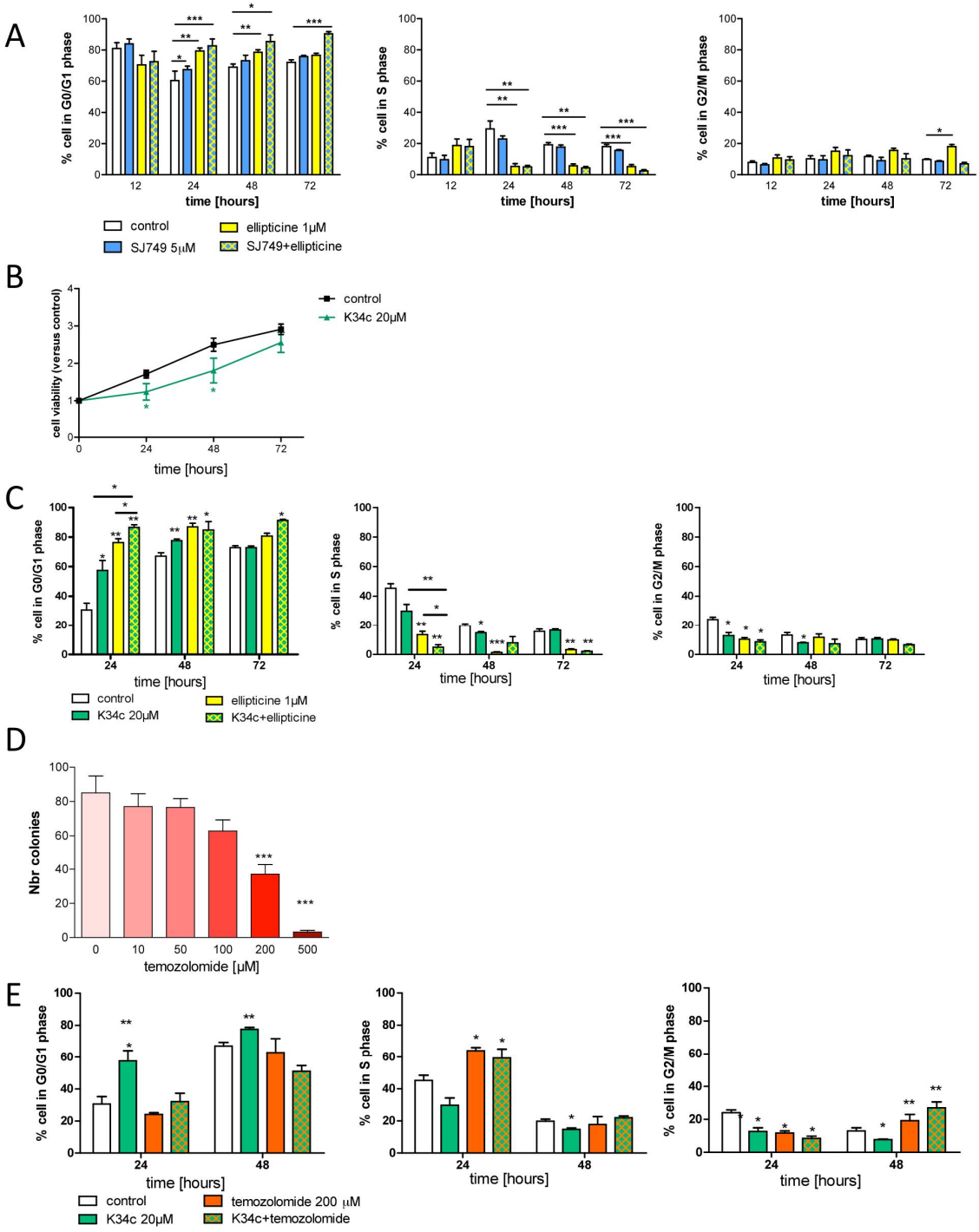

Figure 21: Effects of the chemotherapy combined with an α5β1 integrin antagonist on U87MG glioblastoma cell line. **A**. Cell cycle analysis. U87MG cells were treated for 24, 48, and 72 hours in 2% serum medium either with solvent, 5 µM SJ749, 1 µM ellipticine or with a combination of both drugs before propidium iodide staining and cell cycle analysis by flow cytometry. **B**. Proliferation assay. Cells were grown in 2% FBS containing medium and treated either with solvent (DMSO), or K34c (20 µM). Viability was measured every 24 hours using the MTS assay. Results are expressed as the relative number of living cells versus cells at the time of plating (n=3 in sextuplates). **C.** U87MG cells were treated for 24, 48, and 72 hours in 2% serum medium either with solvent, 20 µM K34c, 1 µM ellipticine or with a combination of both drugs before propidium iodide staining and cell cycle analysis by flow cytometry. **D.** Clonogenicity. Cells were grown in 2% FBS containing medium and

treated either with different concentrations of temozolomide (0 - 500 µM) for 72 hours and then grown in 10% FBS containing medium for 7 more days. After fixtion and staining, numver of colonies was determined. **E**. U87MG cells were treated for 24 and 48 hours in 2% serum medium either with solvent, 20 µM K34c, 200 µM temozolomide or with a combination of both drugs before propidium iodide staining and cell cycle analysis by flow cytometry. Data represent the percentage of cells in G0/G1, S, G2/M.

Combination therapy of glioblastoma: ellipticine with K34c

We used also another α5β1 integrin antagonist, K34c, first synthetized by Pr Kessler`s team (Heckmann et al. , 2008). It antagonizes α5β1 integrin as well as αvβ3, but its affinity for the α5β1 is much more important compared to that for αvβ3. Our previous results have shown that K34c significantly inhibits cell proliferation of U87MG at the concentration of 20 µM after 48 hours of treatment [**Figure 21**b].

K34c had similar effects on U87MG cell cycle progression as SJ749: 20 µM K34c treatment led to the G0/G1 cycle arrest at 24 and 48 hours reaching 58% and 78% respectively, but did not persist till 72 hours. Simultaneously, S and G2/M phase populations decreased.

Concomitant K34c-ellipticine treatment affected U87MG cell cycle in the same manner like SJ749 + ellipticine did, that is G0/G1 cell cycle arrest that persisted till 72 hours [**Figure 21**c].

Combination therapy of glioblastoma: temozolomide with K34c

Recently, temozolomide (TMZ) became a reference drug for glioblastoma chemotherapy. Therefore we employed this agent to expand our study. We have shown that temozolomide inhibits clonogenicity of U87MG cells [**Figure 21**d]. Two-hundred micromolar concentration was used in combination therapy experiments.

Temozolomide blocked cell cycle of U87MG cells in S (rising from 19.8 % to 22.0 %) and G2/M (rising from 13.1 % to 27.0 %) phases instead of the G0/G1 phase. In combination with K34c, the G2/M cycle arrest was even more pronounced (27.0 % compared to 19.2 % for temozolomide alone) [**Figure 21**e].

These results show that the two integrin antagonists, SJ749 and K34c, arrest U87MG cell cycle in G0/G1 phase. However, such cycle arrest did not persist more than 48 hours. Ellipticine-induced G0/G1 cell cycle arrest was intensified and prolonged by addition of integrin antagonist. Since temozolomide blocked the cell cycle rather in S and G2/M phases, integrin antagonist tended to exhibit inverse effects on cell cycle distribution when used in combination. However, temozolomide effects overrode those

of integrin antagonist. This finding underlines the importance of chemotherapeutic drug mechanisms of action when used in combination with integrin antagonist, since their effect on the cell cycle distribution might be either additive, or inverse.

3. Apoptosis and senescence in U87MG induced by the chemotherapy combined with an α5β1 integrin antagonist

We have shown that cytotoxic effects of the SJ749 and ellipticine therapy are additive at least in case of proliferation inhibition. As we showed in the first part of this work, ellipticine treatment induces senescence in U87MG cells. Therefore, we examined senescence induction in U87MG after its combination with α5β1 integrin antagonists, SJ749 and K34c.

Senescence induction in U87MG cells

Integrin α5β1 antagonists, SJ749 or K34c, themselves did not affect senescence. Interestingly, senescence induced by ellipticine treatment (29.6% at 72 hours) was repressed by both, SJ749 or K34c, to basal levels (4.1 % for non-treated cells). SJ749 decreased ellipticine-induced senescence from to 3.3% and K34c to 8.8% [**Figure 22**a LEFT]. Effects of integrin antagonists on chemotherapy-induced senescence were confirmed by combining temozolomide with K34c. Single temozolomide treatment resulted in 23.2 % senescence induction, which was decreased by K34c addition to 4.1% [**Figure 22**a RIGHT].

Apoptosis induction in U87MG cells

Since integrin antagonists counteracted chemotherapy induced senescence, while cell proliferation was inhibited more importantly after the combination therapy, we regarded apoptotic cell death as another possible cellular answer to drug-induced stress.

Analyzing the subG1 cell cycle population, we detected a significant increase of apoptotic population after 24 and 48 hours of concomitant treatment with ellipticine and any of the α5β1 integrin antagonists, SJ749 (5 μM) or K34c (20 μM). Single ellipticine treatment did not significantly increase apoptotic population, whereas SJ749 addition led to apoptosis induction reaching 15.8% and 15.1% after 24 and 48 hours, respectively. K34c in combination with ellipticine induced 18.2% and 22.3% after 24 and 48 hours, respectively [**Figure 22**b LEFT]. These important results were confirmed by another drug combination: temozolomide + K34c. After 24 hours of treatment, such combination therapy resulted in 11.5% apoptosis. Although

temozolomide induced apoptotic cell death itself after 48 hours of treatment, its combination with K34c led to further significant apoptotic population increase reaching 16.6 % compared to 9.0% for single temozolomide treatment [**Figure 22**b RIGHT].

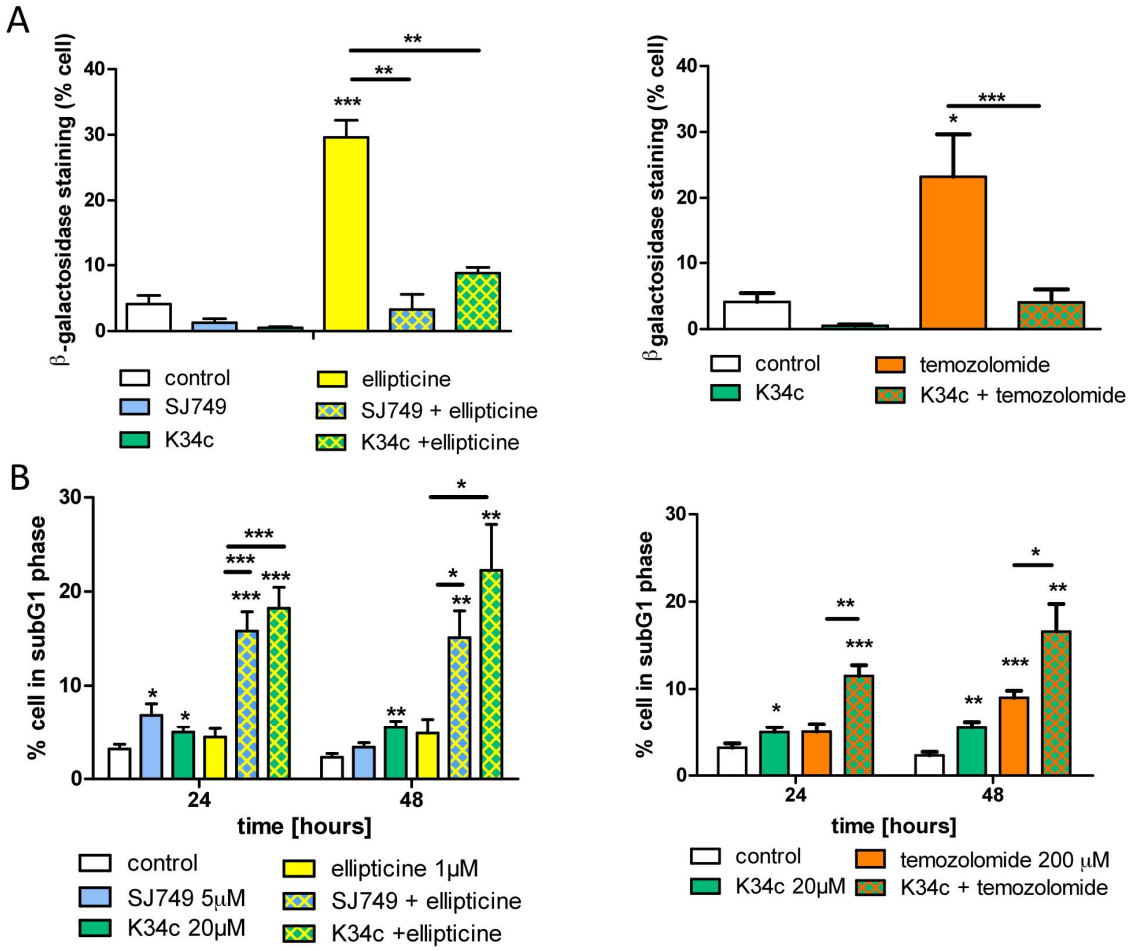

Figure 22: Effect of α5β1 integrin antagonists, chemotherapy and their combination on apoptosis and senescence of U87MG cells. **A**. LEFT: U87MG cells were treated 3 days with either solvent, SJ749 (5 μM), K34c (20μM), ellipticine (1 μM) or combinations before the detection of β-galactosidase activity at pH 6. (n=3). RIGHT: Similar experiments with temozolomide (200 μM) and K34c combination (n=3). **B**. LEFT: U87MG cells were treated 24 or 48 hours with solvent, SJ749 (5 μM), K34c (20 μM), ellipticine (1 μM) or combinations, stained with propidium iodide and subG1 cell population detected by FACS analysis (n=5-10). RIGHT: Similar experiments with K34c and temozolomide (200 μM) (n=4).

These key results of our study show for the first time that α5β1 antagonists modulate cellular response to chemotherapy. Chemotherapy-induced senescence is depressed by the addition of an α5β1 antagonist, while apoptosis is concomitantly increased. Integrin antagonists are thus favoring apoptotic cell death to senescence after drug-induced stress stimuli.

4. The role of the p53 pathway in cellular response of the U87MG cell line (p53wt) to the chemotherapy combined with α5β1 integrin antagonists

We further investigated the effects of the combination therapy on regulatory proteins and genes implemented in senescence and cellular survival regulation. We focused on the p53 signaling pathway as a key regulator of cell cycle, senescence and apoptosis. p53 pathway is known to be affected by ellipticine in diverse cell types (Kuo et al. , 2006, Peng et al. , 2003) and was shown to be strongly activated in U87MG cells in the first part of this work. Similarly, temozolomide chemotherapy was reported to have a connection with the p53 pathway (Li et al., 2009b). Therefore, we examined how the various treatment combinations influenced the p53 expression and activity.

As shown in

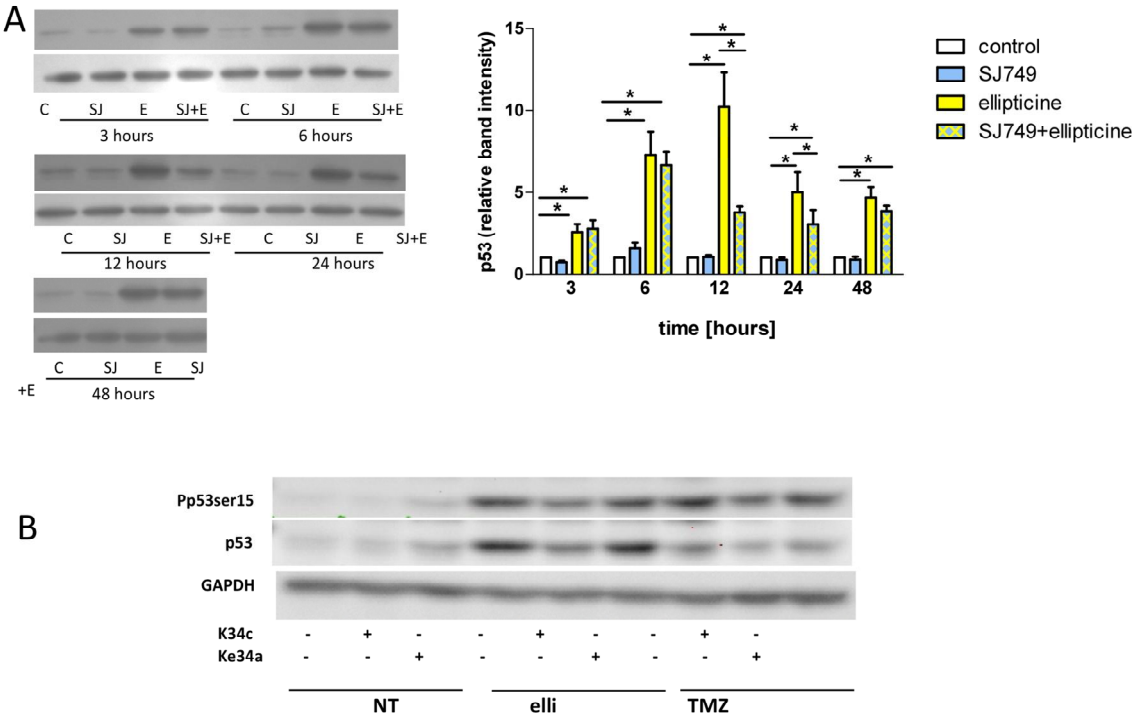

Figure 23a, SJ749 did not affect p53 basal level at any time tested, which contrasts with the striking increase of p53 protein cells exposed to ellipticine with a maximal activity at 12 hours. Combination

of both drugs increased p53 protein, but not mRNA expression above the basal level but significantly less than with ellipticine alone after 12 hours co-treatment. [

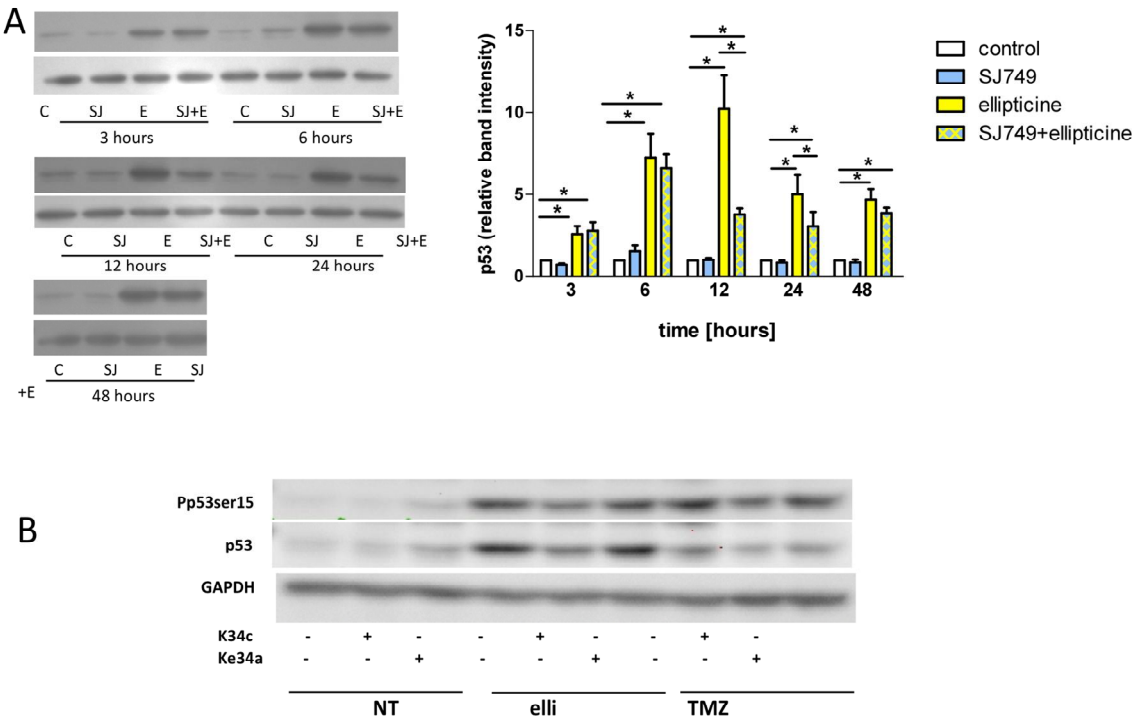

Figure 23a,b]. In addition, p53 activity measured by its phosphorylation at Ser15 was increased by ellipticine and temozolomide and decreased by K34c [

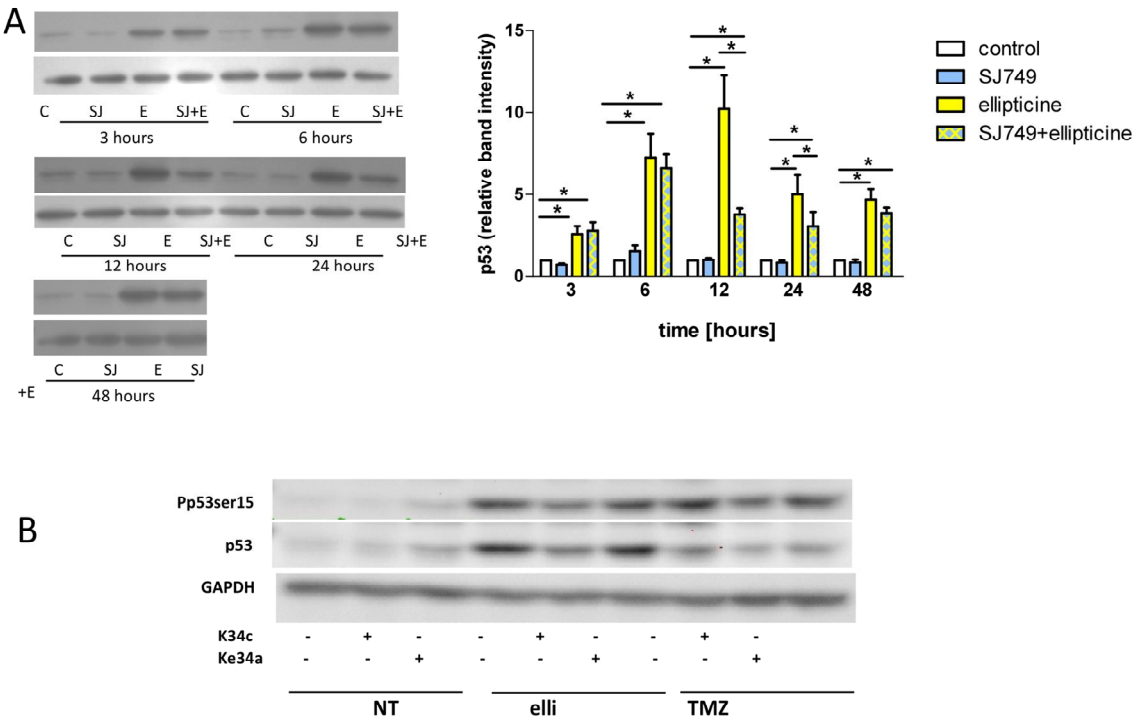

Figure 23b].

To confirm the specificity of the antagonists for the integrin α5β1, we used another integrin antagonist Ke34a, which is structurally similar to K34c, but exhibits 2000 times less affinity to α5β1 integrin than K34c (Heckmann et al. , 2008). Ke34a exhibited no effect on stabilization or activation of p53 protein confirming that α5β1 integrin and p53 functions are related
[

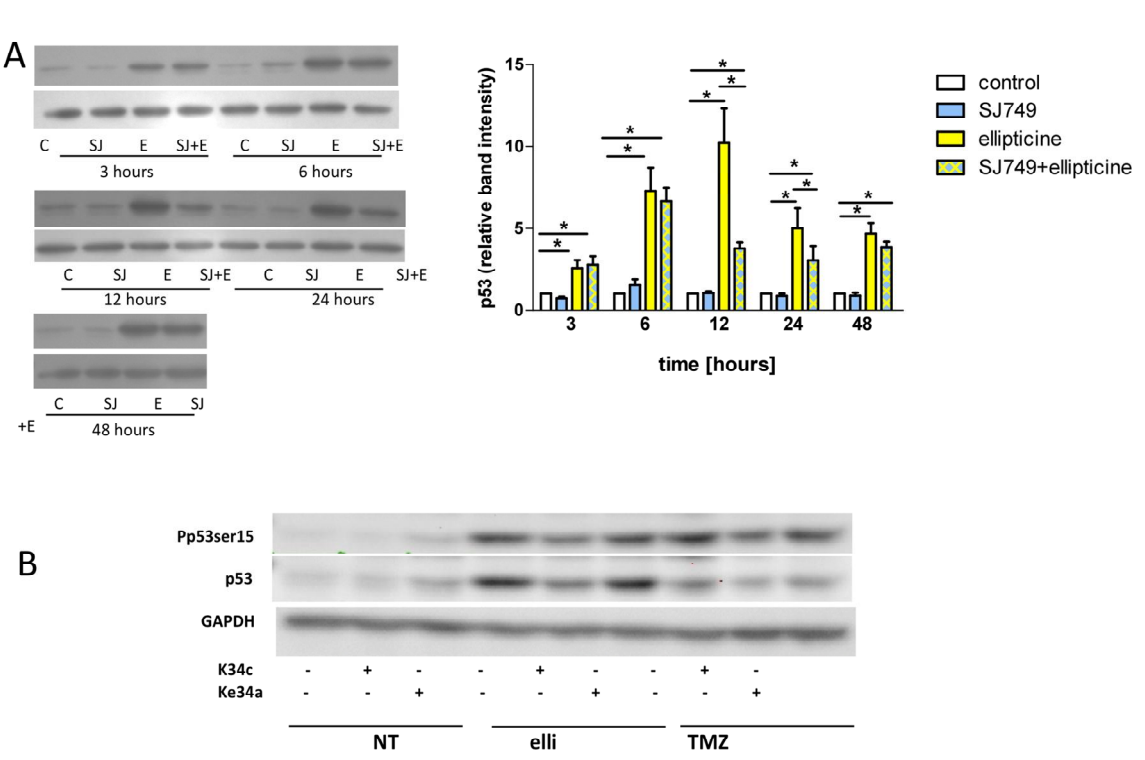
A
C SJ E SJ+E C SJ E SJ+E
3 hours
6 hours
C SJ E SJ+E C SJ E SJ+E
12 hours
24 hours
C SJ E SJ
+E
48 hours
p53 (relative band intensity)
15
10
5
0
3
6
12
24
48
time [hours]
control
SJ749
ellipticine
SJ749+ellipticine
B
Pp53ser15
p53
GAPDH
K34c - + - - + - - + -
Ke34a - - + - - + - - +
NT
elli
TMZ

Figure 23b].

The effects on p53 activity were confirmed regarding mRNA expression of the p53 downstream targets: p21, Mdm-2, Fas, and Apaf-1. All these genes were induced by ellipticine and temozolomide treatment. However, the expression of p21 and Mdm-2 mRNA was significantly decreased by adding integrin antagonist, either SJ749 or K34c, whereas Fas and Apaf-1 levels remained unchanged [

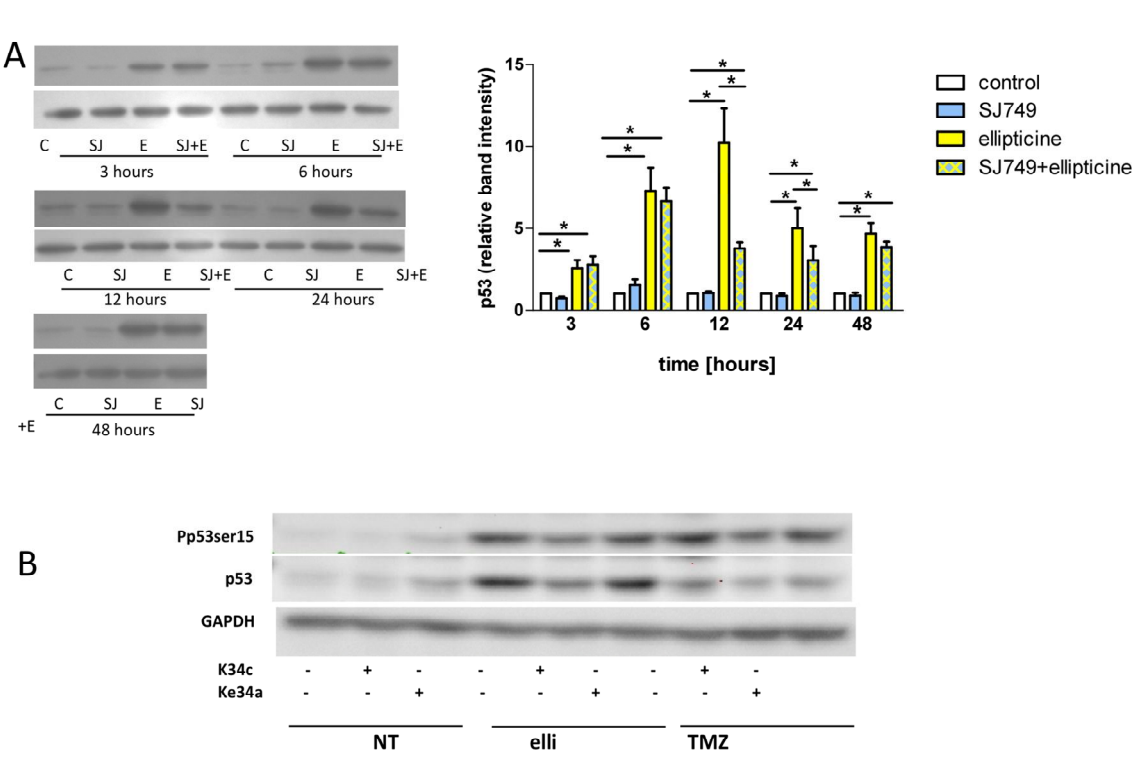
A
C SJ E SJ+E C SJ E SJ+E
3 hours
6 hours
C SJ E SJ+E C SJ E SJ+E
12 hours
24 hours
C SJ E SJ
+E
48 hours
p53 (relative band intensity)
15
10
5
0
3
6
12
24
48
time [hours]
control
SJ749
ellipticine
SJ749+ellipticine
B
Pp53ser15
p53
GAPDH
K34c - + - - + - - + -
Ke34a - - + - - + - - +
NT
elli
TMZ

Figure 23c-e].

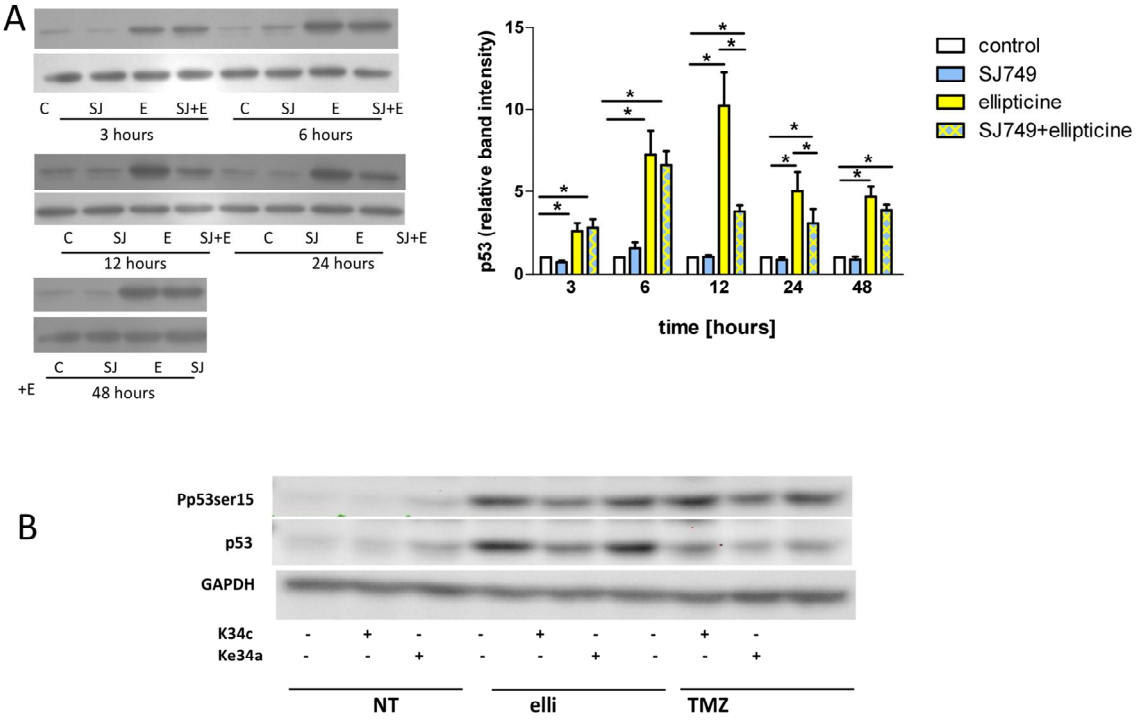

Figure 23: Integrin antagonists modulate the chemotherapy-induced p53 signaling. **A.** Protein p53 expression in U87MG cells treated with SJ749 (5 µM) and/or ellipticine (1 µM) for 3, 6, 12, 24 and 48 hours. Membranes were probed with anti-p53 antibodies. GAPDH was used as a loading control. A

representative blot is shown and the graph displays means of the p53/GAPDH ratios (n=3-4). **B**. Protein p53 expression and activation in U87MG cells treated for 24 hours with ellipticine (1 µM) or temozolomide (200 µM) in combination with the α5β1 integrin antagonist K34c (20 µM) or the 2000 times less affine α5β1 integrin ligand Ke34a (20 µM). Membranes were probed with anti-phospho p53 Ser15 antibodies followed by anti- p53 antibodies. GAPDH was used as loading control. A representative blot out of three is shown. **C.** qPCR analysis of p53, p21, human mdm2, Fas, Apaf-1, Bad and Bax mRNA levels. Cells were treated with SJ749 (5 µM) and/or ellipticine (1 µM). **D.** qPCR analysis of p21, human mdm2, Fas and Apaf-1 mRNA levels. Cells were treated with K34c (20 µM) and/or ellipticine (1 µM). **E.** qPCR analysis of p21, human mdm2, Fas and Apaf-1 mRNA levels. Cells were treated with SJ749 (5 µM), K34c (20 µM), temozolomide (200 µM) or combinations of drugs. (n=3). Scattergrams represent the fold increase of mRNA in U87MG cells treated during 12 hours as compared to control cells and normalised with the reporter gene, cyclophilin (n=3).

5. Effects of chemotherapy combined with α5β1 integrin antagonists in U373 cell line with non-functional p53 pathway

Since chemotherapy-induced p53 pathway activation was shown to be modulated by the addition of integrin antagonists, we further investigated effects of such combination treatment on glioblastoma cell line expressing non-functional p53, U373. We confirmed previously that the p53 in U373 was not functional, nor inducible by ellipticine treatment [

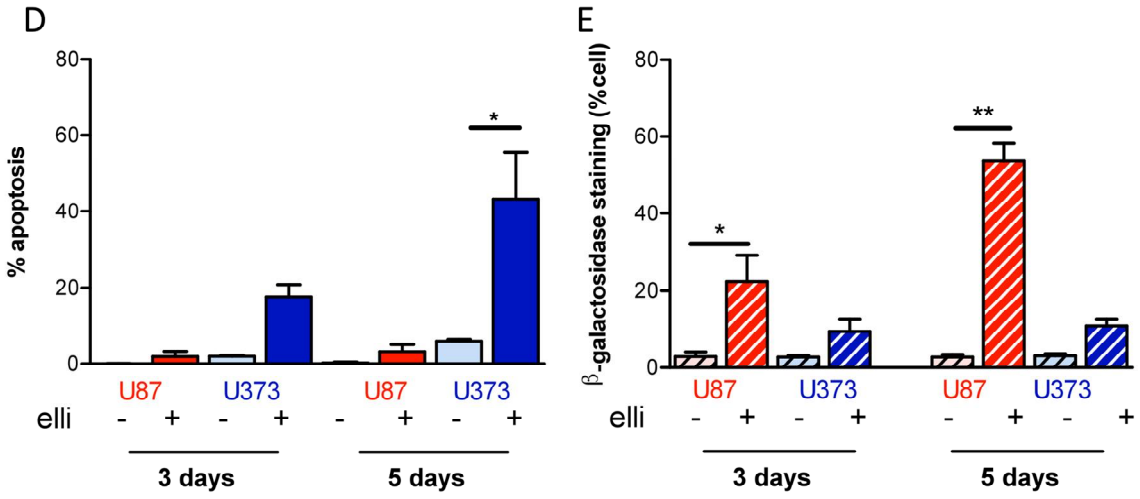

Figure 15a,b, p 71].

In contrast to U87MG cells, single ellipticine therapy significantly increased apoptotic population in the U373 cell line reaching 14 %, but had no ability to induce senescence. Addition of an integrin antagonist, SJ749, had no additional effect either on apoptosis [**Figure 24**a], or senescence [**Figure 24**b]. Senescent population did not exceed 10 % whatever the treatment tested.

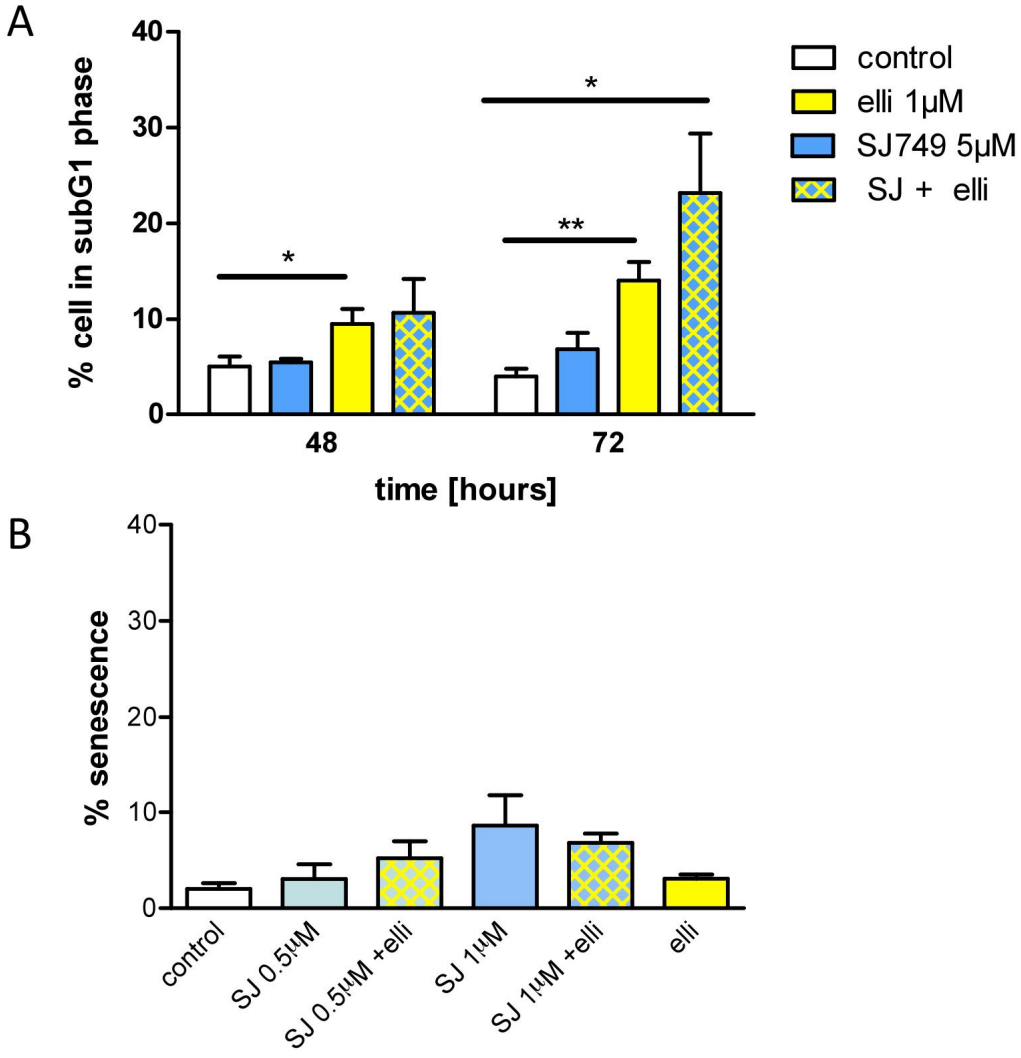

Figure 24: Effect of α5β1 integrin antagonists, chemotherapy and their combination on apoptosis and senescence in U373 glioblastoma cells. **A.** U373 cells were treated 24 or 48 hours with solvent, SJ749 (5 µM), K34c (20 µM), ellipticine (1 µM) or combinations, stained with propidium iodide and subG1 cell population detected by FACS analysis. **B.** U373 cells were treated 3 days with either solvent, SJ749 (5 µM), K34c (20µM), ellipticine (1 µM) or combinations before the detection of β-galactosidase activity at pH 6.

The results mentioned above suggest that the cellular response to such therapy depends on p53 pathway status. To elucidate the results obtained, we continued our further work with several models:

1. Chemical inhibition of the functional p53 in U87MG cells by its specific inhibitor pifithrin-α;
2. U373 cells transfected by a p53wt-expressing plasmid;
3. U87MG cells with suppressed p53 expression using small interfering RNA (siRNA)

4. Isogenic colon carcinoma cell lines HCT116 either expressing p53wt (HCT116+/+), or p53 knock-outed (HCT116-/-).

Ad. Model 1: Effects of ellipticine chemotherapy in U87MG cells with p53wt chemically inhibited by pifithrin-α (PFT-α)

Pifithrin-α at the concentration of 20 μM repressed the ellipticine-induced p53 protein expression starting at 6 hours of co-treatment, while the p53 mRNA level remained unchanged. In contrast, mRNA levels of p53 downstream targets p21 and Fas, which are induced by ellipticine treatment, were affected by addition of pifithrin-α. While p21 induction was decreased, Fas was even more induced when ellipticine and pifithrin-α were administered together compared to single ellipticine treatment [**Figure 25**a].

At the concentration used, pifithrin-α had no significant effects on the U87MG cell cycle itself at any time tested (24, 48 and 72 hours). Moreover, it did not modify ellipticine-induced G0/G1 cycle arrest. In accordance with SJ749 + ellipticine co-treatment, pifithrin-α in combination with ellipticine significantly increased apoptosis reaching 28% after 72 hours of treatment. As well, ellipticine-induced senescence was altered by pifithrin-α in the same manner as in the case of SJ749, reducing it from 22% to 8% [**Figure 25**b].

To confirm whether these effects of pifithrin-α were due to the chemical inhibition of p53, U373 cells expressing p53mut were co-treated with ellipticine and pifithrin-α. It was found out that ellipticine-induced apoptosis was not further increased by the PFT-α addition [**Figure 25**c LEFT]. As well, senescence was induced neither by pifithrin-α separately, nor in combination with ellipticine [**Figure 25**c RIGHT].

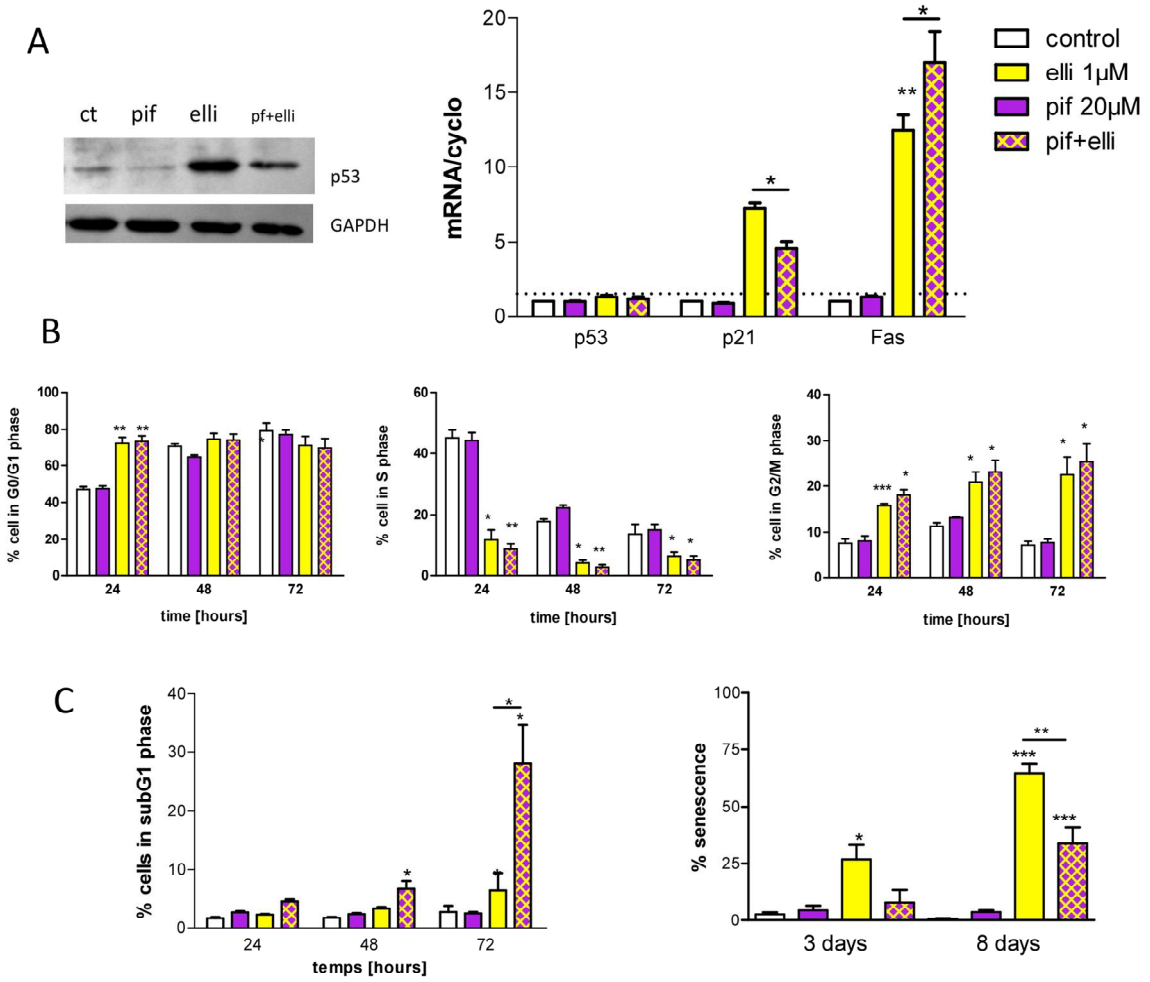

Figure 25: Effects of chemical inhibition of p53 protein by pifithrin-α on U87MG cellular response to ellipticine chemotherapy. **A.** LEFT: Protein p53 expression in U87MG cells treated with pifithrin-α (20 µM) and/or ellipticine (1 µM) for 12 hours. Membranes were probed with anti-p53 antibodies. GAPDH was used as a loading control. A representative blot is shown. RIGHT: qPCR analysis of p53, p21 and Fas mRNA levels. Cells were treated with pifithrin-α (20 µM) and/or ellipticine (1 µM). Scattergram represents the fold increase of mRNA in U87MG cells treated during 12 hours as compared to control cells and normalised with the reporter gene, cyclophilin (n=3). **B.** Cell cycle analysis. Cells were treated for 24, 48, and 72 hours in 2% serum medium either with solvent, 20 µM pifithrin-α and/or 1 µM ellipticine before propidium iodide staining and cell cycle analysis by flow cytometry. Data represent the percentage of cells in G0/G1, S, G2/M. **C.** LEFT: Cells were treated 24, 48 or 72 hours with pifithrin-α (20 µM) and/or ellipticine (1 µM), stained with propidium iodide and subG1 cell population detected by FACS analysis. RIGHT: Cells were treated 3 or 8 days with pifithrin-α (20 µM) and/or ellipticine (1 µM) before the detection of β-galactosidase activity at pH 6.

Ad. Model 2: Effects of ellipticine chemotherapy in U373 cells transfected with a p53wt expressing plasmid

The p53wt expression [**Figure 26**a] into U373 cells resulted in an important cell cycle perturbation as shown in **Figure 26**b. After 3 days of treatment, U373-p53wt cells appeared more sensitive to SJ749-induced or ellipticine-induced apoptosis as compared to mock-transfected cells (24% compared to 14%). SJ749 combination with ellipticine resulted in no further significant apoptosis increase either in mock-transfected cells, or in U373-p53wt [**Figure 26**c].

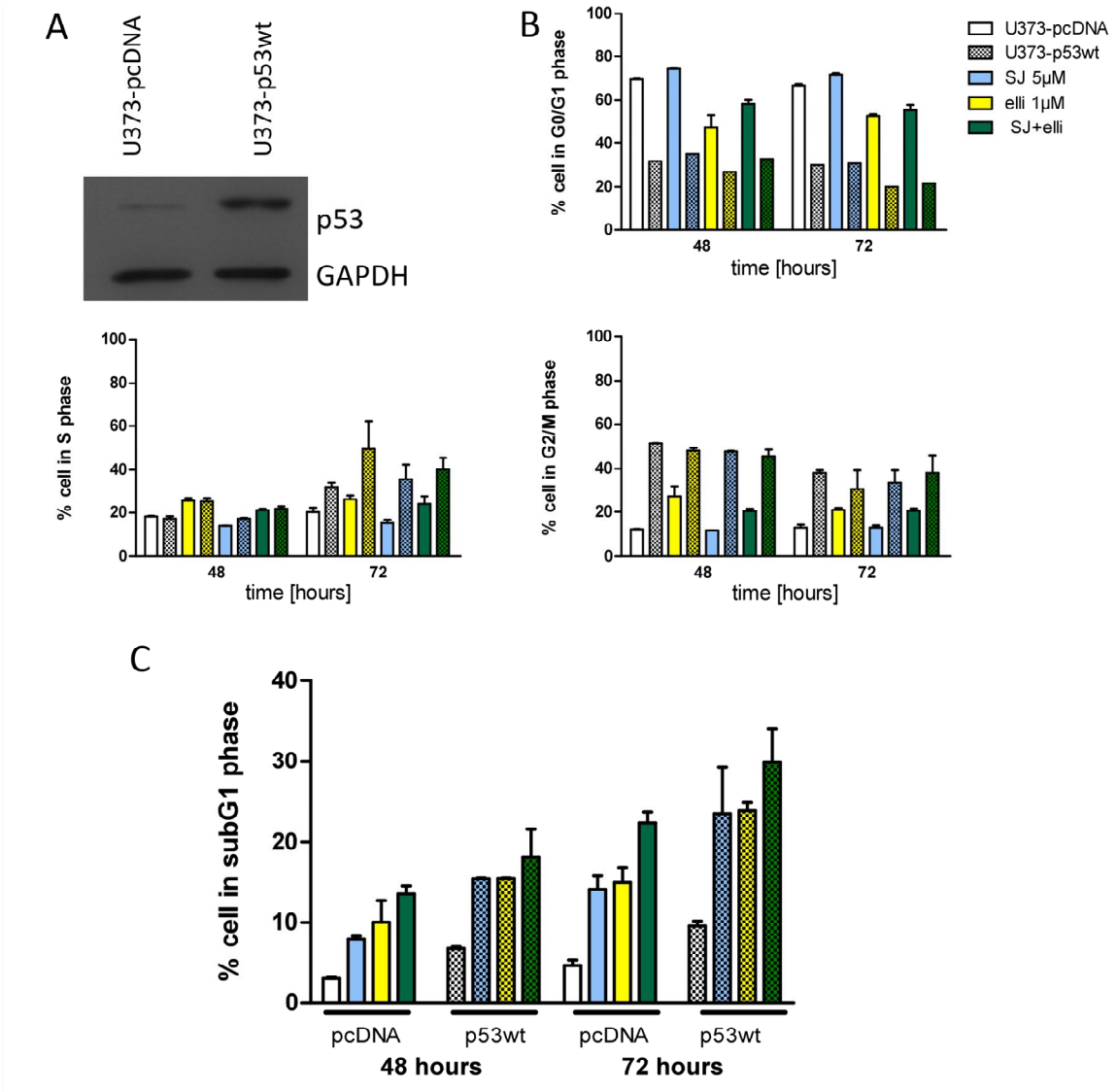

Figure 26: Effect of p53wt transfection in U373 response to ellipticine. **A.** Protein p53 expression in U373 mock or p53wt-transfected cells. Membranes were probed with anti-p53 antibodies. GAPDH was used as a loading control. **B.** U373 mock or p53wt-transfected cells were treated for 48 and 72 hours in 2% FBS medium with 5 µM SJ749 and/or 1 µM ellipticine before propidium iodide staining and flow cytometry analysis. Data represent the percentage of cells in G0/G1, S and G2/M phases. **C.** U373 mock or p53wt-transfected cells were treated for 48 and 72 hours with 5 µM SJ749 and/or

1 µM ellipticine before propidium iodide staining. Apoptotic cells quantified by FACS analysis of the cell cycle are represented as the percent of cells in the subG1 phase.

Ad. Model 3: Effects of the combination therapy in U87MG cells transfected with p53-targeted siRNA

The expression of p53 protein was inhibited by siRNA in U87MG cells. As the basal level of this tumor suppressor is very low, we stimulated the cells by 6 hours ellipticine treatment to insure fruitfulness of the siRNA transfection. In contrast to mock-transfected U87MG, no significant induction of p53 protein expression was detected in transfected cells [**Figure 27**a].

The p53-siRNA alone slightly changed the U87MG cell cycle distribution towards G2/M phase. Ellipticine treatment (48 hours) yielded to important S (rising from 37% to 46%) and G2/M (rising from 15% to 27%) cell cycle arrests in p53-siRNA U87MG cells instead of G0/G1 block in mock-transfected ones. Simultaneously, G0/G1 population decreased (lowering from 48% tp 27%). K34c addition resulted in no further important cell cycle alterations when p53 was inhibited. As temozolomide blocks the cell cycle rather G2/M than the G0/G1 phase, p53-inhibition had no fundamental effects when comparing to mock-transfected cells [**Figure 27**b].

Ellipticine induced apoptosis in p53-siRNA transfected, but not in mock-transfected U87MG cells. As expected, integrin antagonist K34c increased the ellipticine- or temozolomide-induced apoptosis in mock-transfected cells reaching 16% without affecting significantly the chemotherapy-induced apoptosis in p53-siRNA transfected cells [**Figure 27**c].

In addition, temozolomide-induced senescence was decreased by silencing the p53 in U87MG cells. Moreover, K34c decreased significantly the temozolomide-induced senescence in cells transfected with control non-targeting siRNA without affecting significantly the residual senescence of cells transfected with siRNA targeted on p53 [**Figure 27**d].

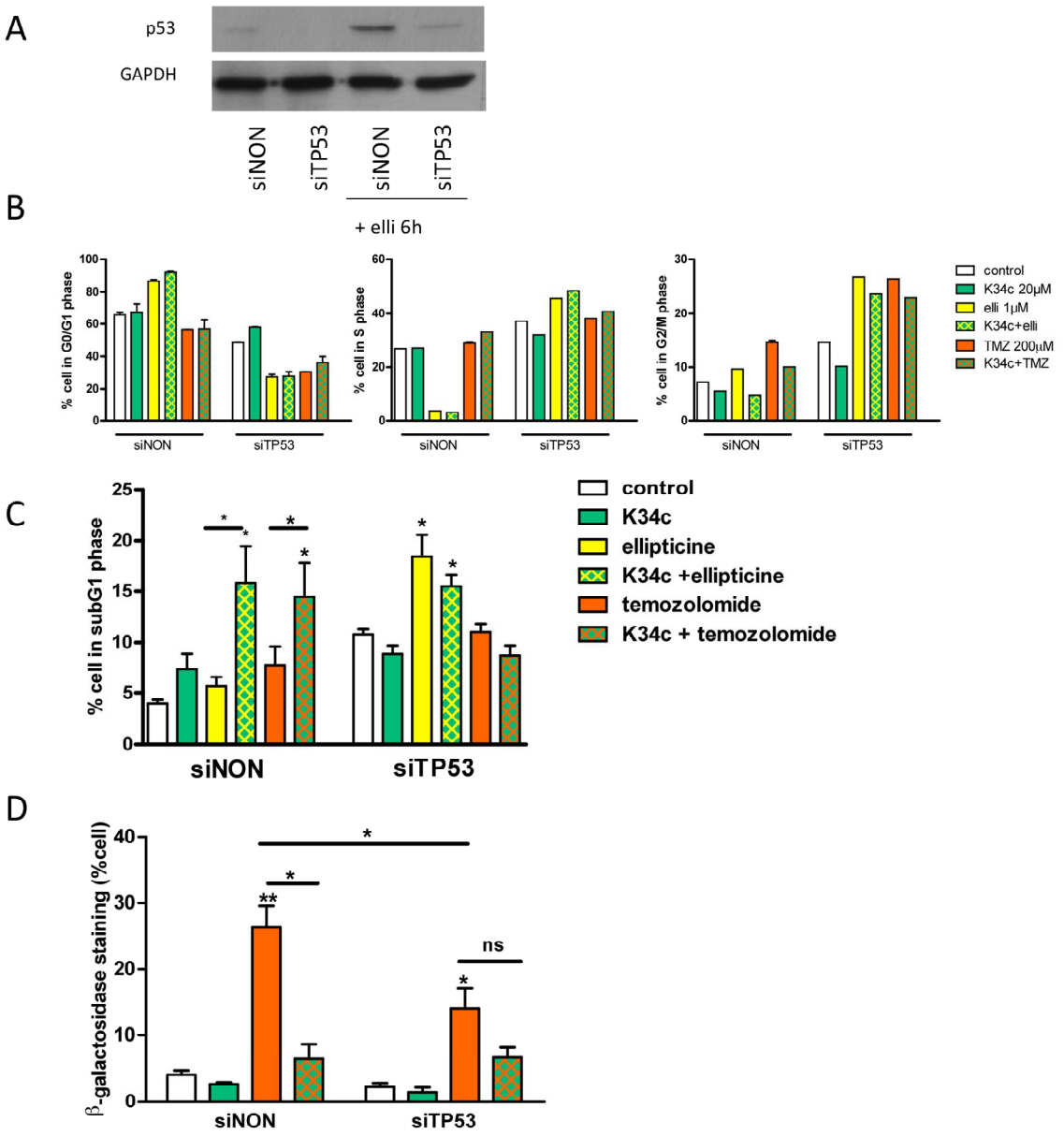

Figure 27: Effects of depletion of p53wt in U87MG cells on the cell answer to chemotherapy and integrin antagonists. **A.** U87MG cells were transfected with non targeting (siNON) or p53 targeted siRNA (siTP53). Western blot with anti p53 antibodies of transfected cells before and after 1 µM ellipticine treatment. **B.** Transfected cells were treated for 72 hours in 2% FBS medium with 20 µM K34c and/or 1 µM ellipticine and/or 200 µM temozolomide before propidium iodide staining and flow cytometry analysis. Data represent the percentage of cells in G0/G1, S and G2/M phases. **C.** Transfected cells were treated for 72 hours in 2% FBS medium with 20 µM K34c and/or 1 µM ellipticine and/or 200 µM temozolomide before propidium iodide staining. Apoptotic cells quantified by FACS analysis of the cell cycle are represented as the percent of cells in the subG1 phase. **D.** Transfected cells were treated for 72 hours in 2% FBS medium with 20 µM K34c and/or 1 µM ellipticine and/or 200 µM temozolomide before the detection of β-galactosidase activity at pH 6.

Ad. Model 4: Effects of the combination therapy in colon carcinoma cell lines HCT116+/+ and HCT116-/-

To confirm our results suggesting the p53 responsibility of the cellular responses, we used isogenic colon cancer cell lines HCT116 p53+/+ and HCT116 p53-/-. Both cell lines express identical levels of α5 integrin subunit [**Figure 28**a LEFT]. As well, p53 knock-out was proven [**Figure 28**a RIGHT].

Analogically to U87MG and U373, ellipticine provoked cell cycle arrest in G0/G1 phase in HCT116 p53+/+, whereas HCT116 p53-/- were blocked in G2/M phase. K34c molecule tended to block the cell cycle in G0/G1 phase regardless of the p53 status. Its combination with ellipticine either intensified the G0/G1 arrest, either acted against G2/M cycle block in HCT116 p53-/- [**Figure 28**b].

As expected, HCT116 p53+/+ senesced significantly more than HCT116 p53 -/- after ellipticine treatment and integrin antagonist K34c inhibited senescence in HCT116 p53+/+ cells without affecting senescence in HCT116 p53-/- cells [**Figure 28**c].

Inversely, the HCT116 p53-/- cells exhibited significantly more apoptosis in the presence of ellipticine compared to HCT116 p53+/+. The SJ749 integrin antagonist significantly increased the ellipticine-induced apoptosis in HCT116 p53+/+ but did not induce further apoptosis when combined with ellipticine in HCT116 p53 -/- [**Figure 28**d].

As confirmed using various models, in p53wt-expressing cells, single chemotherapy induced preferentially senescence than apoptosis. This phenomenon is accompanied by a strong activation of the p53 pathway. Such p53 signaling is down-modulated by integrin α5β1 addition and leads to favorization of apoptosis against senescence. In contrast, in the system, where p53 is not functional/present, single chemotherapy induces apoptotic cell death, but no or little senescence. Here, the α5β1 integrin antagonist addition brings no further benefits such as further apoptotic population increase.

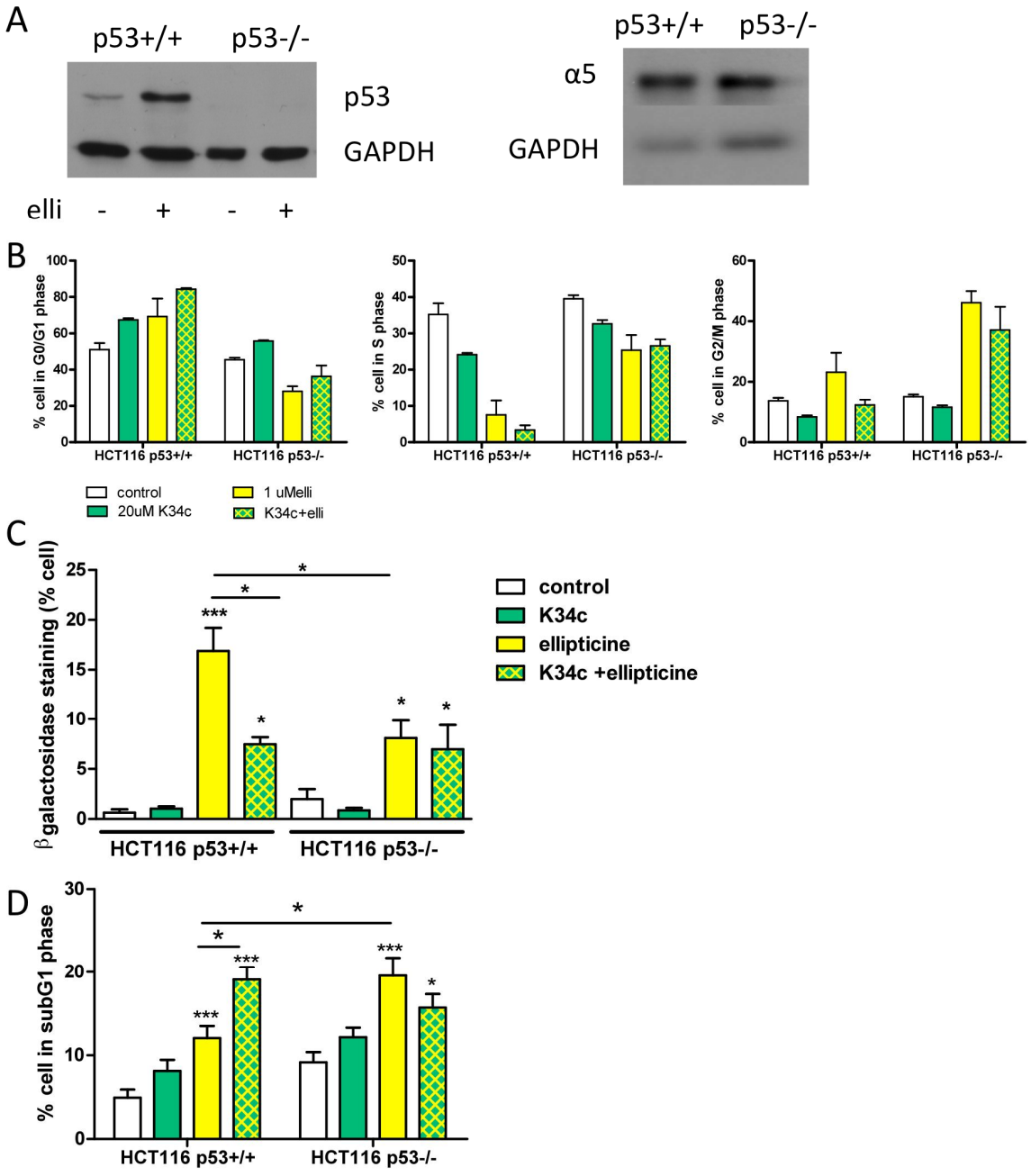

Figure 28: Effects of integrin antagonists on apoptosis and senescence in HCT116 p53+/+ and HCT116 p53-/- cells treated with ellipticine. **A.** Western blot analysis of α5 integrin subunit expression in HCT116 p53+/+ and HCT116 p53 -/- total protein extracts. GAPDH was used as a loading control. **B.** HCT116 p53+/+ and HCT116 p53-/- cells were treated for 48 hours with ellipticine (1 µM), K34c (20 µM) or combination of both drugs before propidium iodide staining and flow cytometry analysis. Data represent the percentage of cells in G0/G1, S and G2/M phases. **C.** HCT116 p53+/+ and HCT116 p53-/- cells were treated for 5 days with ellipticine (1 µM), K34c (20 µM) or combination of both drugs before detection of senescent cells. (n=3) **D.** HCT116 p53+/+ and HCT116 p53-/- cells were treated for 3 days with ellipticine (1 µM), SJ749 (5 µM) or combination of both drugs. After propidium iodide staining, population of subG1 cell population was detected by FACS analysis. (n=3).

6. The α5β1 role in cellular response of human glioblastoma cell lines to the chemotherapy combined with α5β1 integrin antagonists

6.1 Ellipticine chemotherapy in U87MG cells with integrin α5β1 activated by fibronectin

Apparently, antagonizing integrin α5β1 leads to and altered ellipticine chemotherapy outcome in U87MG cells as it favors apoptosis to senescence. Therefore, we activated integrin by plating the U87MG cells on its specific ECM ligand, fibronectin.

Cell proliferation neither of non-treated cells, nor of ellipticine-treated cells was affected [**Figure 29**a]. As well, cell cycle alterations induced by ellipticine described in the first part of this work seemed unaffected by fibronectin binding to α5β1 [**Figure 29**b].

Similarly, ellipticine-induced apoptosis did not reach significantly different levels when cells were placed on fibronectin compared to plastic [**Figure 29**c]. In contrast, after ellipticine treatment they senesced more easily in presence of fibronectin reaching 46% compared to 22% for cells cultured on plastic [**Figure 29**d].

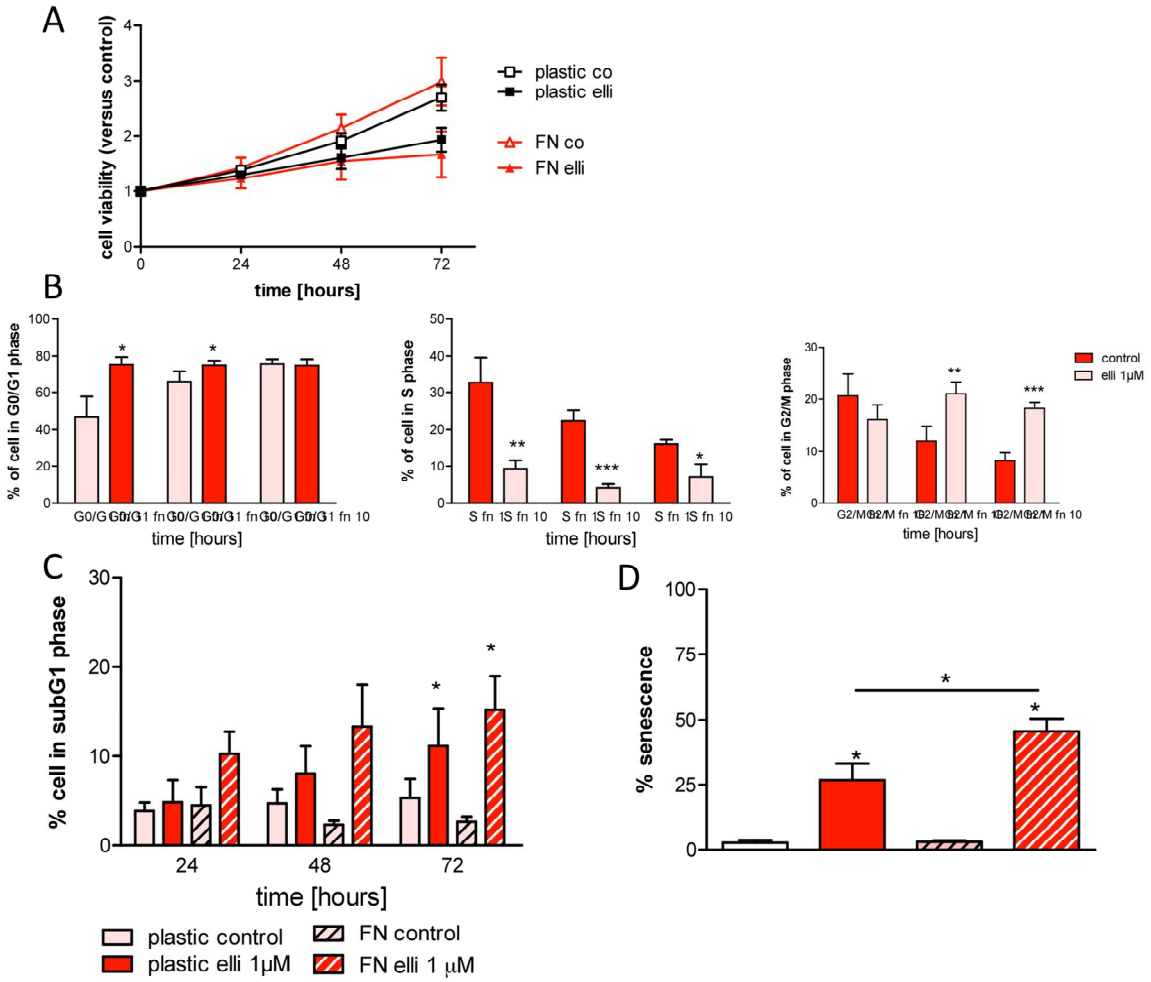

Figure 29: Effects of α5β1 integrin activation by fibronectin on U87MG cellular response to ellipticine chemotherapy. **A.** Proliferation assay. U87MG cells were plated either on plastic, or 1 µg/ml bovine fibronectine treated 24, 48 or 72 hours in 2% FBS medium with either solvent (dimethyl sulfoxide) or 1 µM ellipticine before measuring mitochondrial activity. **B.** Cell cycle analysis. U87MG cells were plated either on plastic, or 1 µg/ml bovine fibronectine and treated 24, 48 or 72 hours in 2% FBS medium with either solvent or 1 µM ellipticine before propidium iodide staining and cell cycle analysis by flow cytometry. Data represent the percentage of cells in G0/G1, S, G2/M. **C.** Apoptosis. cells were plated either on plastic, or 1 µg/ml bovine fibronectine and treated 24, 48 or 72 hours in 2% FBS medium with either solvent or 1 µM ellipticine before propidium iodide staining, population of subG1 cell population was detected by FACS analysis. **D**. Senescence. Cells were plated either on plastic, or 1 µg/ml bovine fibronectine and treated 3 days in 2% FBS medium with either solvent or 1 µM ellipticine before the detection of β-galactosidase activity at pH 6.

Expectedly, α5β1 integrin activation by fibronectin resulted in increase of ellipticine-induced senescence. These results are in accordance with the study of combination of ellipticine with integrin antagonists, in which antagonizing integrin led to ellipticine-induced senescence depression.

6.2 *Ellipticine chemotherapy in U87MG overexpressing α5 integrin subunit*

Since SJ749 antagonist effects were shown to be influenced by the α5β1 integrin expression levels (Maglott et al. , 2006, Martin et al., 2009), we transfected U87MG cells with a α5 integrin-containing plasmid to obtain a model clone F8 overexpressing this integrin. β1 integrin subunit expression remained unchanged [**Figure 30**a].

Having such a model, we studied effects of ellipticine on F8 clone compared to mock-transfected cells (empty pcDNA3.1 plasmid). Neither proliferation, nor cell cycle was affected in a different manner in F8 compared to control pcDNA cells [**Figure 30**b,c].

In contrast, F8 cells exhibited resistance to 72 hours of 1 µM ellipticine therapy followed by one week without treatment in the test of clonogenicity. Sixty-seven percent F8 cells developed colonies compared to only 40% pcDNA. In the same experiment, 200 µM temozolomide therapy resulted in 90% colony formation in F8 compared to 43% in pcDNA cells [**Figure 30**d].

Ellipticine-induced senescence was significantly more important in F8 than in pcDNA cells (46.5 % for F8 and 25.6 % for pcDNA) [**Figure 30**e]. However, ellipticine treatment led to same levels of apoptosis in both these models [**Figure 30**f].

Although α5 integrin overexpression in U87MG cells did not represent any advantage regarding cell proliferation, high levels of this integrin confer chemoresistance to U87MG cells to ellipticine and temozolomide treatment regarding clonogenicity. The increased senescence induction by ellipticine in F8 (α5-overexpressing) compared to pcDNA cells may at least partially contribute to the explanation of this chemoresistance.

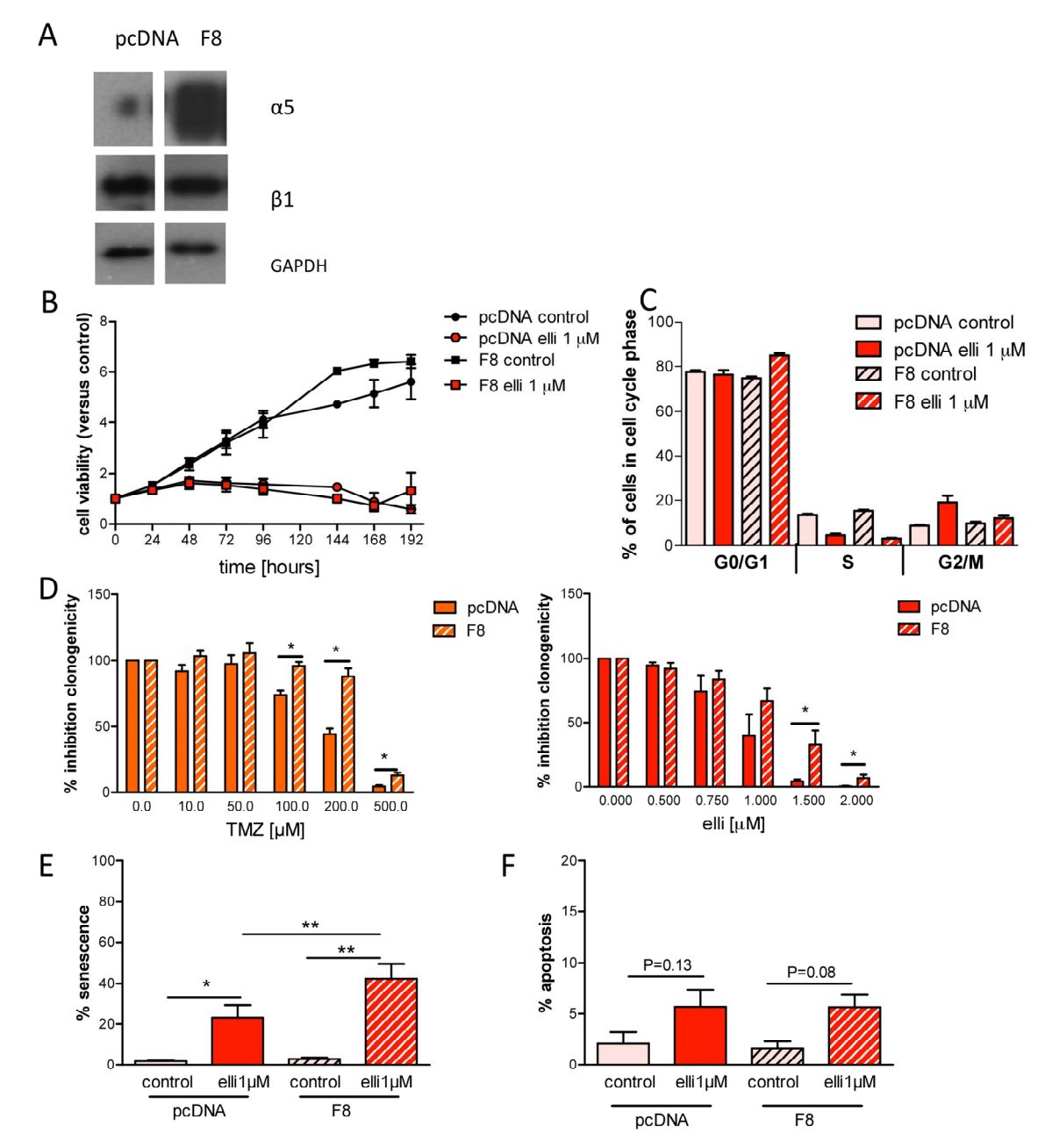

Figure 30: Ellipticine effects on U87MG cells overexpressing α5 integrin (clone F8). **A.** Western blot analysis of α5 integrin subunit expression in mock-transfected (pcDNA) and α5-transfected (F8) U87MG cells` total protein extracts. GAPDH was used as a loading control. B. Proliferation assay. Control (pcDNA) and F8 cells were treated 24, 48, 72, 96, 168 or 192 hours in 2% FBS medium with either solvent (dimethyl sulfoxide) or 1 μM ellipticine (n=7-8). **C.** Control (pcDNA) and F8 cells were treated for 72 hours in 2% FBS medium with 1 μM ellipticine before propidium iodide staining and flow cytometry analysis. Data represent the percentage of cells in G0/G1, S and G2/M phases. **D.** Clonogenicity of control (pcDNA) and F8 cells after 72 hours temozolomide (LEFT) or ellipticine (RIGHT) treatment, different drug concentrations. Results are represented as percentage of number of colonies compared to non-treated cells (n=5-8). **E.** Control (pcDNA) and F8 cells were treated for 72 hours in 2% FBS medium with 1 μM ellipticine before the detection of β-galactosidase activity at pH 6. **F.** Control (pcDNA) and F8 cells were treated for 72 hours in 2% FBS medium with 1 μM before propidium iodide staining. Apoptotic cells quantified by FACS analysis of the cell cycle are represented as the percent of cells in the subG1 phase.

6.3 Ellipticine chemotherapy in U87MG depleted from α5 integrin subunit

To repress the α5 integrin subunit expression in U87MG cell line, we used an α5-targeted shRNA and selected clone D4 for further studies. β1 integrin subunit expression remained unaffected [

Figure 31a]. Control cells (NS1) were stably transfected with non-silencing shRNA.

D4 cells prolifered significantly more than control NS1 cells. However, proliferation of both, NS1 and D4 cells, was completely blocked by ellipticine treatment

[

Figure 31b]. As well, cell cycle was altered in the same manner by ellipticine in NS1 as in D4 [

Figure 31c].

Unlike our expectations, no sensibilization to ellipticine treatment was observed regarding clonogenicity

[

Figure 31d LEFT]. On the contrary, D4 cells were more sensitive to 200 and 500 μM temozolomide in the clonogenicity test
[

Figure 31d RIGHT].

Surprisingly, α5 integrin depletion yielded to premature senescence even in non-treated cells. Furthermore, 72 hours ellipticine treatment led to an outstanding senescence increase reaching 74% compared to 25% senescent NS1 cells
[

Figure 31e]. Apoptosis remained unaffected
[

Figure 31f].

U87MG cells stably depleted in the α5 integrin subunit (D4) hardly stabilized and activated the p53 protein after ellipticine treatment as compared to control cells [**Figure 31**g].

Based on our results with α5 integrin overexpressing U87MG cells (F8) and our experiments with integrin antagonists, we expected higher sensitivity of α5-depleted U87MG cells (D4) to chemotherapeutic agents tested. Surprisingly, D4 cells were more sensitive to temozolomide, but not to ellipticine treatment. Even more surprisingly, D4 cells responded to ellipticine treatment by strong senescence induction as contrasted to integrin antagonizing.

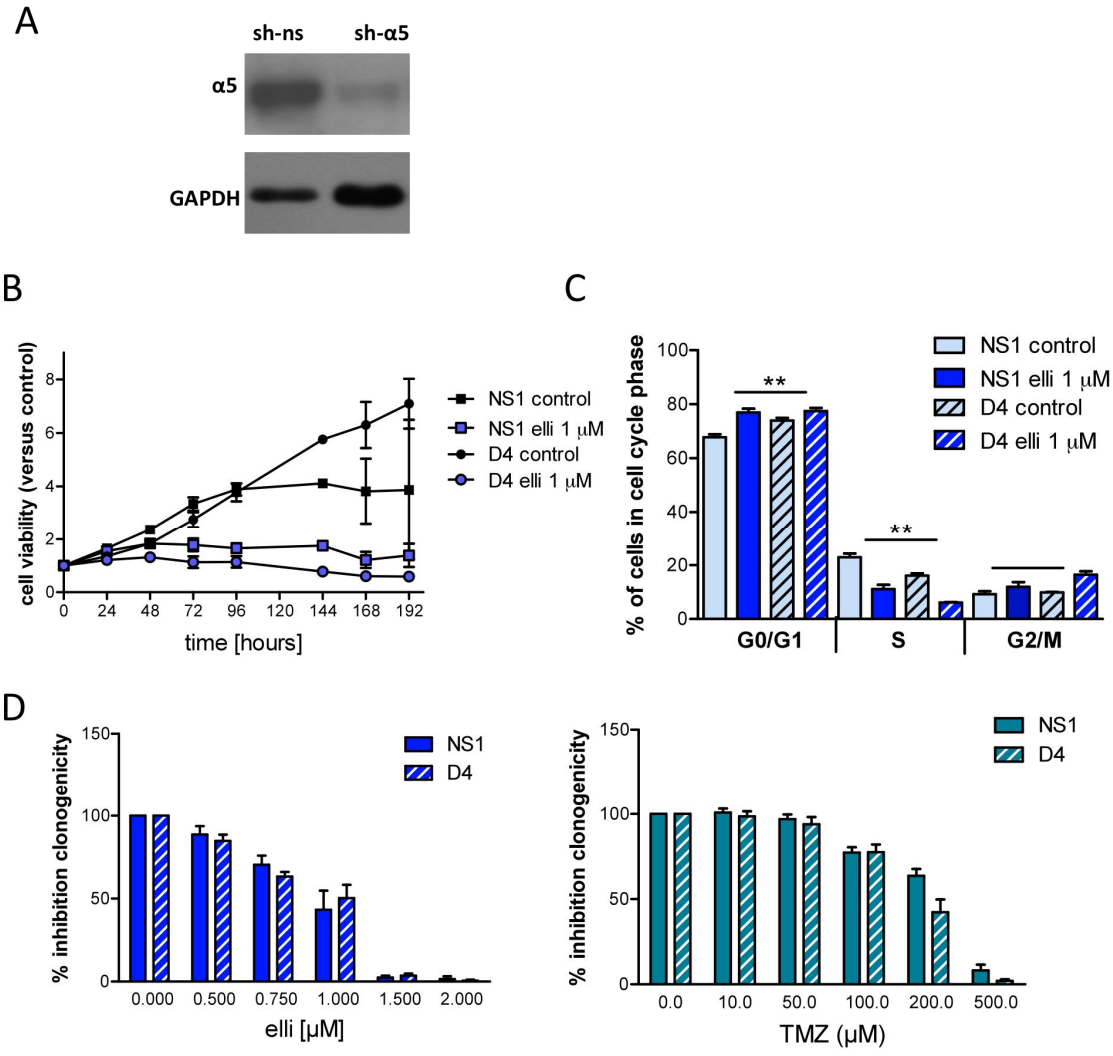

Figure 31: Ellipticine effects on U87MG cells depleted from α5 integrin using shRNA(clone D4). **A.** Western blot analysis of α5 integrin subunit expression in mock-transfected (NS1) and shRNA-α5-transfected (D4) U87MG cells` total protein extracts. GAPDH was used as a loading control. **B.** Proliferation assay. Control (NS1) and D4 cells were treated 24, 48, 72, 96, 168 or 192 hours in 2% FBS medium with either solvent (DMSO) or 1 μM ellipticine (n=7-8). **C.** Control (NS1) and D4 cells were treated for 72 hours in 2% FBS medium with 1 μM ellipticine before propidium iodide staining and flow cytometry analysis. Data represent the percentage of cells in G0/G1, S and G2/M phases. **D.** Clonogenicity of control (NS1) and D4 cells after 72 hours ellipticine (LEFT) or temozolomide (RIGHT) treatment, different drug concentrations. Results are represented as percentage of number of colonies compared to non-treated cells (n=5-8). **E.** Control (NS1) and D4 cells were treated for 72 hours in 2% FBS medium with 1 μM ellipticine before the detection of β-galactosidase activity at pH 6. **F.** Control (NS1) and D4 cells were treated for 72 hours in 2% FBS medium with 1 μM before propidium iodide staining. Apoptotic cells quantified by FACS analysis of the cell cycle are represented as the percent of cells in the subG1 phase. **G.** Protein p53 expression and activation in control (NS1) and D4 cells treated for 6, 12 or 24 hours with ellipticine (1 μM) Membranes were probed with anti-phospho p53 Ser15 antibodies followed by anti-p53 antibodies. GAPDH was used as loading control. A representative blot out of three is shown.

6.4 Ellipticine chemotherapy in U373 overexpressing or depleted from α5 integrin subunit

U373 cells expressed lower amounts of α5 and higher amounts of β1 integrin in comparison to U87MG cell line. The U373α5+ clone D7, generated by transfecting pcDNA plasmid containing α5 integrin subunit into U373 cells, got closer to U87MG line regarding the α5

level [**Figure 32**a]. Such α5 level increase resulted in an unusual cell phenotype with altered internal structure [**Figure 32**b] and multiple nuclei [**Figure 32**c].

A large portion of these multinucleated cells exhibited hallmarks of premature senescence. The percentage of senescent cells even increased after the treatment with ellipticine (increasing from 19% to 27% for D7 compared to 3% for pcDNA) [**Figure 32**d]. Treatment with integrin antagonist SJ749 also resulted in senescence induction in dose-dependent manner.

Interestingly, when antagonists combined with ellipticine, D7 cells senesced even more easily reaching 54.2 % for 1 µM SJ749 after 72 hours treatment [**Figure 32**d].

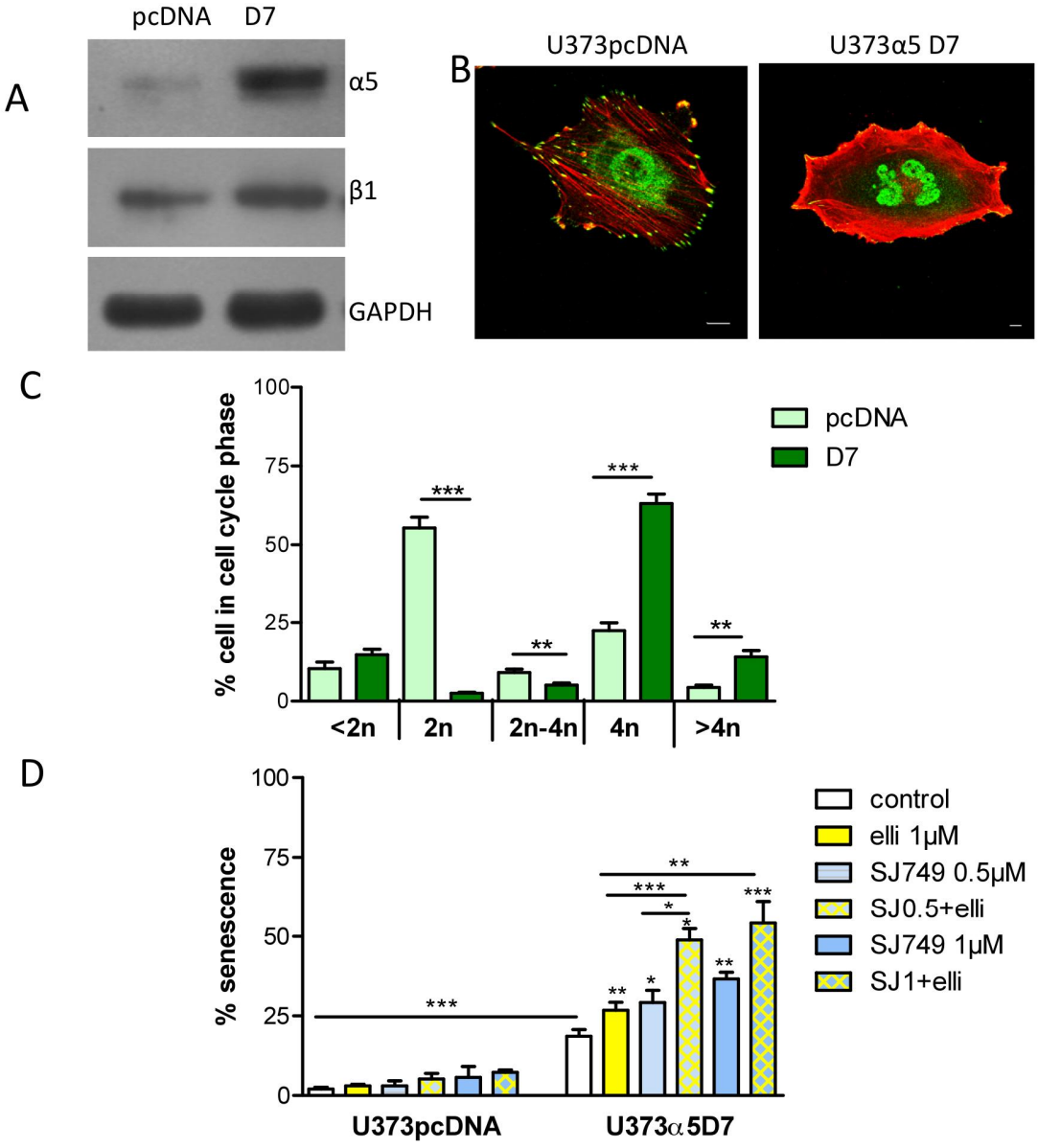

Figure 32: Ellipticine effects on U373 cells overexpressing α5 integrin (clone D7). **A.** Western blot analysis of α5 and β1 integrin subunits expression in mock-transfected (pcDNA) and α5-transfected (D7) U87MG cells` total protein extracts. GAPDH was used as a loading control. B. Immunocytochemical colocalization of actin fibres (phalloidin-rhodamine) and paxillin (FITC), scale = 10 μm. C. Cell cycle analysis by flow cytometry after propidium iodide staining. D. Senescence. Cells were treated for 72 hours as indicated before the detection of β-galactosidase activity at pH 6.

Interestingly, in the context of non-functional p53, α5 integrin overexpression resulted in multinucleated cell phenotype and senescence induction even in non-treated cells. This senescence is increased by both, single (SJ749 or ellipticine) and combination treatment.

Combination therapy of chemotherapeutics and α5β1 integrin antagonists: Conclusions and discussion

The second part of this work is dealing with combination of a conventional chemotherapy with an integrin α5β1-targeted therapy in glioblastomas. The integrin α5β1 has been reported to be overexpressed in a high percentage of these brain tumors (Uhm et al., 1999b). Moreover, its expression seems to be related to tumor aggressiveness (Martin et al. , 2009). Recently, SJ749, a specific α5β1 integrin antagonist, has been shown to inhibit proliferation and clonogenicity of U87MG glioblastoma cell line (Maglott et al. , 2006). From this point of view, antagonizing this integrin might have a positive impact on a chemotherapy outcome. Most of currently tested anti-cancer therapeutic approaches combine a specifically targeted therapy with some conventional chemotherapeutic agent or radiotherapy. Targeted therapies present molecules interfering with altered tumor signaling pathways. For example, perifosin, an Akt inhibitor, is undergoing phase II clinical trials (Omuro, 2008), and enzastaurin, a GSK3β (PKC-activated kinase) inhibitor is being tested in single glioma therapy as well in combination with radiotherapy (Rieger et al. , 2008, Sathornsumetee and Rich, 2008).

a) combination therapy: effect on cell cycle

Combination of SJ749 with ellipticine led to a complete block of U87MG cell proliferation, which was not achieved by either of the agents when used separately. Both integrin antagonists were found to arrest the cell cycle in G0/G1 phase. Therefore, ellipticine-induced G0/G1 cell cycle arrest was intensified and prolonged by addition of integrin antagonist. Since temozolomide blocks the cell cycle rather in S and G2/M phases (Mhaidat et al., 2007), integrin antagonist tended to exhibit inverse effects on cell cycle distribution when used in

combination. However, temozolomide effects overrode those of integrin antagonist. This finding underlines the importance of chemotherapeutic drug mechanisms of action when used in combination with integrin antagonist, since their effect on the cell cycle distribution might be either additive, or inverse.

b) combination therapy: senescence *versus* apoptosis

What is more important than the therapy effects on cell cycle distribution, the are effects of such a therapy on programmed cell death and premature drug-induced senescence. Integrin antagonists in combination with ellipticine or temozolomide induced significantly higher apoptosis compared to any of the agents used separately. Simultaneously, chemotherapy-induced senescence was notably decreased in presence of integrin antagonist. These results suggest an existence of a sort of balance between senescence and apoptosis, where blockade of integrin function by its antagonist shifts this balance towards apoptosis. Moreover, this phenomenon seems to be independent from mechanisms of action of the chemotherapeutic agent, as it was identical for both drugs tested.

Senescence has been first described in human fibroblasts as a phenomenon related to ageing including end of proliferation capacity of the cells (Hayflick, 1965). Nowadays, it is known to be one of common cellular answers to stress stimuli including DNA damage (te Poele et al., 2002, Xue et al., 2007). Senescent cells do not proliferate, but conserve their metabolic activation as well as capacity of signal transduction. After some specific mutations, they might also re-enter the cell cycle (Sage et al., 2003). Altogether, senescent phenotype may provide a sort of protection against therapy effects. Furthermore, senescent cells were reported to have capacity to secrete growth factors even stimulating surrounding cells to proliferate and thus may modulate the overall sensitivity to chemotherapy (Schmitt, 2007, Schmitt et al., 2002).

Our results suggested that the α5β1 integrin is positively implicated in the premature senescence obtained after chemotherapy, which may be blocked by the specific antagonists. Indeed, when integrins were activated by fibronectin, we observed a significant senescence increase after ellipticine treatment. Moreover, same results were obtained in U87MG cells overexpressing the α5 integrin subunit. In U373 cells, overexpression of α5 subunit restores the capability of cells to exhibit senescence with or without chemotherapy. These results confirm a role of α5β1 integrin in the phenomenon of senescence.

In line with this finding, we expected that α5 integrin repression in U87MG cells should favor apoptosis and not senescence upon chemotherapy treatment, same as integrin antagonists. Surprisingly, U87MG cells depleted in α5 integrin subunit senesced even in absence of chemotherapy stress. When treated with ellipticine, senescent population reached extreme percentage. To entirely explain these contradictory results requires further investigations.

c) combination therapy: impact of p53 status

It was previously reported that inhibition of p53 sensitizes cells to temozolomide treatment (Dinca et al., 2008, Xu et al., 2005) and topoisomerase I inhibitors (Wang et al., 2004). In contrast, some works had inverse results claiming that p53wt expressing gliomas were more sensitive to temozolomide (Roos et al., 2007). Therefore, p53 status plays an important, although sometimes contradictory, role in cellular response to diverse therapies.

In presence of functional p53 (U87MG), ellipticine therapy provoked premature senescence, whereas in U373 expressing p53 mutant, cells died from apoptosis after ellipticine treatment (see Part IV.A). In combination with integrin antagonists, ellipticine induced apoptosis instead of senescence in U87MG cells [**Figure 22**]. In contrast, in U373 cells expressing p53 mutant, ellipticine treatment itself resulted in apoptosis, which was not further affected by addition of integrin antagonists. We observed similar differences in cellular responses to ellipticine single therapy when comparing U87MG and U373 cells as when comparing ellipticine mono-therapy and ellipticine plus integrin antagonist combination treatment in U87MG cells.

Moreover we showed that the integrin antagonists decreased the p53 pathway activation elicited by ellipticine and selectively affect p53 target genes. α5β1 antagonists selectively inhibit or rather modulate the p53 signaling pathway and such selectivity may at least partially explain the switch of cellular response to chemotherapy-induced DNA damages from senescence to apoptosis in p53wt cells.

p21 has been reported to be the main senescence regulator (Han et al., 2002), whereas Fas and Apaf-1 both act as pro-apoptotic proteins involved in death-receptor and mitochondrial pathway, respectively. The currently accepted model is that p53 shift cells towards apoptosis

or senescence after a genotoxic stress by transactivating genes involved either in apoptosis (BAX, PUMA, Fas, PIG3, Apaf-1…), or in cell cycle arrest (p21, 14-3-3δ, GADD-45…). Such selectivity seems to be related to modulators directing p53 binding to promoters of genes involved in growth arrest or in apoptosis (Das et al., 2007, Tanaka et al., 2007). It should be noted that p53-dependent proapoptotic genes (for example the Fas and APAF1 genes in our experiments) could be activated by chemotherapeutic stress even without inducing apoptosis (Chang et al., 2002). It was previously reported that p21 overexpression may confer glioblastomas chemoresistance (Ruan et al., 1998), while its attenuation sensitizes these cells to apoptosis induced by carmustine and cisplatin (Ruan et al., 1999). We thus hypothesize that if p21 levels are strongly induced by single ellipticine or temozolomide, cell tends to senesce, while upon integrin antagonist-mediated p53 modulation leading to weaker p21 activation, other pro-apoptotic signals (here Fas and Apaf-1) outbalance the system towards apoptosis.

Another integrin antagonist Ke34a, which has affinity rather to αvβ3 than to α5β1, did not affect either the p53 stabilization or activity. This finding confirms the specificity of α5β1 in the impact on p53 pathway. Thereby, we confirmed our hypothesis and we demonstrated for the first time a relationship between the α5β1 integrin and p53 tumor suppressor.

To elucidate whether the differences in cellular responses to chemotherapy alone and in combination with an α5β1 antagonist are really due to altered p53 pathway activation, different approaches were used:

- ⇒ inhibition of p53wt by pifithrin-α in U87MG cells;
- ⇒ silencing of p53wt with specific siRNA in U87MG cells;
- ⇒ expression of p53wt in U373 mutant p53-expressing cells;
- ⇒ exploration of isogenic cell lines either expressing or not p53wt (colon carcinoma HCT116)

Chemical inhibition of p53 by pifithrin-α resulted in apoptosis induction after ellipticine treatment and concomitantly repressed ellipticine-induced senescence. Pifithrin-α-mediated p53 inhibition led to similar impacts on ellipticine-stimulated p53 downstream targets, same as in the case of integrin α5β1 antagonists. Such results underline the complexity of p53 signaling pathway regulation. Similarly, temozolomide`s cytotoxic effects on U87MG cell line were increased in presence of pifithrin-α and these results were confirmed also with intracranial glioblastoma xenografts (Dinca et al. , 2008).

We further confirmed the key role of p53, since significantly lower percentage of U87MG cells with silenced p53 expression senesced cells upon temozolomide treatment (compared to p53wt-expressing cells. Ellipticine induced apoptotic cell death only in p53-lacking cells, as expected from experiments with U373 cell line. In addition, integrin antagonist addition resulted in apoptosis increase only in control cells, but not in those depleted from p53.

As already described, U373 cells exhibited apoptosis rather than senescence after ellipticine treatment. Integrin antagonist had no additional effects on ellipticine-induced apoptosis, nor any impact on senescence. In these cells, expression of p53wt by itself completely perturbated cell cycle and the system seems to be already stimulated by the p53wt transfection-mediated stress. However, SJ749 treatment increased cell apoptosis significantly more in U373 cells expressing a p53wt protein than in mock-transfected cells. Results thus revealed again a functional link between α5β1 integrin and p53.

Our results were confirmed even in isogenic colon carcinoma cell lines HCT116, expressing p53wt, and its analogue with p53 knock-out, which are widely used as model systems when studying p53 pathway (Kim et al., 2009). Similarly to U87MG, HCT116 expressing functional p53 reacted on ellipticine therapy by senescence induction. Presence of integrin antagonist yielded to a decrease of senescent cells and a simultaneous increase of apoptotic cell population. Ellipticine induced apoptosis in HCT116 p53KO and low senescence, which was not affected by the presence of α5β1 integrin antagonists.

All these data suggest that functional p53 is essential for integrin α5β1 antagonists to affect cellular response to chemotherapy. Disruption of α5β1 integrin function using small molecule inhibitors might enhance the chemotherapeutic effect in glioblastoma expressing wild-type p53 and indispensable level of α5β1 integrin. Molecular mechanisms controlling the α5β1 integrin-dependent input to the p53 pathway as well as senescence regulation remain to be characterized.

In p53 mutant and high α5β1 levels-expression cell context, the combination therapy may also bring benefits due to an increased senescence induction.

Integrins have been reported to regulate DNA damage-induced apoptosis by modulating p53 in some cell types, which do not require adhesion for their survival. In such context cell detachment from ECM confers resistance to DNA damages, which is related with p53 and Arf levels repression (Lewis et al. , 2002). We observed chemoresistance to ellipticine and temozolomide treatment in U87MG cells overexpressing α5 integrin (F8) clonogenicity

pointing out that especially integrin α5β1 could have the primary role among other β1 subunit containing integrins in conferring chemoresistance.

We expected higher sensitivity of α5-depleted U87MG cells (D4) to chemotherapeutic agents tested. Surprisingly, D4 cells were more sensitive to temozolomide, but not ellipticine treatment. Here, such chemosensitization might be due to different mechanism of action of both drugs. Temozolomide is a methylating agent, whose DNA damages are repaired by a specific enzyme O^6-methylguanine methyltransferase (MGMT). MGMT promoter is methylated in 40-50% glioblastoma, which leads to MGMT gene silencing. These glioblastomas are then supposed to respond to temozolomide chemotherapy. Interestingly, MGMT is strongly downregulated by absence or inhibition of p53 (Blough et al., 2007). Our results have revealed lower activation and p53 protein stabilization in D4 (α5-depleted) cells compared to control after ellipticine treatment. Our preliminary results confirmed absence of MGMT enzyme in D4 but not in normal U87MG cells. Thus D4 sensitivity to temozolomide might be explained by the downregulation of MGMT repairing temozolomide-induced DNA damages. In contrast, in D4 cells, strong senescence induction might prevent the consequences of ellipticine treatment-induced DNA damages, which do not depend on MGMT activity. Here, senescence may have protective effects as discussed above. However, these findings have just a preliminary character and need further detailed investigation, which are currently being performed in our laboratory.

Taken together, combination therapy outcome of glioblastoma cell lines is principally dependent on p53 pathway status. In the presence of functional p53, integrin α5β1 antagonists seem to be able to counteract its chemotherapy-mediated stabilization and activation resulting in block of senescence induction and simultaneous apoptosis favoring. While in absence of functional p53, cells seem to hardly senesce upon ellipticine treatment, whereas they are more sensitive to ellipticine treatment-mediated apoptosis induction. In such context, integrin blockade represents no further benefits when combined with the conventional chemotherapeutics.

According to our results, one original way to alter p53 signaling in glioblastoma is through the inhibition of the α5β1 integrin, which modulates rather than completely inhibits p53 pathway. Thus genotoxic therapies with concomitant partial and selective inhibition of the transcriptional activity of p53 by α5β1 integrin antagonists may be of outstanding interest in glioblastoma therapy.

General Conclusions & Perspectives

Current oncology is still lacking therapies efficient enough to cure highly aggressive tumors such as glioblastomas. Neither of the conventional therapeutic approaches brings crucial survival benefits for patients suffering from this aggressive type of cancer. Therefore, strategies aimed to target specifically altered pathways in tumor cells in combination with conventional approaches represent a great challenge for scientists and clinicians nowadays.

This work is dealing with ellipticine and its combination with α5β1 integrin-targeted therapy of glioblastomas. Ellipticine has already been used in clinical praxis against other aggressive and metastatic cancers. It has been reported to exhibit certain specificity for brain tumors in studies *in vitro* as well. Former results of our laboratory provided evidences that it overcomes the blood-brain barrier in rats and thus is able to reach the tumor of interest. Since it is considered a pro-drug being metabolized by cytochrome P450 and peroxidases, its activity depends on these biotransformation enzymes expression pattern of each patient as well as of the tumoral tissue. Among the ellipticine-activating enzymatic systems, e.g. CYP1B1 has been reported to be specifically expressed in astrocytic tumours but not in healthy brain tissue (Murray et al. , 1997). Due to its selective activation, ellipticine exhibits certain specificity to tumors.

Here we demonstrated sensitivity of two glioblastoma cell lines to ellipticine treatment and pointed out the importance of p53 status in cellular response to ellipticine therapy. Whereas both, p53wt and p53mt expressing, cell lines were sensitive to ellipticine, the mechanisms of their cellular answers were completely different. While p53wt-expressing U87MG cell line answered to ellipticine treatment by senescence induction, in U373 (p53mt) ellipticine provoked apoptotic cell death. Both cell lines were proven to express biotransformation enzymes metabolizing ellipticine. Moreover, in U87MG cells, some of these enzymes were ellipticine-inducible. Thereby, ellipticine is regulating its own metabolism in targeted tissue. Ellipticine concentration and thus degree of selective cytochrome P450 induction plays a key role in metabolic activation-dependent mechanisms of ellipticine`s action such as covalent DNA adducts formation.

Despite these promising findings, possible extensive utilization of ellipticine in clinical praxis remains a bit quastionable. Firstly, it considers a drug that was already withdrawn in the past

from the pharmaceutical market due to its cardiotoxicity. Thus it has a kind of negative stigma in view of clinical oncologists. Secondly, its relaunch into clinical practice would not get along without expensive clinical trials. Since ellipticine has already lost its patent protection, it is questionable, whether pharmaceutical industry would be keen on financing its clinical research. Modifying the molecule or patenting a new drug form could overcome this problem. However, ellipticine`s mechanisms of action in the combination therapy may be generalized to other anticancer drugs. Here, all our important results regarding the combination therapy were confirmed with temozolomide, which is currently a reference drug in glioblastoma therapy.

As stated above, glioblastomas are highly aggressive, but also highly resistant tumors, heavily vascularized. As integrins have been reported to possibly confer chemo- or radio-resistance and are simultaneously involved in angiogenesis, integrin-targeted therapies evoke a lot of interest nowadays. Historically, αvβ3 integrin was the first and most extensively explored therapeutic target among the integrin family. Integrin αvβ3-targeted therapy was predominantly aimed on angiogenesis inhibiton. Integrin α5β1 has recently been identified as even more promising therapeutic target for glioblastomas, as it is implicated in multiple stages of tumorigenesis as well as in processes such as tumoral neoangiogenesis and cell invasiveness. Moreover, its expression positively correlates with tumor grade. Here, α5β1 integrin targeted-therapy does not deal with anti-angiogenesis, but rather explores its signalization modulation potential with its effects on tumoral cells directly.

The key finding of our work is that a specific α5β1 integrin non-peptidic small antagonists (SJ749 or K34c) modulates cellular response of p53wt-expressing glioblastoma to conventional chemotherapy (ellipticine or temozolomide) by triggering apoptotic cell death instead of premature senescence. Having noted that senescent cells may re-enter cell cycle and excrete stimulating signals to the cell in their neighborhood, whereas triggering apoptosis brings unexceptional benefits for tumor repression, this results is of great importance. We demonstrated and confirmed a key role of the p53 signaling in this phenomenon, since integrin antagonists were shown to specifically modulate the p53 pathway resulting in affecting the balance between senescence and apoptosis favoring programmed cell death. Thus we presented for the first time a functional link between p53 and α5β1 integrin. Furthermore, our results suggest an unexpected role for the α5β1 integrin in the phenomenon

of senescence. The mechanisms involved remain to be elucidated and are currently under investigation.

We further pointed out that the p53 status is crucial for such combination therapy outcome. In the context of non-functional p53 and high α5 integrin level, ellipticine treatment combined with integrin antagonist resulted not in apoptosis, but senescence induction. Despite combination of chemotherapy with α5β1 integrin antagonist presents certain benefits regardless the p53 status, such combination therapy is supposed to be more suitable for p53wt-expressing tumors due to the controversial benefits of senescence discussed above.

Since all experiments presented in this work were performed *in vitro*, further *in vivo* studies are essential. First and foremost, no studies of SJ749 or K34c integrin antagonist regarding their toxicity in animal models have been realized till today. Similarly, no indications whether these molecules will be able to penetrate through the blood brain barrier do not exist, although such a difficulty might perhaps be solved by use of drug-containing capsules implanted intracranially, similar to Gleevec® (http://www.gleevec.com/patient/gleevec-prescription-medication-information.jsp; cached 15.2.2010). Work is in progress to answer these questions in xenografted human glioblastoma.

In summary, this work provides novel evidences of profitability of combining conventional chemotherapy with α5β1 integrin-targeted therapy underlying the importance of knowing basic tumor characteristics to may estimate the final therapy outcome. The status of p53 has hardly been demonstrated as a predictor of the chemotherapeutic response in glioblastoma (Leuraud et al., 2004, Weller et al., 1998), but concomitant screening of tumors for α5β1 integrin level and p53 status may be more predictive in patients with brain cancer resistant to chemotherapy.

List of Publications and Communications

Publications

Martinkova E, Maglott A, Leger, DY, Bonnet D, Stiborova M, Takeda K, Martin S, Dontenwill M: *α5β1 integrin antagonists reduce chemotherapy-induced premature senescence and facilitate apoptosis in human glioblastoma cells.* Int J Cancer. Accepted. (2010 Jan 22)

Martinkova E, Dontenwill M, Frei E, Stiborová M: *Cytotoxicity of and DNA adduct formation by ellipticine in human U87MG glioblastoma cancer cells.* Neuro Endocrinol Lett 30(Suppl), 60-66 (2009)

Martinkova E, Hodek P, Hudecek J, Frei E, Dontenwill M, Stiborova M: *Oxidation of ellipticine by human and rat cytochromes P450 correlates with its binding to DNA*. Chem. Listy 101, s73−s310 (2007)

Publication in preparation

Léger DY, Maglott A, Martinkova E, Cosset EC, Stiborova M, Martin S, Dontenwill M: *The α5β1 integrin is implicated in human glioblastoma tumorigenicity and chemoresistance.*

Oral Communications

Martinkova E, Maglott A, Leger, DY, Stiborova M, Martin S, Dontenwill M: *Implication of p53 and α5β1 integrin in glioblastoma chemotherapy response.* 5th Meeting of the doctoral schools of the Charles University Prague and Louis Pasteur University Strasbourg, November 12-14, 2008, Strasbourg, France

Posters

Martinkova E, Dontenwill M, Poljakova J, Frei E, Stiborova M: *Cytotoxicity and DNA adduct formation by ellipticine in human U87MG glioblastoma cancer cell line*. XXV. Xenobiochemical Symposium, September 22-25, 2009, Mikulov, Czech Republic

Mrazova B, Kotrbova V, Martinkova E, Frei E, Stiborova M: *The Study on mechanisms of cytochrome b_5-mediated stimulation of ellipticine oxidation by cytochrome P450 3A4.* XXV. Xenobiochemical Symposium, September 22-25, 2009, Mikulov, Czech Republic

Martinkova E, Dontenwill M, Frei E, Stiborova M: *Cytotoxicity and DNA adduct formation by ellipticine in human U87MG glioblastoma cancer cells.* 14th Interdisciplinary Slovak-Czech Toxicology Conference TOXCON, June 1-3, 2009, Brno, Czech Republic

Martinkova E, Maglott A, Leger DY, Stiborova M, Martin S, Dontenwill M: *α5β1integrin expression level and p53 protein status both determine the chemotherapy outcome of human glioblastoma.* ONCOTRANS, March 19-20, 2009, Nancy, France

Dontenwill M, Martinkova E, Maglott A, Stiborova, Martin S: *The α5β1integrin predicts glioblastoma chemotherapy outcome through modulation of p53 pathways.* EACR20. July 6, 2008, Lyon, France

Martinkova E, Maglott A, Martin S, Stiborova M, Dontenwill M: *Sensitization of human glioblastoma to chemotherapy by the treatment with an α5β1 integrin antagonist.* 1er forum du Cancéropôle du Grand-Est, October 19, 2007, Vittel, France

Martinkova E, Hodek P, Hudeček J, Frei E, Dontenwill M, Stiborova M: *Correlation between th e cytochrome P450 specificity in oxidizing the anticancer drug ellipticine and its DNA modification efficiency.* 12th *Interdisciplinary Slovak-Czech Toxicology Conference* TOXCON, June 11-13, 2007, Prague, Czech Republic

Hrabeta J, Figova K, Martinkova E, Cipros S, Cinatl J, Eckschlager T: *The effects of hypoxia on chemoresistance and cell cycle alterations in neuroblastoma cell lines.*

Bibliography

Acton EM, Narayanan VL, Risbood PA, Shoemaker RH, Vistica DT, Boyd MR (1994). Anticancer specificity of some ellipticinium salts against human brain tumors in vitro. J Med Chem. **37**: 2185-9.

Addya S, Anandatheerthavarada HK, Biswas G, Bhagwat SV, Mullick J, Avadhani NG (1997). Targeting of NH2-terminal-processed microsomal protein to mitochondria: a novel pathway for the biogenesis of hepatic mitochondrial P450MT2. J Cell Biol. **139**: 589-99.

Aimova D, Svobodova L, Kotrbova V, Mrazova B, Hodek P, Hudecek J, et al. (2007). The Anticancer Drug Ellipticine Is a Potent Inducer of Rat Cytochromes P450 1A1 and 1A2, Thereby Modulating Its Own Metabolism. Drug Metab Dispos. **35**: 1926-34.

Alghisi GC, Ruegg C (2006). Vascular integrins in tumor angiogenesis: mediators and therapeutic targets. Endothelium. **13**: 113-35.

Anandatheerthavarada HK, Addya S, Dwivedi RS, Biswas G, Mullick J, Avadhani NG (1997). Localization of multiple forms of inducible cytochromes P450 in rat liver mitochondria: immunological characteristics and patterns of xenobiotic substrate metabolism. Arch Biochem Biophys. **339**: 136-50.

Aoudjit F, Vuori K (2001). Integrin signaling inhibits paclitaxel-induced apoptosis in breast cancer cells. Oncogene. **20**: 4995-5004.

Arguello F, Alexander MA, Greene JF, Jr., Stinson SF, Jorden JL, Smith EM, et al. (1998). Preclinical evaluation of 9-chloro-2-methylellipticinium acetate alone and in combination with conventional anticancer drugs for the treatment of human brain tumor xenografts. J Cancer Res Clin Oncol. **124**: 19-26.

Ashby J, Elliott BM, Styles JA (1980). Norharman and ellipticine: a comparison of their albilities to interact with DNA in vitro. Cancer Lett. **9**: 21-33.

Askari JA, Buckley PA, Mould AP, Humphries MJ (2009). Linking integrin conformation to function. J Cell Sci. **122**: 165-70.

Baker SD, Wirth M, Statkevich P, Reidenberg P, Alton K, Sartorius SE, et al. (1999). Absorption, metabolism, and excretion of 14C-temozolomide following oral administration to patients with advanced cancer. Clin Cancer Res. **5**: 309-17.

Barak Y, Gottlieb E, Juven-Gershon T, Oren M (1994). Regulation of mdm2 expression by p53: alternative promoters produce transcripts with nonidentical translation potential. Genes Dev. **8**: 1739-49.

Baumann F, Bjeljac M, Kollias SS, Baumert BG, Brandner S, Rousson V, et al. (2004). Combined thalidomide and temozolomide treatment in patients with glioblastoma multiforme. J Neurooncol. **67**: 191-200.

Beglova N, Blacklow SC, Takagi J, Springer TA (2002). Cysteine-rich module structure reveals a fulcrum for integrin rearrangement upon activation. Nat Struct Biol. **9**: 282-7.

Bertrand JR, Giacomoni PU (1985). Ellipticines: correlation between in vitro DNA intercalation and physiological properties? Chemioterapia. **4**: 445-53.

Blandino G, Levine AJ, Oren M (1999). Mutant p53 gain of function: differential effects of different p53 mutants on resistance of cultured cells to chemotherapy. Oncogene. **18**: 477-85.

Blough MD, Zlatescu MC, Cairncross JG (2007). O6-methylguanine-DNA methyltransferase regulation by p53 in astrocytic cells. Cancer Res. **67**: 580-4.

Bogler O, Huang HJ, Kleihues P, Cavenee WK (1995). The p53 gene and its role in human brain tumors. Glia. **15**: 308-27.

Bork P, Doerks T, Springer TA, Snel B (1999). Domains in plexins: links to integrins and transcription factors. Trends Biochem Sci. **24**: 261-3.

Boudreau NJ, Varner JA (2004). The homeobox transcription factor Hox D3 promotes integrin alpha5beta1 expression and function during angiogenesis. J Biol Chem. **279**: 4862-8.

Brandes AA, Scelzi E, Zampieri P, Rigon A, Rotilio A, Amista P, et al. (1997). Phase II trial with BCNU plus alpha-interferon in patients with recurrent high-grade gliomas. Am J Clin Oncol. **20**: 364-7.

Bray D, Levin MD, Morton-Firth CJ (1998). Receptor clustering as a cellular mechanism to control sensitivity. Nature. **393**: 85-8.

Brooks PC, Clark RA, Cheresh DA (1994). Requirement of vascular integrin alpha v beta 3 for angiogenesis. Science. **264**: 569-71.

Buckner JC, Brown LD, Kugler JW, Cascino TL, Krook JE, Mailliard JA, et al. (1995). Phase II evaluation of recombinant interferon alpha and BCNU in recurrent glioma. J Neurosurg. **82**: 430-5.

Buckner JC, Brown PD, O'Neill BP, Meyer FB, Wetmore CJ, Uhm JH (2007). Central nervous system tumors. Mayo Clin Proc. **82**: 1271-86.

Chadwick M, Silveira DM, Platz BB, Hayes D (1978). Comparative physiological disposition of ellipticine in several animal species after intravenous administration. Drug Metab Dispos. **6**: 528-41.

Chamberlain MC (2006). Treatment options for glioblastoma. Neurosurg Focus. **20**: E19.

Chang BD, Swift ME, Shen M, Fang J, Broude EV, Roninson IB (2002). Molecular determinants of terminal growth arrest induced in tumor cells by a chemotherapeutic agent. Proc Natl Acad Sci U S A. **99**: 389-94.

Chang SM, Lamborn KR, Malec M, Larson D, Wara W, Sneed P, et al. (2004). Phase II study of temozolomide and thalidomide with radiation therapy for newly diagnosed glioblastoma multiforme. Int J Radiat Oncol Biol Phys. **60**: 353-7.

Chen RM, Chou MW, Ueng TH (1998). Induction of cytochrome P450 1A in hamster liver and lung by 6-nitrochrysene. Arch Toxicol. **72**: 395-401.

Cianfrocca ME, Kimmel KA, Gallo J, Cardoso T, Brown MM, Hudes G, et al. (2006). Phase 1 trial of the antiangiogenic peptide ATN-161 (Ac-PHSCN-NH(2)), a beta integrin antagonist, in patients with solid tumours. Br J Cancer. **94**: 1621-6.

Ciesielski MJ, Fenstermaker RA (1999). Synergistic cytotoxicity, apoptosis and protein-linked DNA breakage by etoposide and camptothecin in human U87 glioma cells: dependence on tyrosine phosphorylation. J Neurooncol. **41**: 223-34.

Colucci MA, Moody CJ, Couch GD (2008). Natural and synthetic quinones and their reduction by the quinone reductase enzyme NQO1: from synthetic organic chemistry to compounds with anticancer potential. Org Biomol Chem. **6**: 637-56.

Danen EH, Jansen KF, Van Kraats AA, Cornelissen IM, Ruiter DJ, Van Muijen GN (1995). Alpha v-integrins in human melanoma: gain of alpha v beta 3 and loss of alpha v beta 5 are related to tumor progression in situ but not to metastatic capacity of cell lines in nude mice. Int J Cancer. **61**: 491-6.

Das S, Raj L, Zhao B, Kimura Y, Bernstein A, Aaronson SA, et al. (2007). Hzf Determines cell survival upon genotoxic stress by modulating p53 transactivation. Cell. **130**: 624-37.

Datta SR, Dudek H, Tao X, Masters S, Fu H, Gotoh Y, et al. (1997). Akt phosphorylation of BAD couples survival signals to the cell-intrinsic death machinery. Cell. **91**: 231-41.

Denny BJ, Wheelhouse RT, Stevens MF, Tsang LL, Slack JA (1994). NMR and molecular modeling investigation of the mechanism of activation of the antitumor drug temozolomide and its interaction with DNA. Biochemistry. **33**: 9045-51.

Dickins M (2004). Induction of cytochromes P450. Curr Top Med Chem. **4**: 1745-66.

Dillman RO, Shea WM, Tai DF, Mahdavi K, Barth NM, Kharkar BR, et al. (2001). Interferon-alpha2a and 13-cis-retinoic acid with radiation treatment for high-grade glioma. Neuro Oncol. **3**: 35-41.

Dinca EB, Lu KV, Sarkaria JN, Pieper RO, Prados MD, Haas-Kogan DA, et al. (2008). p53 Small-molecule inhibitor enhances temozolomide cytotoxic activity against intracranial glioblastoma xenografts. Cancer Res. **68**: 10034-9.

Donate F, Parry GC, Shaked Y, Hensley H, Guan X, Beck I, et al. (2008). Pharmacology of the novel antiangiogenic peptide ATN-161 (Ac-PHSCN-NH2): observation of a U-shaped dose-response curve in several preclinical models of angiogenesis and tumor growth. Clin Cancer Res. **14**: 2137-44.

Ertl RP, Winston GW (1998). The microsomal mixed function oxidase system of amphibians and reptiles: components, activities and induction. Comp Biochem Physiol C Pharmacol Toxicol Endocrinol. **121**: 85-105.

Faddeeva MD, Beliaeva TN (1997). [Sanguinarine and ellipticine cytotoxic alkaloids isolated from well-known antitumor plants. Intracellular targets of their action]. Tsitologiia. **39**: 181-208.

Fang J, Nakamura H, Iyer AK (2007). Tumor-targeted induction of oxystress for cancer therapy. J Drug Target. **15**: 475-86.

Farber K, Synowitz M, Zahn G, Vossmeyer D, Stragies R, van Rooijen N, et al. (2008). An alpha5beta1 integrin inhibitor attenuates glioma growth. Mol Cell Neurosci. **39**: 579-85.

Fine HA, Figg WD, Jaeckle K, Wen PY, Kyritsis AP, Loeffler JS, et al. (2000). Phase II trial of the antiangiogenic agent thalidomide in patients with recurrent high-grade gliomas. J Clin Oncol. **18**: 708-15.

Fine HA, Wen PY, Robertson M, O'Neill A, Kowal J, Loeffler JS, et al. (1997). A phase I trial of a new recombinant human beta-interferon (BG9015) for the treatment of patients with recurrent gliomas. Clin Cancer Res. **3**: 381-7.

Foster BA, Coffey HA, Morin MJ, Rastinejad F (1999). Pharmacological rescue of mutant p53 conformation and function. Science. **286**: 2507-10.

Frei E, Bieler CA, Arlt VM, Wiessler M, Stiborova M (2002). Covalent binding of the anticancer drug ellipticine to DNA in V79 cells transfected with human cytochrome P450 enzymes. Biochem Pharmacol. **64**: 289-95.

Friedler A, Hansson LO, Veprintsev DB, Freund SM, Rippin TM, Nikolova PV, et al. (2002). A peptide that binds and stabilizes p53 core domain: chaperone strategy for rescue of oncogenic mutants. Proc Natl Acad Sci U S A. **99**: 937-42.

Friedman HS, Kerby T, Calvert H (2000). Temozolomide and treatment of malignant glioma. Clin Cancer Res. **6**: 2585-97.

Froelich-Ammon SJ, Patchan MW, Osheroff N, Thompson RB (1995). Topoisomerase II binds to ellipticine in the absence or presence of DNA. Characterization of enzyme-drug interactions by fluorescence spectroscopy. J Biol Chem. **270**: 14998-5004.

Frost JA, Steen H, Shapiro P, Lewis T, Ahn N, Shaw PE, et al. (1997). Cross-cascade activation of ERKs and ternary complex factors by Rho family proteins. EMBO J. **16**: 6426-38.

Garbett NC, Graves DE (2004). Extending nature's leads: the anticancer agent ellipticine. Curr Med Chem Anticancer Agents. **4**: 149-72.

Giancotti FG, Ruoslahti E (1999). Integrin signaling. Science. **285**: 1028-32.

Gonzalez FJ, Gelboin HV (1994). Role of human cytochromes P450 in the metabolic activation of chemical carcinogens and toxins. Drug Metab Rev. **26**: 165-83.

Gouyette A, Huertas D, Droz JP, Rouesse J, Amiel JL (1982). Pharmacokinetics of 2-methyl-9-hydroxyellipticinium acetate (NSC-264137) in cancer patients (phase I study). Eur J Cancer Clin Oncol. **18**: 1285-92.

Gu J, Tamura M, Pankov R, Danen EH, Takino T, Matsumoto K, et al. (1999). Shc and FAK differentially regulate cell motility and directionality modulated by PTEN. J Cell Biol. **146**: 389-403.

Guengerich FP, Shimada T (1991). Oxidation of toxic and carcinogenic chemicals by human cytochrome P-450 enzymes. Chem Res Toxicol. **4**: 391-407.

Guengerich FP, Shimada T (1998). Activation of procarcinogens by human cytochrome P450 enzymes. Mutat Res. **400**: 201-13.

Guo W, Giancotti FG (2004). Integrin signalling during tumour progression. Nat Rev Mol Cell Biol. **5**: 816-26.

Han Z, Wei W, Dunaway S, Darnowski JW, Calabresi P, Sedivy J, et al. (2002). Role of p21 in apoptosis and senescence of human colon cancer cells treated with camptothecin. J Biol Chem. **277**: 17154-60.

Harder T, Simons K (1997). Caveolae, DIGs, and the dynamics of sphingolipid-cholesterol microdomains. Curr Opin Cell Biol. **9**: 534-42.

Hayflick L (1965). The Limited in Vitro Lifetime of Human Diploid Cell Strains. Exp Cell Res. **37**: 614-36.

Hazlehurst LA, Damiano JS, Buyuksal I, Pledger WJ, Dalton WS (2000). Adhesion to fibronectin via beta1 integrins regulates p27kip1 levels and contributes to cell adhesion mediated drug resistance (CAM-DR). Oncogene. **19**: 4319-27.

Hazlehurst LA, Valkov N, Wisner L, Storey JA, Boulware D, Sullivan DM, et al. (2001). Reduction in drug-induced DNA double-strand breaks associated with beta1 integrin-mediated adhesion correlates with drug resistance in U937 cells. Blood. **98**: 1897-903.

He G, Siddik ZH, Huang Z, Wang R, Koomen J, Kobayashi R, et al. (2005). Induction of p21 by p53 following DNA damage inhibits both Cdk4 and Cdk2 activities. Oncogene. **24**: 2929-43.

Heckmann D, Meyer A, Laufer B, Zahn G, Stragies R, Kessler H (2008). Rational design of highly active and selective ligands for the alpha5beta1 integrin receptor. Chembiochem. **9**: 1397-407.

Hegi ME, Diserens AC, Gorlia T, Hamou MF, de Tribolet N, Weller M, et al. (2005). MGMT gene silencing and benefit from temozolomide in glioblastoma. N Engl J Med. **352**: 997-1003.

Herrlinger U, Rieger J, Steinbach JP, Nagele T, Dichgans J, Weller M (2005). UKT-04 trial of continuous metronomic low-dose chemotherapy with methotrexate and cyclophosphamide for recurrent glioblastoma. J Neurooncol. **71**: 295-9.

Hoyt DG, Rusnak JM, Mannix RJ, Modzelewski RA, Johnson CS, Lazo JS (1996). Integrin activation suppresses etoposide-induced DNA strand breakage in cultured murine tumor-derived endothelial cells. Cancer Res. **56**: 4146-9.

Humphries JD, Byron A, Humphries MJ (2006). Integrin ligands at a glance. J Cell Sci. **119**: 3901-3.

Hynes RO (1992). Integrins: versatility, modulation, and signaling in cell adhesion. Cell. **69**: 11-25.

Kamijo T, Weber JD, Zambetti G, Zindy F, Roussel MF, Sherr CJ (1998). Functional and physical interactions of the ARF tumor suppressor with p53 and Mdm2. Proc Natl Acad Sci U S A. **95**: 8292-7.

Kim EH, Lee YJ, Bae S, Lee JS, Kim J, Lee YS (2009). Heat shock factor 1-mediated aneuploidy requires a defective function of p53. Cancer Res. **69**: 9404-12.

Kim S, Bell K, Mousa SA, Varner JA (2000a). Regulation of angiogenesis in vivo by ligation of integrin alpha5beta1 with the central cell-binding domain of fibronectin. Am J Pathol. **156**: 1345-62.

Kim S, Harris M, Varner JA (2000b). Regulation of integrin alpha vbeta 3-mediated endothelial cell migration and angiogenesis by integrin alpha5beta1 and protein kinase A. J Biol Chem. **275**: 33920-8.

Kivisto KT, Kroemer HK, Eichelbaum M (1995). The role of human cytochrome P450 enzymes in the metabolism of anticancer agents: implications for drug interactions. Br J Clin Pharmacol. **40**: 523-30.

Kleihues P, Burger PC, Scheithauer BW (1993). The new WHO classification of brain tumours. Brain Pathol. **3**: 255-68.

Komarov PG, Komarova EA, Kondratov RV, Christov-Tselkov K, Coon JS, Chernov MV, et al. (1999). A chemical inhibitor of p53 that protects mice from the side effects of cancer therapy. Science. **285**: 1733-7.

Kuo PL, Hsu YL, Chang CH, Lin CC (2005a). The mechanism of ellipticine-induced apoptosis and cell cycle arrest in human breast MCF-7 cancer cells. Cancer Lett. **223**: 293-301.

Kuo PL, Hsu YL, Kuo YC, Chang CH, Lin CC (2005b). The anti-proliferative inhibition of ellipticine in human breast mda-mb-231 cancer cells is through cell cycle arrest and apoptosis induction. Anticancer Drugs. **16**: 789-95.

Kuo YC, Kuo PL, Hsu YL, Cho CY, Lin CC (2006). Ellipticine induces apoptosis through p53-dependent pathway in human hepatocellular carcinoma HepG2 cells. Life Sci. **78**: 2550-7.

Kuwada SK (2007). Drug evaluation: Volociximab, an angiogenesis-inhibiting chimeric monoclonal antibody. Curr Opin Mol Ther. **9**: 92-8.

Lain S, Xirodimas D, Lane DP (1999). Accumulating active p53 in the nucleus by inhibition of nuclear export: a novel strategy to promote the p53 tumor suppressor function. Exp Cell Res. **253**: 315-24.

Lane DP, Lain S (2002). Therapeutic exploitation of the p53 pathway. Trends Mol Med. **8**: S38-42.

Le Pecq JB, Nguyen Dat X, Gosse C, Paoletti C (1974). A new antitumoral agent: 9-hydroxyellipticine. Possibility of a rational design of anticancerous drugs in the series of DNA intercalating drugs. Proc Natl Acad Sci U S A. **71**: 5078-82.

Lesca P, Monsarrat B, Cros S, Paoletti C (1981). Influence of inducers of monooxygenases on cytotoxic efficiency of ellipticine on leukemia L1210 cells. J Natl Cancer Inst. **67**: 871-6.

Leuraud P, Taillandier L, Medioni J, Aguirre-Cruz L, Criniere E, Marie Y, et al. (2004). Distinct responses of xenografted gliomas to different alkylating agents are related to histology and genetic alterations. Cancer Res. **64**: 4648-53.

Lewis JM, Schwartz MA (1995). Mapping in vivo associations of cytoplasmic proteins with integrin beta 1 cytoplasmic domain mutants. Mol Biol Cell. **6**: 151-60.

Lewis JM, Truong TN, Schwartz MA (2002). Integrins regulate the apoptotic response to DNA damage through modulation of p53. Proc Natl Acad Sci U S A. **99**: 3627-32.

Li R, Maminishkis A, Zahn G, Vossmeyer D, Miller SS (2009a). Integrin alpha5beta1 mediates attachment, migration, and proliferation in human retinal pigment epithelium: relevance for proliferative retinal disease. Invest Ophthalmol Vis Sci. **50**: 5988-96.

Li S, Zhang W, Chen B, Jiang T, Wang Z (2009b). Prognostic and predictive value of p53 in low MGMT expressing glioblastoma treated with surgery, radiation and adjuvant temozolomide chemotherapy. Neurol Res.

Livak KJ, Schmittgen TD (2001). Analysis of relative gene expression data using real-time quantitative PCR and the 2(-Delta Delta C(T)) Method. Methods. **25**: 402-8.

Louis DN, Ohgaki H, Wiestler OD, Cavenee WK, Burger PC, Jouvet A, et al. (2007). The 2007 WHO classification of tumours of the central nervous system. Acta Neuropathol. **114**: 97-109.

Lu X, Lu D, Scully M, Kakkar V (2008). The role of integrins in cancer and the development of anti-integrin therapeutic agents for cancer therapy. Perspect Medicin Chem. **2**: 57-73.

Luo BH, Springer TA (2006). Integrin structures and conformational signaling. Curr Opin Cell Biol. **18**: 579-86.

Maglott A, Bartik P, Cosgun S, Klotz P, Ronde P, Fuhrmann G, et al. (2006). The small alpha5beta1 integrin antagonist, SJ749, reduces proliferation and clonogenicity of human astrocytoma cells. Cancer Res. **66**: 6002-7.

Maher EA, Furnari FB, Bachoo RM, Rowitch DH, Louis DN, Cavenee WK, et al. (2001). Malignant glioma: genetics and biology of a grave matter. Genes Dev. **15**: 1311-33.

Maier AK, Kociok N, Zahn G, Vossmeyer D, Stragies R, Muether PS, et al. (2007). Modulation of hypoxia-induced neovascularization by JSM6427, an integrin alpha5beta1 inhibiting molecule. Curr Eye Res. **32**: 801-12.

Mansuy D (1998). The great diversity of reactions catalyzed by cytochromes P450. Comp Biochem Physiol C Pharmacol Toxicol Endocrinol. **121**: 5-14.

Martin S, Cosset EC, Terrand J, Maglott A, Takeda K, Dontenwill M (2009). Caveolin-1 regulates glioblastoma aggressiveness through the control of alpha(5)beta(1) integrin expression and modulates glioblastoma responsiveness to SJ749, an alpha(5)beta(1) integrin antagonist. Biochim Biophys Acta. **1793**: 354-67.

Mattern RH, Read SB, Pierschbacher MD, Sze CI, Eliceiri BP, Kruse CA (2005). Glioma cell integrin expression and their interactions with integrin antagonists: Research Article. Cancer Ther. **3A**: 325-40.

Mellinghoff IK, Wang MY, Vivanco I, Haas-Kogan DA, Zhu S, Dia EQ, et al. (2005). Molecular determinants of the response of glioblastomas to EGFR kinase inhibitors. N Engl J Med. **353**: 2012-24.

Mhaidat NM, Zhang XD, Allen J, Avery-Kiejda KA, Scott RJ, Hersey P (2007). Temozolomide induces senescence but not apoptosis in human melanoma cells. Br J Cancer. **97**: 1225-33.

Miyamoto S, Teramoto H, Gutkind JS, Yamada KM (1996). Integrins can collaborate with growth factors for phosphorylation of receptor tyrosine kinases and MAP kinase activation: roles of integrin aggregation and occupancy of receptors. J Cell Biol. **135**: 1633-42.

Mizejewski GJ (1999). Role of integrins in cancer: survey of expression patterns. Proc Soc Exp Biol Med. **222**: 124-38.

Moll UM, Petrenko O (2003). The MDM2-p53 interaction. Mol Cancer Res. **1**: 1001-8.

Momand J, Zambetti GP, Olson DC, George D, Levine AJ (1992). The mdm-2 oncogene product forms a complex with the p53 protein and inhibits p53-mediated transactivation. Cell. **69**: 1237-45.

Morgan ET, Sewer MB, Iber H, Gonzalez FJ, Lee YH, Tukey RH, et al. (1998). Physiological and pathophysiological regulation of cytochrome P450. Drug Metab Dispos. **26**: 1232-40.

Morgan SE, Kastan MB (1997). p53 and ATM: cell cycle, cell death, and cancer. Adv Cancer Res. **71**: 1-25.

Mould AP, Askari JA, Aota S, Yamada KM, Irie A, Takada Y, et al. (1997). Defining the topology of integrin alpha5beta1-fibronectin interactions using inhibitory anti-alpha5 and anti-beta1 monoclonal antibodies. Evidence that the synergy sequence of fibronectin is recognized by the amino-terminal repeats of the alpha5 subunit. J Biol Chem. **272**: 17283-92.

Murray GI (2000). The role of cytochrome P450 in tumour development and progression and its potential in therapy. J Pathol. **192**: 419-26.

Murray GI, Taylor MC, McFadyen MC, McKay JA, Greenlee WF, Burke MD, et al. (1997). Tumor-specific expression of cytochrome P450 CYP1B1. Cancer Res. **57**: 3026-31.

Nabors LB, Mikkelsen T, Rosenfeld SS, Hochberg F, Akella NS, Fisher JD, et al. (2007). Phase I and correlative biology study of cilengitide in patients with recurrent malignant glioma. J Clin Oncol. **25**: 1651-7.

Nakamura M, Watanabe T, Klangby U, Asker C, Wiman K, Yonekawa Y, et al. (2001). p14ARF deletion and methylation in genetic pathways to glioblastomas. Brain Pathol. **11**: 159-68.

Nebert DW, McKinnon RA, Puga A (1996). Human drug-metabolizing enzyme polymorphisms: effects on risk of toxicity and cancer. DNA Cell Biol. **15**: 273-80.

Nelson DR, Koymans L, Kamataki T, Stegeman JJ, Feyereisen R, Waxman DJ, et al. (1996). P450 superfamily: update on new sequences, gene mapping, accession numbers and nomenclature. Pharmacogenetics. **6**: 1-42.

O'Connor L, Strasser, A, Bennett M, Macdonald K, Chan S-W, et al. (1999). Fas, p53, and Apoptosis. Science. **284**: 1431b-.

Ohashi M, Sugikawa E, Nakanishi N (1995). Inhibition of p53 protein phosphorylation by 9-hydroxyellipticine: a possible anticancer mechanism. Jpn J Cancer Res. **86**: 819-27.

Ohgaki H, Kleihues P (2005). Population-based studies on incidence, survival rates, and genetic alterations in astrocytic and oligodendroglial gliomas. J Neuropathol Exp Neurol. **64**: 479-89.

Ohgaki H, Kleihues P (2007). Genetic pathways to primary and secondary glioblastoma. Am J Pathol. **170**: 1445-53.

Oliner JD, Kinzler KW, Meltzer PS, George DL, Vogelstein B (1992). Amplification of a gene encoding a p53-associated protein in human sarcomas. Nature. **358**: 80-3.

Omuro AM (2008). Exploring multi-targeting strategies for the treatment of gliomas. Curr Opin Investig Drugs. **9**: 1287-95.

Paulus W, Baur I, Schuppan D, Roggendorf W (1993). Characterization of integrin receptors in normal and neoplastic human brain. Am J Pathol. **143**: 154-63.

Penas-Prado M, Gilbert MR (2007). Molecularly targeted therapies for malignant gliomas: advances and challenges. Expert Rev Anticancer Ther. **7**: 641-61.

Peng Y, Li C, Chen L, Sebti S, Chen J (2003). Rescue of mutant p53 transcription function by ellipticine. Oncogene. **22**: 4478-87.

Plewka D, Plewka A, Nowaczyk G, Kaminski M, Rutkowski T, Ludyga T, et al. (2000). Neoplastic lesions of the human liver in relation to the activity of the cytochrome P-450 dependent monooxygenase system. Med Sci Monit. **6**: 244-8.

Poljakova J, Eckschlager T, Hrabeta J, Hrebackova J, Smutny S, Frei E, et al. (2009). The mechanism of cytotoxicity and DNA adduct formation by the anticancer drug ellipticine in human neuroblastoma cells. Biochem Pharmacol. **77**: 1466-79.

Poljakova J, Frei E, Gomez JE, Aimova D, Eckschlager T, Hrabeta J, et al. (2007). DNA adduct formation by the anticancer drug ellipticine in human leukemia HL-60 and CCRF-CEM cells. Cancer Lett. **252**: 270-9.

Porter TD (2002). The roles of cytochrome b5 in cytochrome P450 reactions. J Biochem Mol Toxicol. **16**: 311-6.

Pozzi A, Wary KK, Giancotti FG, Gardner HA (1998). Integrin alpha1beta1 mediates a unique collagen-dependent proliferation pathway in vivo. J Cell Biol. **142**: 587-94.

Pramanik D, Majeti BK, Mondal G, Karmali PP, Sistla R, Ramprasad OG, et al. (2008). Lipopeptide with a RGDK tetrapeptide sequence can selectively target genes to proangiogenic alpha5beta1 integrin receptor and mouse tumor vasculature. J Med Chem. **51**: 7298-302.

Reardon DA, Fink KL, Mikkelsen T, Cloughesy TF, O'Neill A, Plotkin S, et al. (2008a). Randomized phase II study of cilengitide, an integrin-targeting arginine-glycine-aspartic acid peptide, in recurrent glioblastoma multiforme. J Clin Oncol. **26**: 5610-7.

Reardon DA, Nabors LB, Stupp R, Mikkelsen T (2008b). Cilengitide: an integrin-targeting arginine-glycine-aspartic acid peptide with promising activity for glioblastoma multiforme. Expert Opin Investig Drugs. **17**: 1225-35.

Reinmuth N, Liu W, Ahmad SA, Fan F, Stoeltzing O, Parikh AA, et al. (2003). Alphavbeta3 integrin antagonist S247 decreases colon cancer metastasis and angiogenesis and improves survival in mice. Cancer Res. **63**: 2079-87.

Rendic S, Di Carlo FJ (1997). Human cytochrome P450 enzymes: a status report summarizing their reactions, substrates, inducers, and inhibitors. Drug Metab Rev. **29**: 413-580.

Ricart AD, Tolcher AW, Liu G, Holen K, Schwartz G, Albertini M, et al. (2008). Volociximab, a chimeric monoclonal antibody that specifically binds alpha5beta1 integrin: a phase I, pharmacokinetic, and biological correlative study. Clin Cancer Res. **14**: 7924-9.

Rieger J, Lemke D, Maurer G, Weiler M, Frank B, Tabatabai G, et al. (2008). Enzastaurin-induced apoptosis in glioma cells is caspase-dependent and inhibited by BCL-XL. J Neurochem. **106**: 2436-48.

Roos WP, Batista LF, Naumann SC, Wick W, Weller M, Menck CF, et al. (2007). Apoptosis in malignant glioma cells triggered by the temozolomide-induced DNA lesion O6-methylguanine. Oncogene. **26**: 186-97.

Ruan S, Okcu MF, Pong RC, Andreeff M, Levin V, Hsieh JT, et al. (1999). Attenuation of WAF1/Cip1 expression by an antisense adenovirus expression vector sensitizes glioblastoma cells to apoptosis induced by chemotherapeutic agents 1,3-bis(2-chloroethyl)-1-nitrosourea and cisplatin. Clin Cancer Res. **5**: 197-202.

Ruan S, Okcu MF, Ren JP, Chiao P, Andreeff M, Levin V, et al. (1998). Overexpressed WAF1/Cip1 renders glioblastoma cells resistant to chemotherapy agents 1,3-bis(2-chloroethyl)-1-nitrosourea and cisplatin. Cancer Res. **58**: 1538-43.

Sage J, Miller AL, Perez-Mancera PA, Wysocki JM, Jacks T (2003). Acute mutation of retinoblastoma gene function is sufficient for cell cycle re-entry. Nature. **424**: 223-8.

Sathornsumetee S, Reardon DA, Desjardins A, Quinn JA, Vredenburgh JJ, Rich JN (2007). Molecularly targeted therapy for malignant glioma. Cancer. **110**: 13-24.

Sathornsumetee S, Rich JN (2008). Designer therapies for glioblastoma multiforme. Ann N Y Acad Sci. **1142**: 108-32.

Sato N, Mizumoto K, Kusumoto M, Niiyama H, Maehara N, Ogawa T, et al. (1998). 9-Hydroxyellipticine inhibits telomerase activity in human pancreatic cancer cells. FEBS Lett. **441**: 318-21.

Sawada K, Mitra AK, Radjabi AR, Bhaskar V, Kistner EO, Tretiakova M, et al. (2008). Loss of E-cadherin promotes ovarian cancer metastasis via alpha 5-integrin, which is a therapeutic target. Cancer Res. **68**: 2329-39.

Schacter BA, Meyer UA, Marver HS (1972). Hemoprotein catabolism during stimulation of microsomal lipid peroxidation. Biochim Biophys Acta. **279**: 221-7.

Schlaepfer DD, Hanks SK, Hunter T, van der Geer P (1994). Integrin-mediated signal transduction linked to Ras pathway by GRB2 binding to focal adhesion kinase. Nature. **372**: 786-91.

Schmitt CA (2007). Cellular senescence and cancer treatment. Biochim Biophys Acta. **1775**: 5-20.

Schmitt CA, Fridman JS, Yang M, Lee S, Baranov E, Hoffman RM, et al. (2002). A senescence program controlled by p53 and p16INK4a contributes to the outcome of cancer therapy. Cell. **109**: 335-46.

Schwaller MA, Allard B, Lescot E, Moreau F (1995). Protonophoric activity of ellipticine and isomers across the energy-transducing membrane of mitochondria. J Biol Chem. **270**: 22709-13.

Schwartzbaum JA, Fisher JL, Aldape KD, Wrensch M (2006). Epidemiology and molecular pathology of glioma. Nat Clin Pract Neurol. **2**: 494-503; quiz 1 p following 16.

Serini G, Valdembri D, Bussolino F (2006). Integrins and angiogenesis: a sticky business. Exp Cell Res. **312**: 651-8.

Shi LM, Fan Y, Myers TG, O'Connor PM, Paull KD, Friend SH, et al. (1998a). Mining the NCI anticancer drug discovery databases: genetic function approximation for the QSAR study of anticancer ellipticine analogues. J Chem Inf Comput Sci. **38**: 189-99.

Shi LM, Myers TG, Fan Y, O'Connor PM, Paull KD, Friend SH, et al. (1998b). Mining the National Cancer Institute Anticancer Drug Discovery Database: cluster analysis of ellipticine analogs with p53-inverse and central nervous system-selective patterns of activity. Mol Pharmacol. **53**: 241-51.

Smallheer JM, Weigelt CA, Woerner FJ, Wells JS, Daneker WF, Mousa SA, et al. (2004). Synthesis and biological evaluation of nonpeptide integrin antagonists containing spirocyclic scaffolds. Bioorg Med Chem Lett. **14**: 383-7.

Springer TA (1997). Folding of the N-terminal, ligand-binding region of integrin alpha-subunits into a beta-propeller domain. Proc Natl Acad Sci U S A. **94**: 65-72.

Springer TA, Wang JH (2004). The three-dimensional structure of integrins and their ligands, and conformational regulation of cell adhesion. Adv Protein Chem. **68**: 29-63.

Stevens MF, Newlands ES (1993). From triazines and triazenes to temozolomide. Eur J Cancer. **29A**: 1045-7.

Stiborova M, Arlt VM, Henderson CJ, Wolf CR, Kotrbova V, Moserova M, et al. (2008). Role of hepatic cytochromes P450 in bioactivation of the anticancer drug ellipticine: studies

with the hepatic NADPH:cytochrome P450 reductase null mouse. Toxicol Appl Pharmacol. **226**: 318-27.

Stiborova M, Bieler CA, Wiessler M, Frei E (2001). The anticancer agent ellipticine on activation by cytochrome P450 forms covalent DNA adducts. Biochem Pharmacol. **62**: 1675-84.

Stiborova M, Fernando RC, Schmeiser HH, Frei E, Pfau W, Wiessler M (1994). Characterization of DNA adducts formed by aristolochic acids in the target organ (forestomach) of rats by 32P-postlabelling analysis using different chromatographic procedures. Carcinogenesis. **15**: 1187-92.

Stiborova M, Martinek V, Rydlova H, Hodek P, Frei E (2002). Sudan I is a potential carcinogen for humans: evidence for its metabolic activation and detoxication by human recombinant cytochrome P450 1A1 and liver microsomes. Cancer Res. **62**: 5678-84.

Stiborova M, Poljakova J, Ryslava H, Dracinsky M, Eckschlager T, Frei E (2007a). Mammalian peroxidases activate anticancer drug ellipticine to intermediates forming deoxyguanosine adducts in DNA identical to those found in vivo and generated from 12-hydroxyellipticine and 13-hydroxyellipticine. Int J Cancer. **120**: 243-51.

Stiborova M, Rupertova M, Aimova D, Ryslava H, Frei E (2007b). Formation and persistence of DNA adducts of anticancer drug ellipticine in rats. Toxicology. **236**: 50-60.

Stiborova M, Rupertova M, Schmeiser HH, Frei E (2006). Molecular mechanisms of antineoplastic action of an anticancer drug ellipticine. Biomed Pap Med Fac Univ Palacky Olomouc Czech Repub. **150**: 13-23.

Stiborova M, Sejbal J, Borek-Dohalska L, Aimova D, Poljakova J, Forsterova K, et al. (2004). The anticancer drug ellipticine forms covalent DNA adducts, mediated by human cytochromes P450, through metabolism to 13-hydroxyellipticine and ellipticine N2-oxide. Cancer Res. **64**: 8374-80.

Stiborova M, Stiborova-Rupertova M, Borek-Dohalska L, Wiessler M, Frei E (2003). Rat microsomes activating the anticancer drug ellipticine to species covalently binding to deoxyguanosine in DNA are a suitable model mimicking ellipticine bioactivation in humans. Chem Res Toxicol. **16**: 38-47.

Stoeltzing O, Liu W, Reinmuth N, Fan F, Parry GC, Parikh AA, et al. (2003). Inhibition of integrin alpha5beta1 function with a small peptide (ATN-161) plus continuous 5-FU infusion reduces colorectal liver metastases and improves survival in mice. Int J Cancer. **104**: 496-503.

Stott FJ, Bates S, James MC, McConnell BB, Starborg M, Brookes S, et al. (1998). The alternative product from the human CDKN2A locus, p14(ARF), participates in a regulatory feedback loop with p53 and MDM2. EMBO J. **17**: 5001-14.

Stupack DG, Puente XS, Boutsaboualoy S, Storgard CM, Cheresh DA (2001). Apoptosis of adherent cells by recruitment of caspase-8 to unligated integrins. J Cell Biol. **155**: 459-70.

Stupp R, Mason WP, van den Bent MJ, Weller M, Fisher B, Taphoorn MJ, et al. (2005). Radiotherapy plus concomitant and adjuvant temozolomide for glioblastoma. N Engl J Med. **352**: 987-96.

Sugikawa E, Hosoi T, Yazaki N, Gamanuma M, Nakanishi N, Ohashi M (1999a). Mutant p53 mediated induction of cell cycle arrest and apoptosis at G1 phase by 9-hydroxyellipticine. Anticancer Res. **19**: 3099-108.

Sugikawa E, Yazaki N, Tsunoda S, Nakanishi N, Ohashi M (1999b). Inhibition of mutant p53 phosphorylation at serine 15 or serine 315 partially restores the function of wild-type p53. Biochem Biophys Res Commun. **261**: 256-63.

Tadokoro S, Shattil SJ, Eto K, Tai V, Liddington RC, de Pereda JM, et al. (2003). Talin binding to integrin beta tails: a final common step in integrin activation. Science. **302**: 103-6.

Takagi J, Petre BM, Walz T, Springer TA (2002). Global conformational rearrangements in integrin extracellular domains in outside-in and inside-out signaling. Cell. **110**: 599-11.

Takagi J, Springer TA (2002). Integrin activation and structural rearrangement. Immunol Rev. **186**: 141-63.

Tan SM, Robinson MK, Drbal K, van Kooyk Y, Shaw JM, Law SK (2001). The N-terminal region and the mid-region complex of the integrin beta 2 subunit. J Biol Chem. **276**: 36370-6.

Tanaka T, Ohkubo S, Tatsuno I, Prives C (2007). hCAS/CSE1L associates with chromatin and regulates expression of select p53 target genes. Cell. **130**: 638-50.

te Poele RH, Okorokov AL, Jardine L, Cummings J, Joel SP (2002). DNA damage is able to induce senescence in tumor cells in vitro and in vivo. Cancer Res. **62**: 1876-83.

Tentori L, Dorio AS, Muzi A, Lacal PM, Ruffini F, Navarra P, et al. (2008). The integrin antagonist cilengitide increases the antitumor activity of temozolomide against malignant melanoma. Oncol Rep. **19**: 1039-43.

Tentori L, Graziani G (2002). Pharmacological strategies to increase the antitumor activity of methylating agents. Curr Med Chem. **9**: 1285-301.

Tucker GC (2002). Inhibitors of integrins. Curr Opin Pharmacol. **2**: 394-402.

Tuettenberg J, Friedel C, Vajkoczy P (2006). Angiogenesis in malignant glioma--a target for antitumor therapy? Crit Rev Oncol Hematol. **59**: 181-93.

Tuettenberg J, Grobholz R, Korn T, Wenz F, Erber R, Vajkoczy P (2005). Continuous low-dose chemotherapy plus inhibition of cyclooxygenase-2 as an antiangiogenic therapy of glioblastoma multiforme. J Cancer Res Clin Oncol. **131**: 31-40.

Uhm JH, Dooley NP, Kyritsis AP, Rao JS, Gladson CL (1999a). Vitronectin, a glioma-derived extracellular matrix protein, protects tumor cells from apoptotic death. Clin Cancer Res. **5**: 1587-94.

Uhm JH, Gladson CL, Rao JS (1999b). The role of integrins in the malignant phenotype of gliomas. Front Biosci. **4**: D188-99.

Ullrich R, Hofrichter M (2007). Enzymatic hydroxylation of aromatic compounds. Cell Mol Life Sci. **64**: 271-93.

Umeda N, Kachi S, Akiyama H, Zahn G, Vossmeyer D, Stragies R, et al. (2006). Suppression and regression of choroidal neovascularization by systemic administration of an alpha5beta1 integrin antagonist. Mol Pharmacol. **69**: 1820-8.

Vistica DT, Kenney S, Hursey ML, Boyd MR (1994). Cellular uptake as a determinant of cytotoxicity of quaternized ellipticines to human brain tumor cells. Biochem Biophys Res Commun. **200**: 1762-8.

Vousden KH (2000). p53: death star. Cell. **103**: 691-4.

Vousden KH (2002). Activation of the p53 tumor suppressor protein. Biochim Biophys Acta. **1602**: 47-59.

Wang Y, Zhu S, Cloughesy TF, Liau LM, Mischel PS (2004). p53 disruption profoundly alters the response of human glioblastoma cells to DNA topoisomerase I inhibition. Oncogene. **23**: 1283-90.

Weller M, Rieger J, Grimmel C, Van Meir EG, De Tribolet N, Krajewski S, et al. (1998). Predicting chemoresistance in human malignant glioma cells: the role of molecular genetic analyses. Int J Cancer. **79**: 640-4.

Wrighton SA, Stevens JC (1992). The human hepatic cytochromes P450 involved in drug metabolism. Crit Rev Toxicol. **22**: 1-21.

Wunderlich M, Berberich SJ (2002). Mdm2 inhibition of p53 induces E2F1 transactivation via p21. Oncogene. **21**: 4414-21.

Xiao T, Takagi J, Coller BS, Wang JH, Springer TA (2004). Structural basis for allostery in integrins and binding to fibrinogen-mimetic therapeutics. Nature. **432**: 59-67.

Xiong JP, Stehle T, Diefenbach B, Zhang R, Dunker R, Scott DL, et al. (2001). Crystal structure of the extracellular segment of integrin alpha Vbeta3. Science. **294**: 339-45.

Xirodimas D, Saville MK, Edling C, Lane DP, Lain S (2001). Different effects of p14ARF on the levels of ubiquitinated p53 and Mdm2 in vivo. Oncogene. **20**: 4972-83.

Xu GW, Mymryk JS, Cairncross JG (2005). Pharmaceutical-mediated inactivation of p53 sensitizes U87MG glioma cells to BCNU and temozolomide. Int J Cancer. **116**: 187-92.

Xue W, Zender L, Miething C, Dickins RA, Hernando E, Krizhanovsky V, et al. (2007). Senescence and tumour clearance is triggered by p53 restoration in murine liver carcinomas. Nature. **445**: 656-60.

Yamakita Y, Totsukawa G, Yamashiro S, Fry D, Zhang X, Hanks SK, et al. (1999). Dissociation of FAK/p130(CAS)/c-Src complex during mitosis: role of mitosis-specific serine phosphorylation of FAK. J Cell Biol. **144**: 315-24.

Yamasaki M, Miyata H, Fujiwara Y, Takiguchi S, Nakajima K, Nishida T, et al. (2009). p53 Genotype Predicts Response to Chemotherapy in Patients with Squamous Cell Carcinoma of the Esophagus. Ann Surg Oncol.

Yung WK, Prados M, Levin VA, Fetell MR, Bennett J, Mahaley MS, et al. (1991). Intravenous recombinant interferon beta in patients with recurrent malignant gliomas: a phase I/II study. J Clin Oncol. **9**: 1945-9.

Zang Q, Springer TA (2001). Amino acid residues in the PSI domain and cysteine-rich repeats of the integrin beta2 subunit that restrain activation of the integrin alpha(X)beta(2). J Biol Chem. **276**: 6922-9.

Zauberman A, Flusberg D, Haupt Y, Barak Y, Oren M (1995). A functional p53-responsive intronic promoter is contained within the human mdm2 gene. Nucleic Acids Res. **23**: 2584-92.

Zhang Z, Vuori K, Reed JC, Ruoslahti E (1995). The alpha 5 beta 1 integrin supports survival of cells on fibronectin and up-regulates Bcl-2 expression. Proc Natl Acad Sci U S A. **92**: 6161-5.

Ziegler DM (2002). An overview of the mechanism, substrate specificities, and structure of FMOs. Drug Metab Rev. **34**: 503-11.

http://www.cancer.org/docroot/PRO/content/PRO_1_1_Cancer_Statistics_2009_Presentation.asp, cached 19.2.2010

http://emedicine.medscape.com/article/283453-overview, cached 30.11.2009

http://rad.usuhs.mil/rad/who/who2b.html; cached 30.11.2009

http://emedicine.medscape.com/ article/283453-overview, cached 30.11.2009

http://p53.free.fr/index.html, cached 1.12.2009

http://www2.unil.ch/cepo_research/introduction.html; cached 17.12.2009

http://cgap.nci.nih.gov/; cached 16.12.1009

http://www.gleevec.com/patient/gleevec-prescription-medication-information.jsp; cached 15.2.2010